

**Characterization of Log Periodic Folded Slot Antenna Array**

By

David Del Río Del Río

A thesis submitted in partial fulfillment of the requirements for the degree of

MASTERS of SCIENCE

in

Electrical Engineering

UNIVERSITY OF PUERTO RICO

MAYAGÜEZ CAMPUS

2005

Approved by:

\_\_\_\_\_  
José Colom Ustariz, PhD.  
Member, Graduate Committee

\_\_\_\_\_  
Date

\_\_\_\_\_  
Sandra Cruz Pol, PhD.  
Member, Graduate Committee

\_\_\_\_\_  
Date

\_\_\_\_\_  
Rafael Rodríguez Solís, PhD.  
President, Graduate Committee

\_\_\_\_\_  
Date

\_\_\_\_\_  
Isidoro Couvertier, PhD.  
Chairperson of the Department

\_\_\_\_\_  
Date

\_\_\_\_\_  
David González Barreto, PhD.  
Representative of Graduate Studies

\_\_\_\_\_  
Date

## **Abstract**

This work studies the log-periodic folded-slot array (LPFSA) using Design of Experiments (DOE) techniques. The LPFSA impedance, gain and time-domain responses were analyzed and regression models were used to predict the antenna responses. The results indicate that the impedance of the central line and the boom length are the most influential factors in the frequency response of the antenna. These factors are responsible for the broad impedance and pattern bandwidth of the antenna. The gain of the antenna is between 7 and 8 dB for a scaling factor of .89 and between 9 and 10 dB for a scaling factor of 0.95. The VSWR was less than two on the bandwidth of the antenna between 3 and 11 GHz for optimal designs. Results also indicate that the log periodic antenna configuration is not suitable for time domain applications. The research also found a stability problem with the radiation pattern of the original LPFSA configuration and consequently a configuration was developed to correct this problem.

## **Resumen**

Este trabajo estudia la antena log periodic de ranura plegada (LPFSA) usando técnicas de diseños de experimentos. La impedancia de la LPFSA, por sus siglas en ingles, ganancia y la respuesta en el dominio del tiempo fueron analizadas y modelos de regresión fueron usados para predecir la respuesta de la antena. Los resultados indican que la impedancia de la línea central y el largo total de la antena son los factores más influyentes en la respuesta de frecuencia de la antena. Estos factores son responsables por el ancho de banda ancha de impedancia y el patrón de la antena. La ganancia de la antena esta entre 7 y 8 dB para un factor de reducción de .89 y entre 9 y 10 dB para un factor de reducción de 0.95. Los resultados también indican que la configuración log periodic no es adecuada para aplicaciones en el dominio del tiempo. La investigación encontró un problema de estabilidad con el patrón de radiación de la configuración original y una configuración alterna fue desarrollada para corregir este problema.

© David Del Río Del Río, 2005

To the Lord, since He gives me strength and wisdom to overcome the difficult situations.

To my parents, for their love, support and faith in me.

## **Acknowledgements**

I would like to thank my advisor Dr. Rafael Rodriguez for his financial support and also for teaching me a lot about antennas. In addition, I would like to thank Dr. Dejan Filipovic from the University of Colorado for his invaluable help to this research. Also, I would like to thank Zoya Popovic for her financial support during the summer I spent at CU and to the members of my committee Dr. Sandra Cruz Pol, Dr. Jose Colom and David Gonzalez.

Special thanks to my friends Alexei, Jaime, Juan, Silvia, Antonio, Carlos, Nestor for their help and friendship.

This work was sponsored by a CAREER award granted by the National Science Foundation.

## TABLE OF CONTENTS

<b>1</b>	<b>INTRODUCTION .....</b>	<b>1</b>
1.1	JUSTIFICATION .....	1
1.2	OBJECTIVES .....	2
1.3	PROJECT DESCRIPTION.....	2
1.4	WORK ORGANIZATION.....	3
<b>2</b>	<b>LITERATURE REVIEW .....</b>	<b>4</b>
2.1	DEFINITION OF LOG PERIODIC ANTENNAS .....	4
2.2	LOG PERIODIC ANTENNA DESIGN PARAMETERS.....	4
2.3	PRINCIPLES OF OPERATION OF LOG PERIODIC ANTENNAS .....	5
2.4	LOG PERIODIC DIPOLE ANTENNA .....	7
2.5	LOG PERIODIC SLOT ANTENNAS AND FEED TYPES .....	12
2.6	APPLICATIONS OF LOG PERIODIC ANTENNAS .....	14
2.7	TIME DOMAIN ANALYSIS OF ANTENNAS.....	15
2.8	LOG PERIODIC FOLDED SLOT ANTENNA .....	19
2.9	COPLANAR WAVEGUIDE TRANSMISSION LINES .....	21
2.10	LOG PERIODIC FOLDED SLOT ANTENNA FEEDLINE.....	23
2.11	FOLDED SLOT ANTENNA .....	23
2.12	DESIGN OF EXPERIMENTS .....	26
<b>3</b>	<b>METHODOLOGY .....</b>	<b>34</b>
3.1	PURPOSE .....	34
3.2	PROCEDURE .....	36
3.3	SIMULATION SOFTWARE .....	37
3.3.1	<i>Electromagnetic Simulator</i> .....	37
3.3.2	<i>Design Expert Software</i> .....	38
3.4	DESIGN EQUATIONS FOR LPFSA .....	38
3.5	LOG PERIODIC FOLDED SLOT ANTENNA DESIGN EXAMPLE.....	40
3.5.1	<i>Input Factors</i> .....	41
3.5.2	<i>Feed line Dimensions</i> .....	41
3.5.3	<i>Elements Connecting Line Dimensions</i> .....	41
3.5.4	<i>Calculated Parameters</i> .....	42
3.5.5	<i>Results</i> .....	43
3.6	SIMULATION RESULTS FROM PRELIMINARY DESIGNS – DATA COLLECTION .....	45
3.7	DESIGN OF EXPERIMENTS .....	49
3.7.1	<i>DOE I</i> .....	49
3.7.2	<i>DOE II</i> .....	51
3.7.3	<i>DOE III</i> .....	51
3.7.4	<i>DOE IV</i> .....	52
3.8	TIME DOMAIN ANALYSIS.....	52
3.9	PROTOTYPE FABRICATION .....	56
<b>4</b>	<b>RESULTS AND DISCUSSION .....</b>	<b>57</b>
4.1	DOE I RESULTS .....	57
4.1.1	<i>Model for the Mean of the Gain</i> .....	61
4.1.2	<i>Model for the Mean of the Reflection Coefficient</i> .....	63
4.1.3	<i>Model for the Minimum of Reflection Coefficient</i> .....	64
4.1.4	<i>Model for the Input Resistance</i> .....	66
4.1.5	<i>Effects in the Antenna Parameters</i> .....	68
4.2	DOE II RESULTS .....	75
4.2.1	<i>Model for the Minimum of the Gain</i> .....	79

4.2.2	<i>Model for the Mean of the Reflection Coefficient</i> .....	80
4.2.3	<i>Model for the Minimum of the Reflection Coefficient</i> .....	82
4.2.4	<i>Model for the Minimum of the VSWR</i> .....	83
4.2.5	<i>Model for the Minimum of the Input Resistance</i> .....	84
4.2.6	<i>Effects in the Antenna Parameters</i> .....	85
4.3	DOE III RESULTS.....	94
4.3.1	<i>Model for the Mean of the Gain</i> .....	97
4.3.2	<i>Model for the Mean of the Reflection Coefficient</i> .....	98
4.3.3	<i>Model for the Minimum of the Input Resistance</i> .....	99
4.3.4	<i>Effects in the Antenna Parameters</i> .....	101
4.4	DOE IV RESULTS .....	109
4.4.1	<i>Model for the Minimum of the Gain</i> .....	111
4.4.2	<i>Model for the Minimum of the Reflection Coefficient</i> .....	113
4.4.3	<i>Model for the Maximum of the Input Resistance</i> .....	114
4.4.4	<i>Model for the Minimum of the Input Resistance</i> .....	116
4.4.5	<i>Effects in the Antenna Parameters</i> .....	117
4.5	TIME DOMAIN ANALYSIS .....	127
4.6	MODULATED IMPEDANCE FEEDER .....	132
4.7	MEASURED RESULTS .....	136
<b>5</b>	<b>CONCLUSIONS AND RECOMMENDATIONS.....</b>	<b>143</b>
5.1	CONCLUSIONS.....	143
5.2	RECOMMENDATIONS.....	145
<b>6</b>	<b>BIBLIOGRAPHY .....</b>	<b>146</b>
<b>7</b>	<b>APPENDIX.....</b>	<b>149</b>

## List of Figures

Figure 2.3.1. Current Distribution of LPFSA design at $f=6.87$ GHz.....	7
Figure 2.3.2. Current Distribution of LPFSA design at 10.59 GHz. ....	7
Figure 2.4.1. Carell’s Design Curves.....	8
Figure 2.4.2. Phase of Reflection Coefficient of a log periodic circuit. ....	9
Figure 2.4.3. Dimensions of LPDA using different optimization methods.....	11
Figure 2.5.1. Log-Periodic Slot Antenna Configuration.....	12
Figure 2.5.2. Return Loss Response for different LPSA designs. ....	13
Figure 2.5.3. Geometry of the microstrip-fed log-periodic slot array. ....	13
Figure 2.5.4. LPDA with each element fed separately. ....	14
Figure 2.7.1. Impulse Response of LPDA. ....	16
Figure 2.7.2. Linear system representing propagation of electromagnetics waves in a medium. ....	17
Figure 2.7.3. Correlation between the receive response of TEM horn antennas and the incident waveform as a function of angle in the H-plane. ....	18
Figure 2.8.1. 3-D view of LPFSA configuration. ....	20
Figure 2.9.1. Coplanar Waveguide Line and Dimensions.....	22
Figure 2.9.2. Coplanar Waveguide Excitation Modes.....	22
Figure 2.11.1. Folded Slot Antenna configuration and its dimensions.....	24
Figure 2.11.2. Input Impedance of Folded Slot Antenna designs as function of substrate thickness.....	25
Figure 2.11.3. Ideal field distribution of folded slot antenna.....	25
Figure 2.12.1. Normal Plot of Residuals.....	27
Figure 2.12.2. Residuals versus Run Number Plot. ....	28

Figure 2.12.3. Residuals versus factor Z(impedance of the feeder line) .....	28
Figure 2.12.4. Predicted versus Actual values.....	29
Figure 2.12.5. Half Normal Plot of Example.....	32
Figure 3.1.1. Top View of LPFSAs.....	35
Figure 3.1.2. Log Periodic Folded Slot Antenna Dimensions.....	36
Figure 3.1.3. Elements Connecting Line Dimensions.....	36
Figure 3.2.1. Procedure Involved in the design of LPFSA.....	37
Figure 3.5.1. Return Loss Response of Example.....	43
Figure 3.5.2. Input Resistance of Example.....	44
Figure 3.5.3. Gain in the direction of maximum radiation ( $\theta=85^\circ$ , $\phi=90^\circ$ ) of Example..	45
Figure 3.6.1. Return Loss Response of designs with different scaling factors.....	46
Figure 3.6.2. Gain ( $\theta=85^\circ$ ) of designs with different scaling factors.....	47
Figure 3.6.3. Return Loss Response of designs with $\epsilon_r=6.15$ .....	48
Figure 3.6.4. Return Loss Response of designs with $\epsilon_r=6.15$ .....	48
Figure 3.6.5. Return Loss Response of designs where the boom length was varied.....	49
Figure 3.8.1. Receiving circuit depiction.....	53
Figure 4.1.1. Graphical method for determining the parameters that affect the mean of the gain using DOE I data.....	61
Figure 4.1.2. Normal Plot of Residuals and Residuals versus Predicted Values Plot for Gain (mean) model for DOE I.....	62
Figure 4.1.3. Graphical method for determining the parameters that affect the mean of the reflection coefficient using DOE I data.....	63
Figure 4.1.4. Graphical method for determining the parameters that affect the minimum of the reflection coefficient using DOE I data.....	65

Figure 4.1.5. Graphical method for determining the parameters that affect the maximum of the input resistance using DOE I data. ....	67
Figure 4.1.6. Return Loss Response for DOE I Design 00000 and Design 00001.....	69
Figure 4.1.7. Return Loss Response for DOE I Design 00100 and Design 00101.....	70
Figure 4.1.8. Return Loss Response for DOE I Design 00010 and Design 00011.....	70
Figure 4.1.9. Gain in the Direction of Maximum Radiation for DOE I Design 00000 and Design 00001. ....	71
Figure 4.1.10. Gain in the Direction of Maximum Radiation for DOE I Design 00100 and Design 00101. ....	71
Figure 4.1.11. Gain in the Direction of Maximum Radiation for DOE I Design 00010 and Design 00011. ....	72
Figure 4.1.12. Gain in the Direction of Maximum Radiation for DOE I Design 00000 and Design 00100. ....	73
Figure 4.1.13. Gain in the Direction of Maximum Radiation for DOE I Design 00010 and Design 00110. ....	73
Figure 4.1.14. Gain in the Direction of Maximum Radiation for DOE I Design 01010 and Design 01110. ....	74
Figure 4.1.15. Return Loss Response for DOE I Design 01010 and Design 01110.....	75
Figure 4.2.1. Graphical method for determining the parameters that affect the minimum of the gain using DOE II data. ....	79
Figure 4.2.2. Graphical method for determining the parameters that affect the mean of the reflection coefficient using DOE II data. ....	81
Figure 4.2.3. Graphical method for determining the parameters that affect the minimum of the reflection coefficient using DOE II data.....	82
Figure 4.2.4. Graphical method for determining the parameters that affect the minimum of the VSWR using DOE II data.....	83
Figure 4.2.5. Graphical method for determining the parameters that affect the minimum of the real part of the input impedance using DOE II data. ....	85

Figure 4.2.6. Gain in the Direction of Maximum Radiation for DOE II Design 10000 and Design 10010. ....	86
Figure 4.2.7. 3-D View of Radiation Pattern for DOE II Design 10000 ( $f = 10.86$ GHz) 87	
Figure 4.2.8. Radiation Pattern ( $\varphi=90^\circ$ ) for DOE II Design 10000 ( $f = 10.86$ GHz). ....	87
Figure 4.2.9. 3-D View of Radiation Pattern for DOE II Design 10010 ( $f = 7.70$ GHz)..	88
Figure 4.2.10. Radiation Pattern ( $\varphi=90^\circ$ ) for DOE II Design 10000 ( $f = 10.70$ GHz). ...	88
Figure 4.2.11. Input Resistance for DOE II Design 00000 and Design 00010.....	89
Figure 4.2.12. Input Resistance for DOE II Design 00101 and Design 00111.....	89
Figure 4.2.13. Input Resistance for DOE II Design 10000 and Design 10010.....	90
Figure 4.2.14. Input Resistance for DOE II Design 00011 and Design 01011.....	91
Figure 4.2.15. Input Resistance for DOE II Design 00110 and Design 10110.....	92
Figure 4.2.16. Input Resistance for DOE II Design 00010 and Design 10010.....	92
Figure 4.2.17. Gain in the Direction of Maximum Radiation for DOE II Design 00000 and Design 10000. ....	93
Figure 4.2.18. Gain in the Direction of Maximum Radiation for DOE II Design 00011 and Design 10011. ....	94
Figure 4.3.1. Graphical method for determining the parameters that affect the mean of the gain using DOE III data. ....	97
Figure 4.3.2. Graphical method for determining the parameters that affect the mean of the reflection coefficient using DOE III data.....	98
Figure 4.3.3. Graphical method for determining the parameters that affect the minimum of the input resistance using DOE III data.....	100
Figure 4.3.4. Return Loss Response for DOE III Design 0000 and Design 0010.....	102
Figure 4.3.5. Gain in the Direction of Maximum Radiation for DOE III Design 0000 and Design 0010. ....	103
Figure 4.3.6. Gain in the Direction of Maximum Radiation for DOE III Design 1101 and Design 1111. ....	103

Figure 4.3.7. Return Loss Response for DOE III Design 0010 and Design 0011.....	104
Figure 4.3.8. Gain in the Direction of Maximum Radiation for DOE III Design 0000 and Design 0001.....	105
Figure 4.3.9. Return Loss Response for DOE III Design 0000 and Design 0100.....	106
Figure 4.3.10. Gain in the Direction of Maximum Radiation for DOE III Design 0010 and Design 0110.....	106
Figure 4.3.11. Return Loss Response for DOE III Design 0110 and Design 1110.....	107
Figure 4.3.12. Return Loss Response for DOE III Design 0011 and Design 1011.....	108
Figure 4.3.13. Gain in the Direction of Maximum Radiation for DOE III Design 0101 and Design 1101.....	108
Figure 4.4.1. Graphical method for determining the parameters that affect the minimum of the gain using DOE IV data.....	112
Figure 4.4.2. Graphical method for determining the parameters that affect the minimum of the reflection coefficient using DOE IV data.....	113
Figure 4.4.3. Graphical method for determining the parameters that affect the maximum of the input resistance using DOE IV data.....	115
Figure 4.4.4. Graphical method for determining the parameters that affect the minimum of the input resistance using DOE IV data.....	116
Figure 4.4.5. Return Loss Response for DOE IV Design 0001 and Design 0011.....	118
Figure 4.4.6. Gain in the Direction of Maximum Radiation for DOE IV Design 0001 and Design 0011.....	118
Figure 4.4.7. Gain in the Direction of Maximum Radiation for DOE IV Design 0000 and Design 0010.....	119
Figure 4.4.8. Return Loss Response for DOE IV Design 0010 and Design 0011.....	120
Figure 4.4.9. Gain in the Direction of Maximum Radiation for DOE IV Design 0010 and Design 0011.....	120
Figure 4.4.10. Return Loss Response for DOE IV Design 1011 and Design 1111.....	121
Figure 4.4.11. Return Loss Response for DOE IV Design 0001 and Design 0101.....	122

Figure 4.4.12. Gain in the Direction of Maximum Radiation for DOE IV Design 1011 and Design 1111. ....	123
Figure 4.4.13. Gain in the Direction of Maximum Radiation for DOE IV Design 0011 and Design 0111. ....	123
Figure 4.4.14. 3-D View of Radiation Pattern for DOE IV Design 0011 ( $f = 5.67$ GHz). .....	124
Figure 4.4.15. Radiation Pattern ( $\phi=90^\circ$ ) for DOE IV Design 0011 ( $f = 5.67$ GHz).....	124
Figure 4.4.16. Return Loss Response for DOE IV Design 0111 and Design 1111.....	125
Figure 4.4.17. Return Loss Response for DOE IV Design 0011 and Design 1011.....	126
Figure 4.4.18. Gain in the Direction of Maximum Radiation for DOE IV Design 0001 and Design 1001. ....	126
Figure 4.4.19. Gain in the Direction of Maximum Radiation for DOE IV Design 0000 and Design 1000. ....	127
Figure 4.5.1. Magnitude and Phase of the Transfer Function from design 00000 from DOE II.....	128
Figure 4.5.2. Frequency Content of Transmitted and Received Pulse from design 00000 from DOE II.....	128
Figure 4.5.3. Transmitted and Received Pulse using design 00000 from DOE 2. ....	129
Figure 4.5.4. Phase and Magnitude of the Transfer Function from design 00010 from DOE II.....	130
Figure 4.5.5. Frequency content of the Received Pulse and Transmitted and Received pulse using design 00010 from DOE II. ....	130
Figure 4.5.6. Phase and Magnitude of the Transfer Function from design 00010 from DOE III. ....	131
Figure 4.5.7. Transmitted and Received Pulse using design 0010 from DOE III. ....	132
Figure 4.6.1. Modulated Impedance Feeder Configuration.....	133
Figure 4.6.2. Gain in the direction of maximum radiation for designs using the modulated impedance feeder. ....	134

Figure 4.6.3. Return Loss Response for designs using the modulated impedance feeder. .....	135
Figure 4.6.4. Return Loss Response for designs using the modulated impedance feeder. .....	135
Figure 4.7.1. Simulated versus Measured Results of Return Loss Response of DOE II Design 00000. ....	137
Figure 4.7.2. Simulated versus Measured Results of VSWR Response of DOE II Design 00000. ....	137
Figure 4.7.3. Far Field Pattern (H-plane) of DOE II Design 00000 (etching), $f=6$ GHz. .....	138
Figure 4.7.4. Far Field Pattern (H-plane) of DOE II Design 00000 (etching), $f=8.4$ GHz. .....	139
Figure 4.7.5. Simulated versus Measured Results of Return Loss Response of DOE II Design 00101. ....	139
Figure 4.7.6. Simulated versus Measured Results of Return Loss Response of DOE III Design 0010. ....	140
Figure 4.7.7. Simulated versus Measured Results of VSWR Response of DOE III Design 0010. ....	141
Figure 4.7.8. Far Field Pattern (H-plane) of DOE III Design 0010 (b) (milling), $f=5.25$ GHz. ....	141
Figure 4.7.9. Far Field Pattern (H-plane) of DOE III Design 0010 (b) (milling), $f=8.6$ GHz. ....	142
Figure 4.7.10. Simulated versus Measured Results of Return Loss Response of DOE IV Design 0011. ....	142

## List of Tables

Table 3.1. LPFSA Design Example Input Factors.....	41
Table 3.2. 50 ohm line Dimensions.....	41
Table 3.3. Elements Connecting Line Dimensions.....	41
Table 3.4. Calculated Parameters of LPFSA Example.....	42
Table 3.5. Element Dimensions.....	42
Table 3.6. Factors and Levels for DOE1.....	50
Table 3.7. Design Matrix for DOE1.....	50
Table 3.8. Factors and Levels for DOE 2.....	51
Table 3.9. Factors and Levels for DOE3.....	52
Table 3.10. Factors and Levels for DOE4.....	52
Table 4.1. Mean and Minimum Values of the Reflection Coefficient of DOE I.....	57
Table 4.2. Mean, Minimum and Maximum Values of VSWR and Input Impedance of DOE I.....	58
Table 4.3. Mean Value of the Gain of DOE I.....	59
Table 4.4. Standard Deviation and Variance of the Gain and Real part of Input Impedance of DOE I.....	60
Table 4.5. Actual and Predicted Values of the Model.....	62
Table 4.6. Mean and Minimum Values of the Reflection Coefficient of DOE II.....	75
Table 4.7. Mean, Minimum and Maximum Values of VSWR and Input Impedance of DOE II.....	76
Table 4.8. Mean, Maximum and Minimum Values of the Gain of DOE II.....	77
Table 4.9. Standard Deviation and Variance of the Gain and Real part of Input Impedance of DOE II.....	78
Table 4.10. Mean and Minimum Values of the Reflection Coefficient for DOE III.....	95

Table 4.11. Mean, Minimum and Maximum Values of VSWR and Input Impedance of DOE III.....	95
Table 4.12. Mean, Maximum and Minimum Values of the Gain of DOE III.....	96
Table 4.13. Mean, Minimum and Maximum Values of VSWR and Input Impedance.....	96
Table 4.14. Mean and Minimum Values of the Reflection Coefficient of DOE IV.....	109
Table 4.15. Mean, Minimum and Maximum Values of VSWR and Input Impedance of DOE IV.....	110
Table 4.16. Mean, Maximum and Minimum Values of the Gain of DOE IV.....	110
Table 4.17. Mean, Minimum and Maximum Values of VSWR and Input Impedance of DOE IV.....	111

# **1 Introduction**

## **1.1 Justification**

There has been a radical change in people's lifestyle. Just 12 years ago most people did not have a cellular phone and when they wanted to get information on a specific subject they went to the library to read from pages and pages of different books to get the information that they were looking for. All of that has changed; right now most people have a cellular phone and use the internet to search for information. As technology evolves we have moved from a wired society to a wireless society. As a consequence, there is a huge demand for wireless home networks. Antennas of all kinds have made this switch possible. Right now, people can get a data rate of 54 Mbps while using 802.11g technology based networks. But people always want more and in this case, more bandwidth. There is a need to optimize antennas for maximum bandwidth.

It is of great interest to us to perform a full characterization of Log Periodic Folded Slot Antennas. Although the Log Periodic principle was discovered five decades ago, there has not been an interest for wireless broadband applications until now. The Log Periodic Folded Slot Antennas are low profile, low cost and easy to fabricate. But there is one problem: it is not easy to achieve impedance matching to 50 ohms. The interest here is to perform a full characterization using Design of Experiments techniques to better understand the factors that affect the frequency response negatively and to develop a simple model that would guarantee good frequency response. Only then, this antenna would become a viable option to develop wireless broadband applications.

## 1.2 Objectives

The main objective of this research is to perform a full characterization of a Log Periodic Folded Slot Antenna using Design of Experiments (DOE). This will help us to identify the factors that affect the impedance and radiation pattern of the antenna. Once these factors are identified, several design of experiments will be used to optimize the response of the antenna and finally develop models that guarantee an optimum frequency response. It is of great interest to analyze the antenna in the time domain to evaluate its fidelity for time domain applications. Finally, the simulated results need to be validated by the construction and measuring of antenna prototypes using the network analyzer and anechoic chamber.

## 1.3 Project Description

The Log Periodic Folded Slot Antenna (LPFSA) is low profile, low cost and easy to fabricate. This antenna is fed using a coplanar waveguide line. This antenna is build on top of a substrate. For this project, three different substrates will be used: RO5880 with an  $\epsilon_r=2.2$  and thickness of .787 mm, RO4350 with a  $\epsilon_r=3.48$  and thickness of .762 mm and RO6003 with a  $\epsilon_r=6.15$  and thickness of .635 mm. Mainly, the focus is on how small changes in the dimensions of the antenna affects positively or negatively the response of the antenna.

This thesis presents a full characterization of LPFSAs using Design of Experiments techniques. This statistical tool allows us to evaluate the output of the process, in this case the frequency response of the antenna when input factors are varied. The input factors are dimensions of the antenna. A  $2^k$  factorial design was used to perform the Design of Experiments to evaluate the interactions between input factors. Responses such as return loss, input impedance, VSWR and gain were analyzed. The characterization helped to identify the factors affecting the frequency response of the antenna and solutions were presented to optimize the antenna performance.

Past research has been focused on how to improve the frequency characteristics of one of the LPFSA closest relatives: the Log Periodic Dipole Array (LPDA) [1]. Also, past research focused on what changes were needed in the structure of LPDAs to improve its time domain response.

## **1.4 Work Organization**

The theory behind Log Periodic Folded Slot Antennas, folded slot antennas, coplanar waveguide transmission lines as well as a review on previous publications on different aspects of log periodic antennas and time domain characterization of antennas is described in Chapter 2. Chapter 3 explains the methodology used to characterize the log periodic folded slot antenna (LPFSA) as well as the procedure used to study the antennas in the time domain. The results are presented in Chapter 4 along with an explanation of those results. Finally, the conclusions and recommendations for future work are presented in Chapter 5.

## 2 Literature Review

### 2.1 Definition of Log Periodic Antennas

Log periodic antennas are considered broadband antennas. They exhibit the same properties at frequencies  $f$  and  $\tau f$ . This is possible because the structure becomes equal to itself by a scaling  $1/\tau$  of its dimensions. Then, the antenna characteristics are a periodic function with period  $|\log \tau|$ , of the logarithm of the frequency. But they are not frequency independent antennas because they have a defined band of operation. On the other hand, a frequency independent antenna is one that has the same characteristics at all frequencies and its structure would be infinite in length. This infinite structure must be truncated in order to be a practical antenna.

### 2.2 Log Periodic Antenna Design Parameters

One of the most important parameters that describe log periodic antennas in general is presented in Equation 2.1. This parameter is known as the scaling factor. This scaling factor allows the antenna dimensions to remain constant in terms of wavelength. The condition is necessary to maintain the same impedance and radiation characteristics over a wide range of frequencies. This factor should be less than 1 and when the frequency is increased by  $1/\tau$ , the input impedance, VSWR and radiation pattern should be very similar to the values from the previous period. Equation 2.2 is related to the spacing between adjacent elements. This space shrinks when frequency increases. One way to make each cycle as similar as the preceding one is to make design parameter  $\alpha$  small (Equation 2.3) which implies that the elements are spaced more closely and more elements will be present in the active region. But one must be careful with parameter  $\alpha$  because if it is set to a value which is too small or too large it will destroy the impedance bandwidth of the antenna. If the antenna elements are placed too close together or are extremely separated the reflection coefficient increases above the -10 dB level destroying

the impedance bandwidth. A detailed design procedure for the log periodic folded slot antenna is presented in Chapter 3.

$$\tau = \frac{l_{i+1}}{l_i} = \frac{d_{i,i+1}}{d_{i-1,i}} \quad (2.1)$$

$$\sigma = \frac{d_{i,i+1}}{2l_i} = \frac{1-\tau}{4\sigma} \quad (2.2)$$

$$\alpha = \tan^{-1}\left(\frac{1-\tau}{4\sigma}\right) \quad (2.3)$$

### 2.3 Principles of Operation of Log Periodic Antennas

The bandwidth of the antenna is usually determined by the cutoff frequencies of the shorter and longest elements in the structure. The largest element with a length of  $\lambda/2$  determines the cutoff frequency at the low end. The shorter element usually has a length of  $\lambda/2$  at cutoff frequency at the higher end. Usually, more elements are added at high frequencies to ensure smooth high frequency characteristics [14].

Typically, log periodic antennas are composed of many antenna elements divided over three main regions depending on the frequency of operation. They are known as the active region, transmission region and unexcited region. The transmission region is composed of the physically smaller elements before the active region. These elements must behave as a transmission line. They are the shortest and most closely spaced elements in the array. These elements are also adjacent to the array feed point. In this region, the phase between adjacent elements is almost opposite and a negligible amount of energy is radiated by them and as a consequence the current is small. In the transmission region, the amplitude of the voltage does not change much from the voltage amplitude present at the input.

The active region is composed of elements whose length is near  $\lambda/2$  at the operating frequency. When the wave reaches the active region, the voltage decreases while the current increases. The linear increase in the current phase in the active region forces the wave in the direction of the smaller elements producing endfire radiation in that direction. The energy from the shorter active elements traveling toward the longer inactive elements decreases very rapidly. Then, a negligible amount of energy is reflected from the truncated end. The elements in the active region, larger in size, produce endfire radiation in the direction of the shorter elements because of the phase reversal between the elements. Also, there is an induced contribution between adjacent elements that adds in phase with the contribution coming from the feed line that prevents the radiation pattern to be steered in the radiation of the longer elements.

The larger elements in the antenna, the ones that must remain unexcited at a given frequency are known as the unexcited region. In the unexcited region, both the voltage and current present in the elements is negligible. This is because all the energy is attenuated in the active region and the amount that reaches the unexcited region is negligible.

The following example illustrates the concept of the active region moving throughout the antenna as frequency increases. In Figure 2.3.1, the current distribution of a log periodic folded slot antenna (LPFSA) is presented. Note that in this case, the elements in the center of the antenna are strongly excited while the other elements in the antenna are unexcited. This is expected because these are the elements that radiate the energy in the middle of the bandwidth of operation (6.87 GHz). In Figure 2.3.2, the smaller elements are excited because the frequency of operation associated with these currents is at the ending of the bandwidth of operation (10.59 GHz). Then, the active region moves in the direction of the feed as frequency increases.

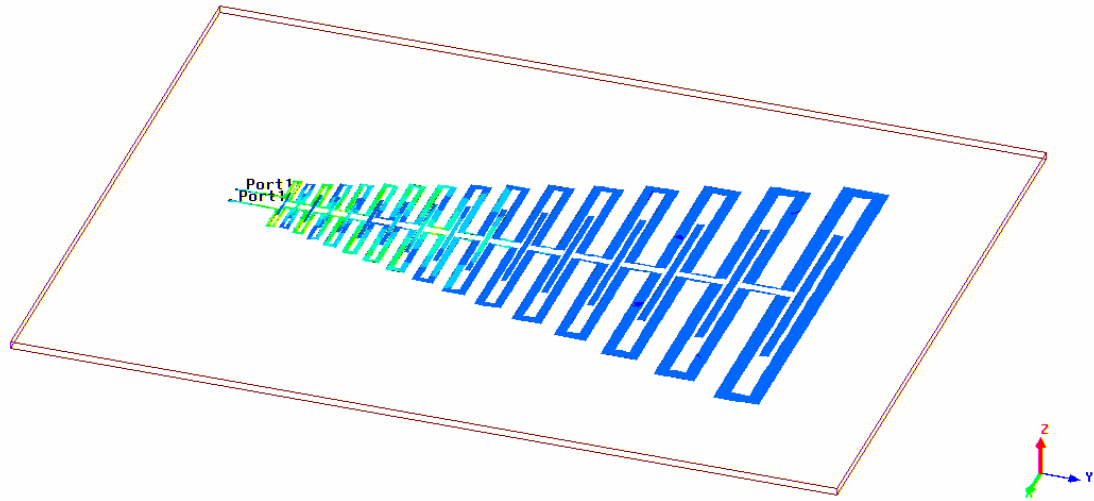


**Figure 2.3.1.** Current Distribution of LPFSA design at  $f=6.87$  GHz.

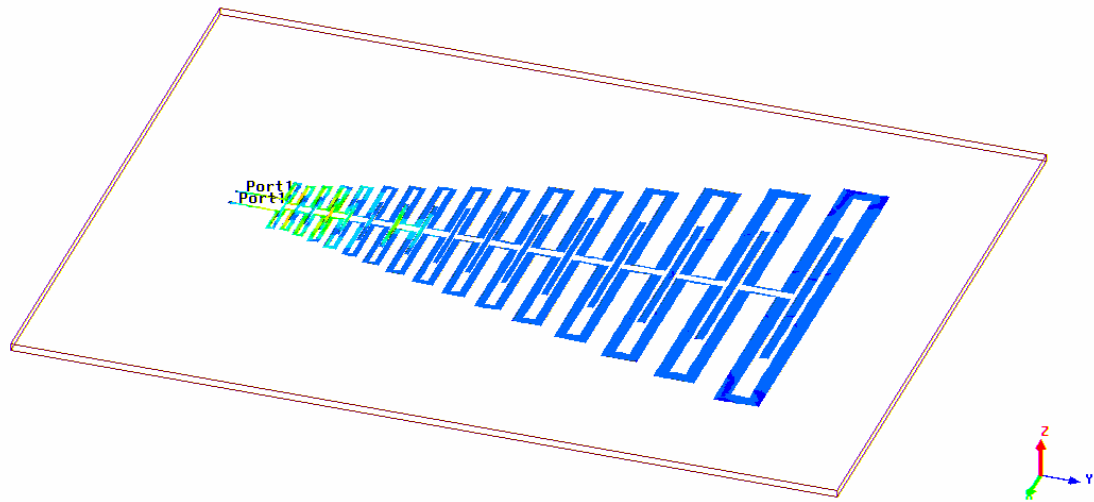


**Figure 2.3.2.** Current Distribution of LPFSA design at 10.59 GHz.

## 2.4 Log Periodic Dipole Antenna

The Log Periodic Dipole Antenna structure was introduced by Isbell [1]. It was studied extensively by Carrel [2]. In his work, he derived mathematical formulas to obtain the input impedance based on the design parameters of the log periodic dipole antenna. The formula is used for Log Periodic Dipole Antennas where the input

impedance of each element is  $Z_a = 73 \Omega$ . He said that the VSWR increases when  $Z_0$  (impedance of the feed line) increases. In contrast, he had designs with a  $Z_0 = 500 \Omega$  that worked within acceptable limits and the efficiency of the antenna increased to nearly 100%. The formula he used to obtain the input impedance of the antenna is presented in Equation 2.4.

$$R_0 = \frac{Z_0}{\sqrt{\frac{Z_0 \sqrt{\tau}}{Z_a 4\sigma} + 1}} \quad (2.4)$$

$Z_0$  – Impedance of the feed line

$R_0$  – Input Impedance of LPDA

$Z_a$  – Input Impedance of a single dipole element

One of the most famous design curves for LPDA design was computed by Carrel and is presented in Figure 2.4.1. This set of curves is based on the scale factor  $\tau$  and the relative spacing between the elements  $\sigma$  to obtain a desired gain. Later on, researchers found out that Carrel made a mistake calculating one of his formulas resulting in a 1 dB difference from the results reported by the initial design curves.

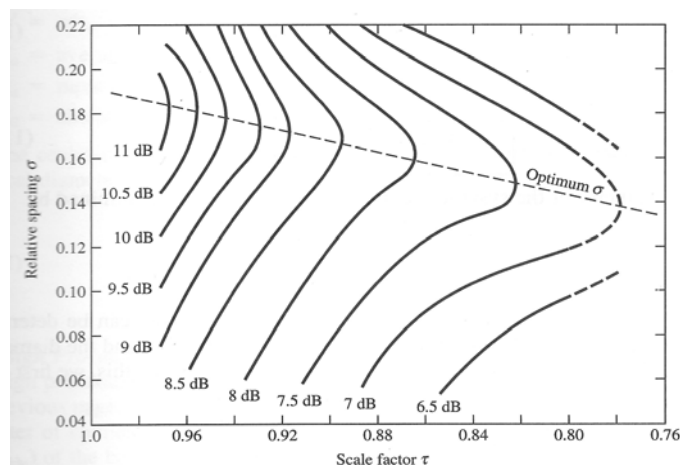


**Figure 2.4.1.** Carrell's Design Curves (Taken from [21]).

Later on, Isbell [1] said that the feeder impedance was not critical to the operation of the LPD antenna. According to Carrel, a reasonable amount of power will remain at the large end of the antenna if the impedance of the feeder line  $Z_0$  is less than  $75 \Omega$ . This “end effect” degrades the radiation characteristic of the antenna.

Du-Hammel [3] said that unexpected jumps in the phase of the reflection coefficient of the antenna when we move from  $f$  to  $\tau f$  indicated a possible end effect. This is presented in Figure 2.4.2. Here, a straight solid line is presented. That line represents the normal behavior of a LPDA without end effect. However, the dashed line presents places where the line is completely vertical. This is an indication of a possible end effect since there are  $180^\circ$  jumps in the phase of the reflection coefficient.

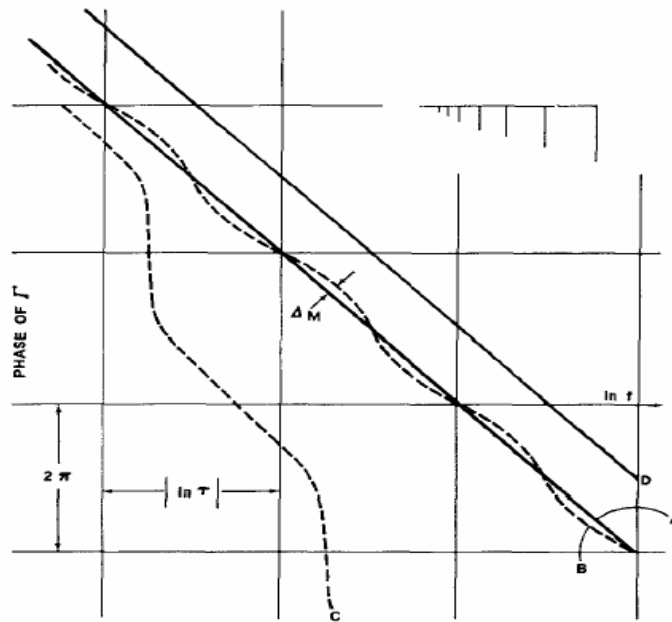


**Figure 2.4.2.** Phase of Reflection Coefficient of a log periodic circuit (Taken from [3]).

In “Optimization of Log-Periodic Dipole Antennas”, Balmain [4] stated that the anomalies present in the radiation pattern such as back lobes and side lobes of a Log Periodic Dipole Antenna would disappear if one increases the feeder impedance up to a certain point. By increasing the impedance of the feeder, the relative backlobe level

decreases. Then, Ingerson [5] stated that higher gain could be obtained from a LPDA by utilizing the antenna elements that make up the LPDA at the third or higher resonance.

The refinement process in the design LPDA continued when De Vito and Stracca [6] exposed that the number of elements that were shorter than the resonating dipole were important for small  $\tau$  values because without them a remarkable degradation of gain and the input impedance could occur. They established that the number of elements in the LPDA is given by the following formula:

$$N = 1 + N_a + \frac{\log(f_{\max} / f_{\min})}{\log(1/\tau)}, \quad N_a = N_1 + N_2 \quad (2.5)$$

$N_1$  and  $N_2$  are elements shorter and longer than the resonant element respectively.

They also said that the gain would decrease when the value of the feeder impedance increases. Finally, they stated that when  $\tau$  is kept constant and the overall length of the antenna increases the gain also increases.

Then, Ingerson [7] pointed out that the input impedance of log periodic antennas composed of monopoles and slots varies greatly with frequency. He reasoned that this was due to reflections between the antenna feed point and the active region of the antenna. Specifically, he said that there was a stop region and this region reflected a portion of the energy at the generator at the feed point preventing the energy from reaching the elements near resonance. This caused the log periodic slot antenna to have a high VSWR. To solve the problem, he proposed a modulated impedance feeder, this means that the impedance of the feeder line is going to change from antenna element to antenna element. Finally, he said that since the slots acted as series inductive elements, they had to be separated considerably from one another to improve radiation characteristics.

An interesting optimization approach for LPDA is presented in [15]. Using a combination of a genetic algorithm along with a Nelder-Mead Downhill Simplex algorithm a hybrid algorithm for optimization is created. The optimized LPDA dimensions show that for the optimum design the scaling factor is not constant. In Figure 2.4.3, a table shows the dimensions of each element of the optimized design. The gain variations and the standard deviation of the VSWR across the passband are reduced with the optimization procedure. Recent studies show that the use of a frequency dependent scaling factor yields better back to front ratios that when a constant scaling factor is used.

Initial 7 element LPDA design, $\tau=0.9$ and $\sigma=0.17$				
Element	Initial design	Optimized		
		Nelder-Mead	GA	GA & Nelder
L1	0.1875	0.1584	0.1982	0.1584
R1	0.005	0.0058	0.0064	0.0058
L2	0.1688	0.1516	0.2168	0.1516
R2	0.005	0.0046	0.0090	0.0046
L3	0.1518	0.1086	0.1520	0.1086
R3	0.005	0.0157	0.0089	0.0157
L4	0.1367	0.1234	0.1366	0.1234
R4	0.005	0.0055	0.0088	0.0055
L5	0.1230	0.1032	0.1230	0.1032
R5	0.004	0.0039	0.0054	0.0039
L6	0.1107	0.0924	0.0950	0.0924
R6	0.003	0.0027	0.0045	0.0027
L7	0.0996	0.0934	0.0836	0.0934
R7	0.003	0.0001	0.0017	0.0001
S1	0.0638	0.0731	0.0607	0.0731
S2	0.0574	0.0404	0.0571	0.0404
S3	0.0516	0.0607	0.0516	0.0607
S4	0.0465	0.0413	0.0542	0.0413
S5	0.0428	0.0399	0.0346	0.0399
S6	0.0376	0.0481	0.0471	0.0481
Gain	8.0673	8.7606	8.0781	8.9040
STD(gain)	1.0326	0.3206	0.3363	0.2816
VSWR	1.8232	1.1051	1.0864	1.0114
STD(VSWR)	0.6935	0.0611	0.0415	0.0110

**Figure 2.4.3.** Dimensions of LPDA using different optimization methods (Taken from [15]).

## 2.5 Log Periodic Slot Antennas and Feed Types

The design procedure of a LPSA is described in [16]. The structure presented in the paper is presented in Figure 2.5.1. A coplanar waveguide line is used to feed the antenna and slot antennas act as the antenna elements. The length of the individual elements in the antenna array is  $\lambda/8$  at their resonant frequency. In this configuration, a bandwidth between 33% and 48% can be obtained depending on the number of slot elements. These antennas were designed on substrates with  $\epsilon_r= 2.2, 10.2$ . The return loss response for LPSA with a scaling factor between .75 and .95 can be observed in Figure 2.5.2.

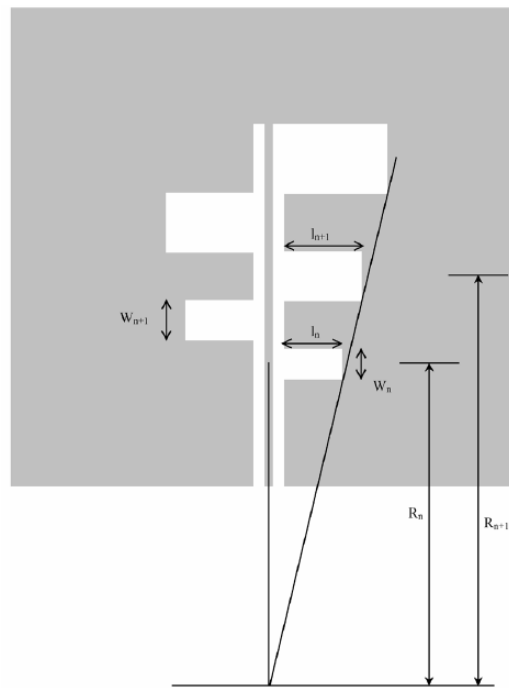


**Figure 2.5.1.** Log-Periodic Slot Antenna Configuration (Taken from [16]).

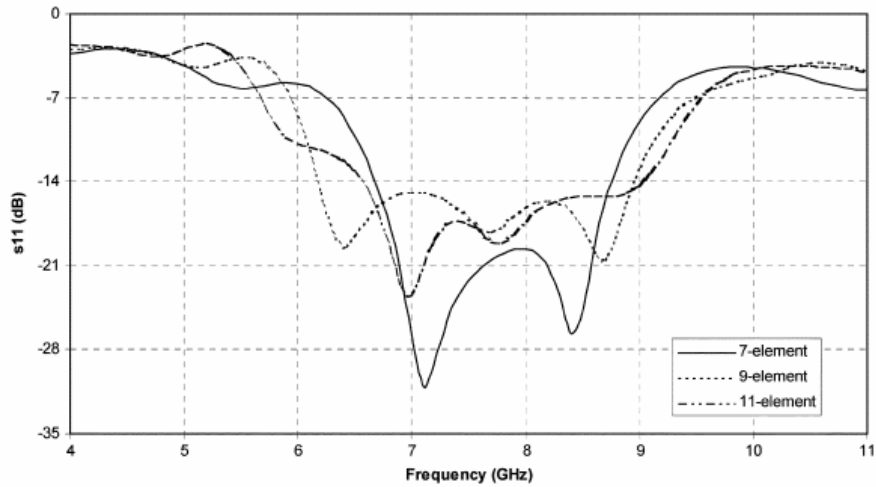


**Figure 2.5.2.** Return Loss Response for different LPSA designs (Taken from [16]).

A log periodic antenna design composed of slots and a microstrip feed is presented in [17]. In this case, the LP antenna is designed using two layers. The first layer is a cavity with slots etched on top. The second layer has a substrate with an  $\epsilon_r = 6.15$ . The antenna is fed using a microstrip line based on the modulated impedance feeder from Ingerson [7] where the characteristic impedance of the feed line exhibits a step change to a lower value near the slots. The configuration is presented in Figure 2.5.3.

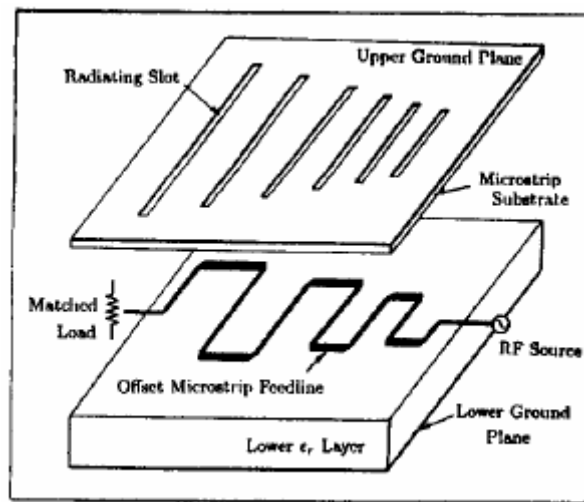


**Figure 2.5.3.** Geometry of the microstrip-fed log-periodic slot array (Taken from [17]).

A novel feed network has been proposed in [11]. Each antenna element in the LPDA is fed independently as presented in Figure 2.5.4. Note that a corporate feed is used to excite the elements with different line lengths. The lengths are adjusted to make the elements to have an independent adjustable time delay. Then, the wave reaches all the elements in the antenna at the same time. This feed is designed for pulse transmission. Transmission of clean pulses for radar and communication applications is possible because the different frequency components of the pulse are transmitted at the same time.

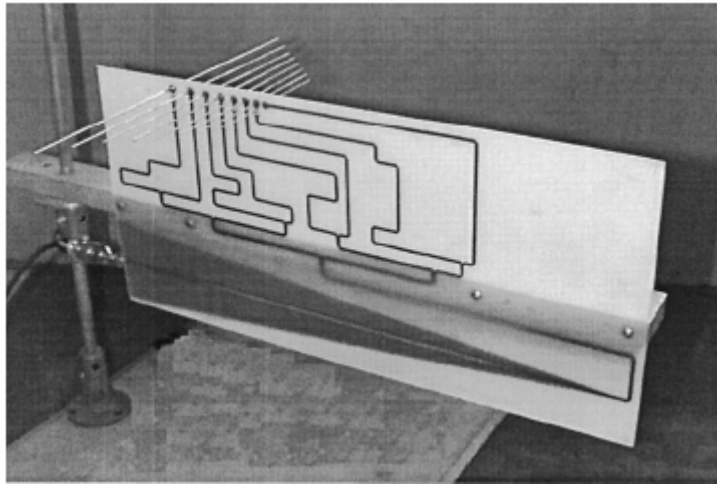


**Figure 2.5.4.** LPDA with each element fed separately (Taken from [11]).

## 2.6 Applications of Log Periodic Antennas

Applications of log periodic antennas have been limited to frequency domain applications. They have been used in a couple of applications because of its wide bandwidth and high directivity. Log periodic antennas have been used as a low cost alternative to conventional VHF / UHF antennas based on the Yagi-Uda Antenna. They also have been used for electromagnetic interference (EMI) testing and electromagnetic compatibility (EMC). Such applications include ANSI C63.4, FCC-15, FCC-18, EN 55022 emissions testing and IEC 61000-4-3 immunity testing. For EMC applications it is necessary that the antenna to have a high power rating to generate the field levels needed

for immunity tests and high gain. Likewise, for EMI applications a sensitive antenna like the log periodic is necessary to pick up unwanted RF and measure the strength of interfering fields. When combined with a monitoring receiver, log periodic antennas make it possible to intercept unauthorized radio transmitters or to determine the angle of incidence (direction finding) and the polarization plane and of electromagnetic waves. For communications applications in the frequency domain, log periodic antennas are popular because its high directivity allows the signal to be concentrated into a specific area without wasting energy on the outskirts. Finally, they can be used as a transmit antenna in the entire frequency range.

## **2.7 Time Domain Analysis of Antennas**

Ultra wide band antennas represent just one of the multiple efforts in the last couple of years to expand the bandwidth of home networks. Ultrawide band signals are wide signals in frequency but very narrow in the time domain. Examples of recent UWB antennas can be found in [18]. These antennas need to be capable to transmit clean short pulses in 15 different bands of 500 MHz present between 3.1 GHz and 10.6 GHz. UWB signals produce an ultra-wide spectrum with zero dc content. The need to analyze the performance of these UWB antennas in the time domain has spawned different methods to verify antennas capabilities in the time-domain. The following paragraphs present just a few examples on time domain analysis for antennas.

In [8] Sorgel performed a time domain analysis on antennas that are usually associated with frequency domain applications. The structures analyzed were the Vivaldi antenna and the LPDA. The study concluded that the Vivaldi antenna seemed well suited for the transmission of clean pulses whereas the LPDA seemed more suited for modulation schemes such as Orthogonal Frequency Division Multiplexing since the scheme uses a large set of independent sub carriers that do not to maintain a fixed phase difference, something critical for the transmission of clean pulses. The impulse response

of the LPDA from the study can be seen in Figure 2.7.1. There are so many peaks that is impossible to discern the shape of the original signal.

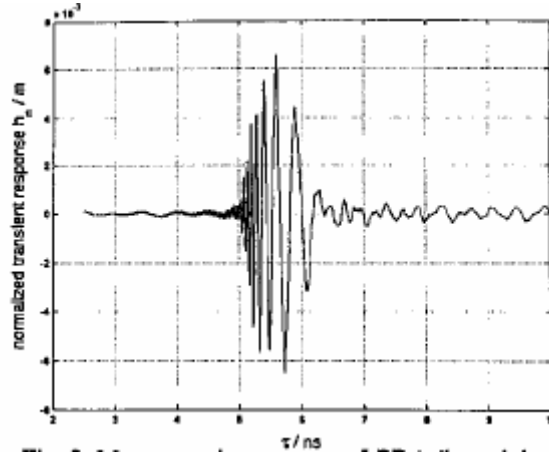


**Figure 2.7.1.** Impulse Response of LPDA (Taken from [8]).

For time domain applications it is important to know if the receiving antenna can receive the pulses or the waveform with the less distortion possible. In [9] Pozar develops a procedure to analyze antennas in the time domain and talks about how we can maximize and optimize the received waveform. The procedure develop by Pozar is used to find the transfer function of the antenna. The transfer needs to be flat against frequency and provide linear phase to ensure the transmission of clean pulses. The transfer function presented in the paper relates the receive antenna load voltage to the generator voltage at the transmit antenna. The receiving antenna with input impedance  $Z_R(\omega)$  is terminated with load impedance  $Z_L(\omega)$ . The receive antenna load voltage present through  $Z_L(\omega)$  is calculated with a simple voltage divisor as shown in formulas 2.6 and 2.7. The transfer function  $H_{LG}(\omega)$  can be obtained from the formulas presented below.  $V_{oc}(\omega)$  is defined as  $V_{oc}(\omega) = \bar{h}(\omega) \square \bar{E}(\omega)$  where  $\bar{h}(\omega)$  represents the effective height and  $\bar{E}(\omega)$  is the electric field incident at the receive antenna.

$$V_L(\omega) = \frac{V_{oc}(\omega)Z_L(\omega)}{Z_L(\omega) + Z_R(\omega)} \quad (2.6)$$

$$V_L(\omega) = H_{LG}(\omega)V_G(\omega)e^{-j\omega r/c} \quad (2.7)$$

In [19], ultra wide band signal transmission is explored in the EHF Band. Specifically, ultra short pulse transmission at 60 GHz is studied. The study focuses in the atmospheric absorptive and dispersive effects on pulse propagation delay, pulse width and distortion given those absorption resonances of oxygen occur at 60 GHz. A transfer function is derived based in the transmitted Electric Field and the received Electric Field. The transfer function allows us to calculate the impulse response of the receiving antenna to determine the atmospheric effects on the transmitted signal. This transfer function takes into account the complex refractivity of the molecules composing the air. Equation 2.8 present the transfer function derived on [19]. The transmitting and receiving links represented as a linear system to be able to calculate the transfer function is presented in Figure 2.7.2.

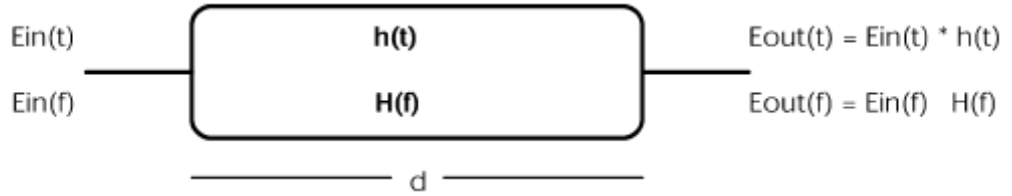


**Figure 2.7.2.** Linear system representing propagation of electromagnetic waves in a medium (Taken from [19]).

$$H(f) = \frac{d_0}{d_0 + d} e^{-j[\alpha(f) + j\beta(f)]d} \quad (2.9)$$

$$\alpha(f) = \frac{2\pi f}{c} N_i(f), \quad \beta(f) = \frac{2\pi f}{c} [1 + N_r(f)] \quad (2.10)$$

$N_r(f)$  and  $N_i(f)$  are the real and imaginary parts of the medium complex refractivity, respectively. The received electric field is presented below.

$$E_{out}(f) = \frac{1}{2} \vec{A}_m(f - f_0) H(f) + \frac{1}{2} \vec{A}_m^*[-(f + f_0)] H^*(f) \quad (2.11)$$

The study assumes that pulse amplitude modulated signals are transmitted. Finally, the results of the study indicate that pulse distortion and propagation delay effects are pronounced at 60 GHz where high absorption of oxygen molecules occurs. Therefore, pulse transmission at 60 GHz is impossible.

In [23], the traditional parameters that describe the behavior of the antenna in the frequency domain are calculated for the time domain. They declare that a high fidelity antenna, one that can transmit clean short pulses need that the normalized cross correlation of how accurately the time integral of the transmitted field reproduces the behavior of the voltage applied to the antenna terminals in the transmitting case should be around .85. For the receiving case, the antenna fidelity is a measure of how accurately the received voltage available at the antenna terminals reproduces the behavior of the transient field incident upon the antenna. This combined with the antenna's effective area and the directivity gives an impression of the fidelity of an antenna for time domain applications.

In the study, a TEM horn and a resistively loaded TEM horn antenna are analyzed to determine their fidelity for pulse transmission. The correlation between the receive response of TEM horn antennas and the incident waveform as a function of angle in the H-plane is presented in Figure 2.7.3. Notice that the TEM horn is good for a beamwidth of 30 degrees (between 0° and 30°) and the resistively loaded TEM horn antenna is good between 150° and 180°. The phase response of the received signal becomes nonlinear outside these areas.

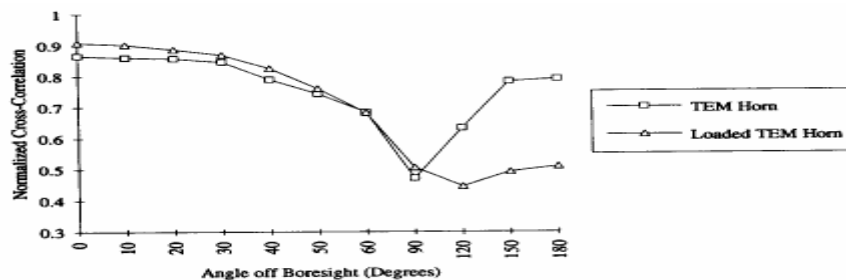


**Figure 2.7.3.** Correlation between the receive response of TEM horn antennas and the incident waveform as a function of angle in the H-plane (Taken from [23]).

A characterization for short pulses antennas in the time domain is presented in [24]. The received voltage in the time domain is expressed as the convolution between the effective height and the incident electric field in the antenna after a rigorous derivation. The result obtained is similar to those presented by Pozar in [9].

The dispersive behavior of the LPDA caused by the nonlinearity in the phase of the radiated field as shown by a formula presented in [10]. That formula is presented below.

$$\phi(\omega) = \frac{\pi}{\ln \tau} \ln \left( \frac{\omega}{\omega_i} \right) \quad (2.12)$$

To solve the problem, the authors proposed to feed the antenna from the larger elements, the ones that carry the low frequency components of the transmitted signal. The antenna continues to radiate in the direction of the smaller elements because a non-transpose feed is used. Therefore, the 180° phase difference between antenna elements present with the transposed feed of traditional LPDA designs is lost. The new feed arrangement causes the incident energy to find electrically large elements between the feed and the principal active region. If the bandwidth is large enough, the antenna will find higher order active regions between the feed and the principal active region. The dispersive behavior of the antenna is eliminated with the new feed arrangement but the gain varies between 10 and 2 dB against frequency which is the typical case for antennas designed for UWB applications.

## 2.8 Log Periodic Folded Slot Antenna

This work will be based on the analysis of different configurations of the log periodic folded slot antenna. The log periodic folded slot antenna (LPFSA) is a member of the family of log periodic antennas. The principle of operation for log periodic antennas was described on Section 2.2. A 3-D view of a LPFSA is presented in Figure 2.8.1. Like others in the log periodic family, a LPFSA is not a frequency independent

antenna because it has a defined band of operation. The purpose of this work is to improve the radiation pattern and the impedance bandwidth of the antenna by using DOE Techniques. The next sections describe the principles of operation behind the feed type used and the individual antenna elements that compose the antenna. Finally, an introduction to DOE is presented.

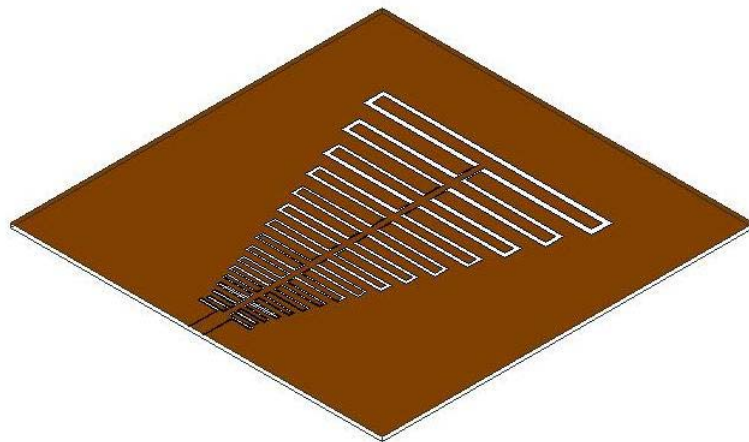


**Figure 2.8.1.** 3-D view of LPFSA configuration.

Previous work on log periodic folded slot antennas can be found at [40] and [14]. Scherer [40] fabricated and tested a large number of log periodic folded slot array antennas over a frequency range between 2 to 12 GHz. He varied the scaling factor between 0.58 to 0.90 and  $\alpha$  was varied from 20 to 35°. The configuration shown in Fig 2.8.2 includes a parasitic slot which helps to stabilize the radiation pattern using a parasitic slot length between  $\alpha/3$  to  $1.5\alpha$ . If the slot length is outside the range or if there is no parasitic slot at all, Scherer found out that the pattern backlobe and sidelobes increased under those circumstances. The design also employs a modulated impedance feeder for the central line that connects all the elements. This means that the impedance of the feeder line is going to change from antenna element to antenna element to eliminate the reflections present between the feedpoint and just before the active region causing the antenna to exhibit a high VSWR if the problem is not eliminated. The work also compares the log periodic folded slot with a log periodic folded monopole.

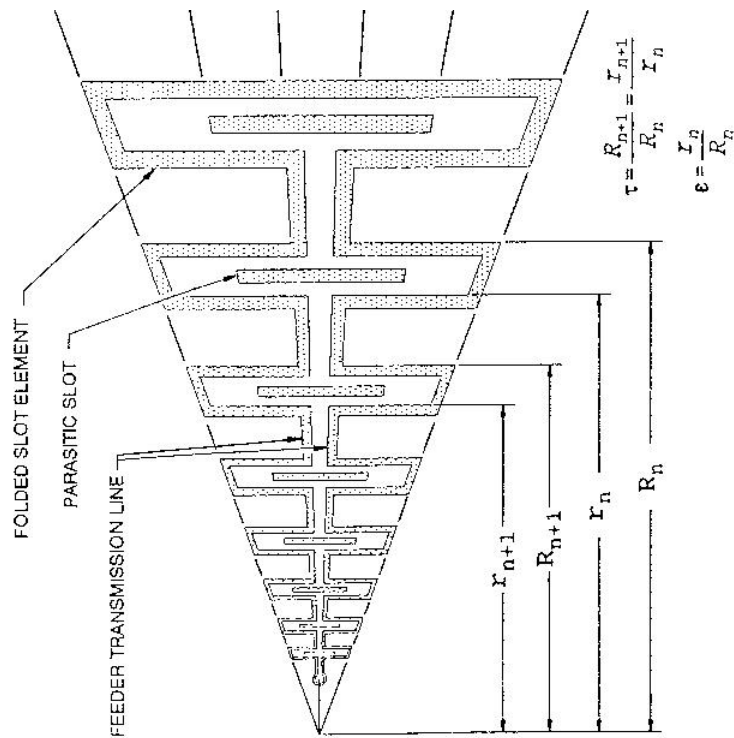


FIG. 14-37 Log-periodic folded-slot array: outline and parameters.

Figure 2.8.2. Log Periodic Folded Slot Array (Taken from [25]).

In [14], the LPFSA was used to build phased arrays. In this case, if the individual elements in a LPFSA are  $\lambda_g/4$  above the ground, a scanning between  $0^\circ$  and  $30^\circ$  from zenith are achieved with small losses in gain. If the scanning angle is increased then more losses are present.

## 2.9 Coplanar Waveguide Transmission Lines

The CPW line consists of two slot lines and a central conductor on top of a substrate. The width of the slots and the central conductor will determine the characteristic impedance of the line. A narrow center conductor with wide slot lines is associated with a line with high impedance. Meanwhile, a wide center conductor and narrow slot lines is associated with a line with low impedance. Coplanar waveguide lines are popular because there is no need for via holes and can be integrated easier with active devices. They have been used to feed all different kinds of antenna configurations [26].

A coplanar waveguide is depicted in Figure 2.9.1. The height of substrate  $h$ , the width of the central conductor  $w$  and the width of the gap  $g$  are the dimensions that describe a CPW line. The cover (gray) is metal, usually copper.

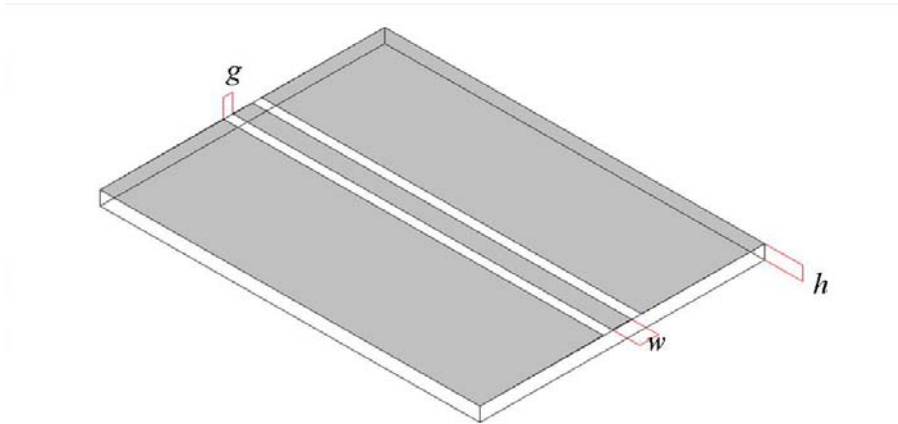


**Figure 2.9.1.** Coplanar Waveguide Line and Dimensions.

The center conductor present in a CPW line allows the transmission line to be excited in two different ways [26]. One excitation mode occurs when the fields on the apertures are in phase (slotline mode). Slotline mode is usually short-circuited with placement of air bridges (due to high radiation losses). The other excitation mode is when the fields on the apertures are  $180^\circ$  out of phase (CPW mode). The two excitation modes for CPW lines are presented in Figure 2.9.2.

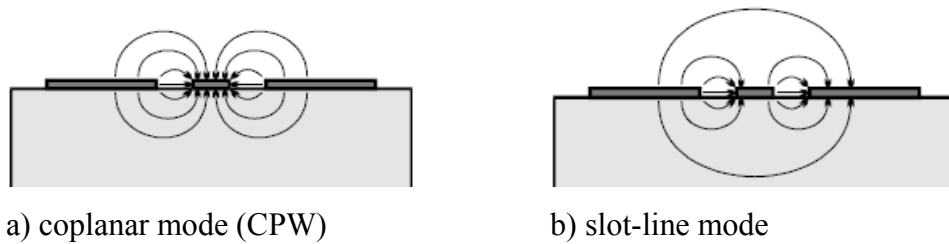


**Figure 2.9.2.** Coplanar Waveguide Excitation Modes. (Taken from [26]).

## 2.10 Log Periodic Folded Slot Antenna Feedline

The feed line of the LPFSA is a coplanar waveguide line. The CPW feed line is an advantage because it provides a  $180^\circ$  phase shift between the elements. Therefore, a  $180^\circ$  phase shift is introduced to the terminal port of each element in the antenna array. This phase shift is required for proper operation of the antenna array because without the mechanism, interference in the pattern occurs because the smaller elements produce an endfire beam in the direction of the longer elements. There is no interference in the direction of the smaller elements because most of the energy is dissipated in the active region. Then, a negligible amount of energy reaches the longer elements is unable to interfere in the direction of the smaller elements.

## 2.11 Folded Slot Antenna

The folded slot antenna is the building block of the LPFSA. They are useful at 2<sup>nd</sup> resonance because the input impedance can be matched to 50 ohms easily [22]. This resonance occurs when the perimeter of the antenna is equal to  $\lambda_g$  at the desired resonant frequency. Figure 2.11.1 presents the folded slot antenna and its dimensions.

The perimeter of the antenna is essential to determine the resonant frequency. Different perimeters are defined in [22] but one of the most common equations to determine the perimeter of the antenna is presented in equation 2.13.

$$C = 2(L_a + S_a + W_{a2} - W_{a1}) \quad (2.13)$$

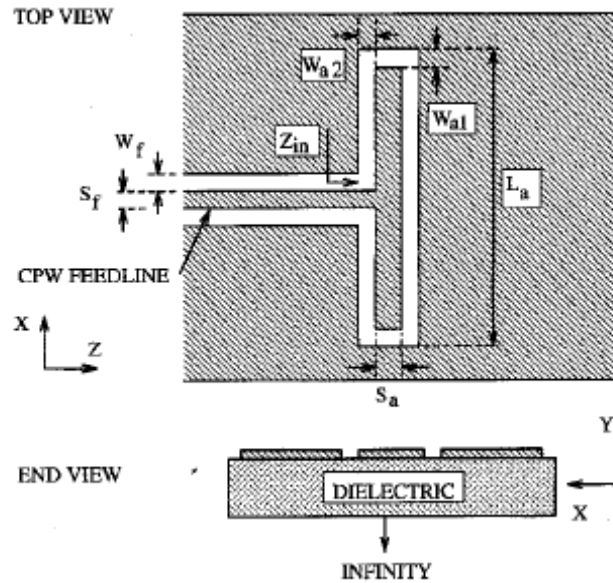


**Figure 2.11.1.** Folded Slot Antenna configuration and its dimensions (Taken from [20]).

In [12] and [13], the folded slot antennas are analyzed using the FDTD method using a Gaussian pulse as excitation. They point out that the waveform reaching the antenna can be different from the one launched due to effects of radiation loss and dispersion. The study mentions that the input impedance is an increasing function of thickness and dielectric constant until  $h/L$  reaches 0.2 ( $h$  is the substrate thickness and  $L$  is the length of the slot), after that the impedance decreases. This can be observed in Figure 2.11.2. In this case, for a substrate with  $\epsilon_r = 10.8$ , the input impedance varies between 100 and 500 ohms. The range where the input impedance varies is reduced when  $\epsilon_r$  decreases. Back to figure 5, the shaded region establishes that there was no well defined resonance with this substrate. When a substrate with  $\epsilon_r = 2.2$  is used, the no self resonance region disappears. Therefore, the resonant impedance of the antenna varies with substrate parameters.

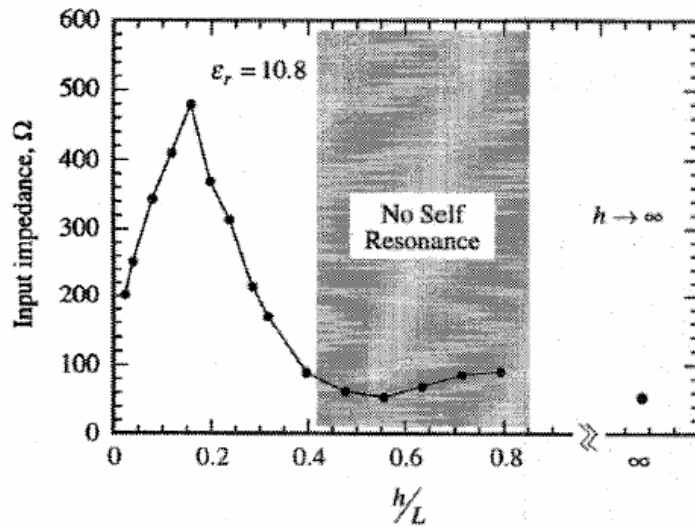


**Figure 2.11.2.** Input Impedance of Folded Slot Antenna designs as function of substrate thickness (Taken from [13]).

A novel impedance matching technique is discussed in the paper. The technique consists of adding additional folded slot elements until the input impedance goal is reached. The input impedance is calculated with the  $Z_{in} = Z_{slot} / n^2$ . The impedance will decrease as more elements are added. The desired field distribution for a folded slot antenna is shown in Figure 2.11.3. The folded slot has its electric field polarized in the direction perpendicular to the slot length. The desired operating mode of this antenna is when the fields in both slots are in phase.

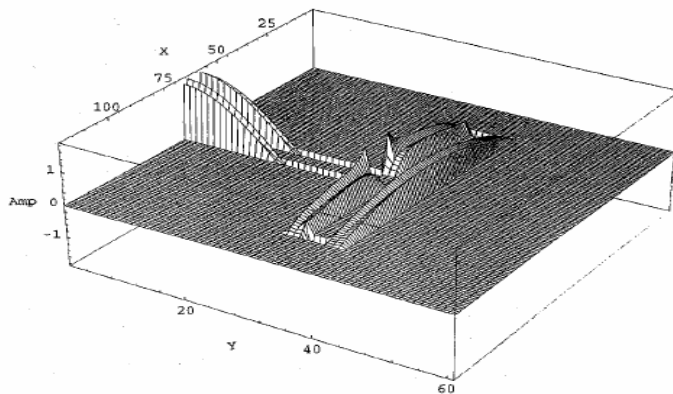


**Figure 2.11.3.** Ideal field distribution of folded slot antenna (Taken from [13]).

Meanwhile, in [20] is said that the radiation characteristics of a FSA is similar to magnetic dipoles. The radiated power into the substrate is proportional to  $\epsilon_r^{1.43}$  at first resonance. The circumference of the antenna should be near  $1 - 1.04 \lambda_g$  to obtain a good response. It is mentioned that by making the slots wider variations in input impedance are reduced and for good performance  $W_{a2} = \lambda_g/60$ . The separation between slots should be small to maintain low cross-polarization levels.

In [22], a full characterization of folded slot antennas is performed using Design of Experiments techniques. The researchers found out that the input impedance at 2<sup>nd</sup> resonance can be lowered by increasing the top slot dimensions. Also, they found out that the resonant frequency can be predicted with a high degree of confidence using the effective permittivity of the antenna. 1<sup>st</sup> and 3<sup>rd</sup> resonances are also discussed and ways of matching the antenna at this reference are also given.

## **2.12 Design of Experiments**

According to Isixsigma [28], A Design of Experiment (DOE) is a structured, organized method for determining the relationship between factors (Xs) affecting a process and the output of that process (Y). The method helps to identify the vital few sources of variation in a process. It also quantifies the effects of the important input factors (Xs) including their interactions.

The main objective of an experiment is to determine the effect that a condition in the experiment has on the output every time is modified. After the experiment is completed and analyzed, a model that describes the output is developed. The model gives insight into the behavior of the process under study when the output of a process is not widely understood. In the next few paragraphs, a general description of Design of Experiments is presented.

An Analysis of Variance (ANOVA) allows us to evaluate the effects that a specific input factor has on the output of the process. It also allows us to evaluate the consistency of the model that describes the output of a process. It works under the following assumptions. The first assumption is that residuals are independent. Second, the residuals must be distributed normally with a mean equal to zero and constant variance. One way to determine if one factor affects the response is to compare the variances of the factor and the error. The factor under study is important to the process if the variance of the factor is big when compared to the variance of the error. To check for the consistency of the model one could do it by observing a couple of graphs. A good sign of a successful experiment is when the normal plot of residuals shows that the residuals follow a normal distribution. A sample graph can be observed in Figure 2.12.1.

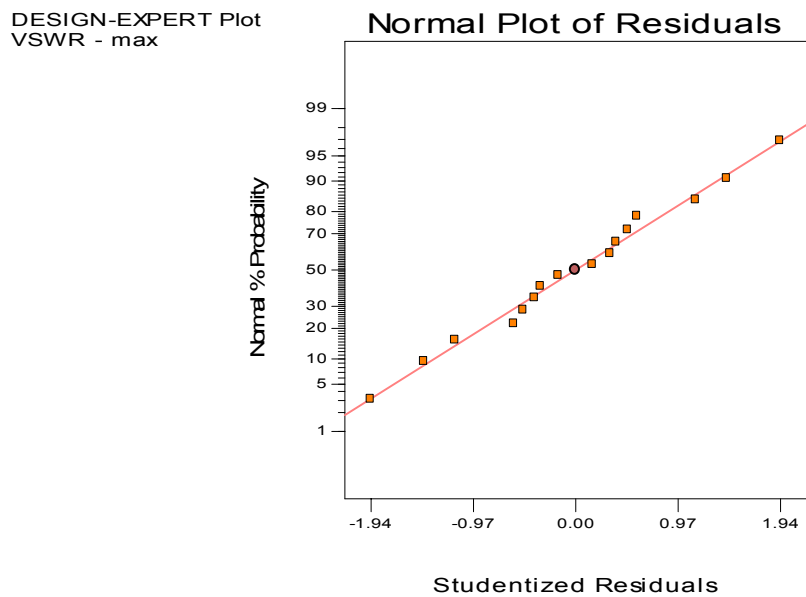


**Figure 2.12.1.** Normal Plot of Residuals.

Another way to check the consistency of the model is to check the errors versus order of the experiment plot. The plot must show a random behavior. The experiment needs to be redesigned again if the plot shows a pattern like a linear or quadratic behavior. This means that there is an unknown source that affects the response in the

experiment. A sample  $2^4$  factorial experiment produces the residuals versus run plot presented in Figure 2.12.2 showing random behavior.

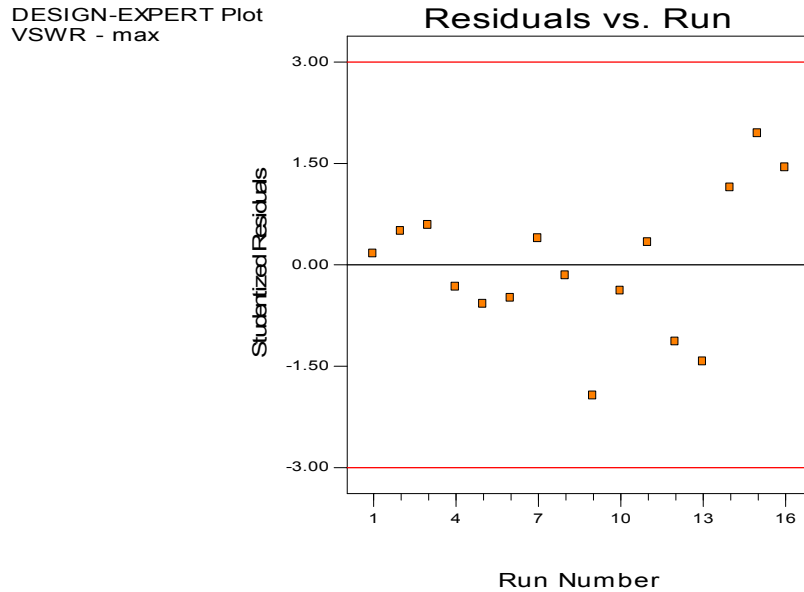


**Figure 2.12.2.** Residuals versus Run Number Plot.

Another way to check the consistency the model is the plot of the residuals versus each of the factors in the experiment. A successful design is one where the small to the large range is less than two times. Figure 2.12.3 presents the expected behavior.

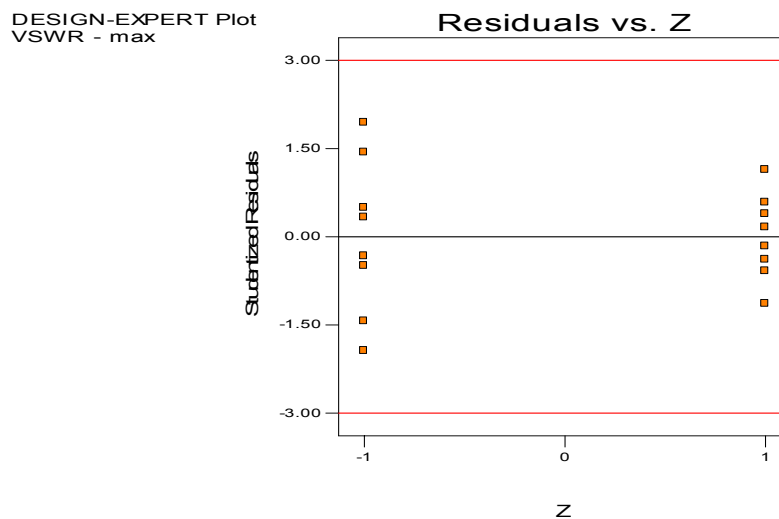


**Figure 2.12.3.** Residuals versus factor Z(impedance of the feeder line)

Finally, one needs to check the plot that shows the observed values versus the predicted values to identify the outliers in the experiment. Figure 2.12.4 shows the predicted versus actual values of a sample experiment.

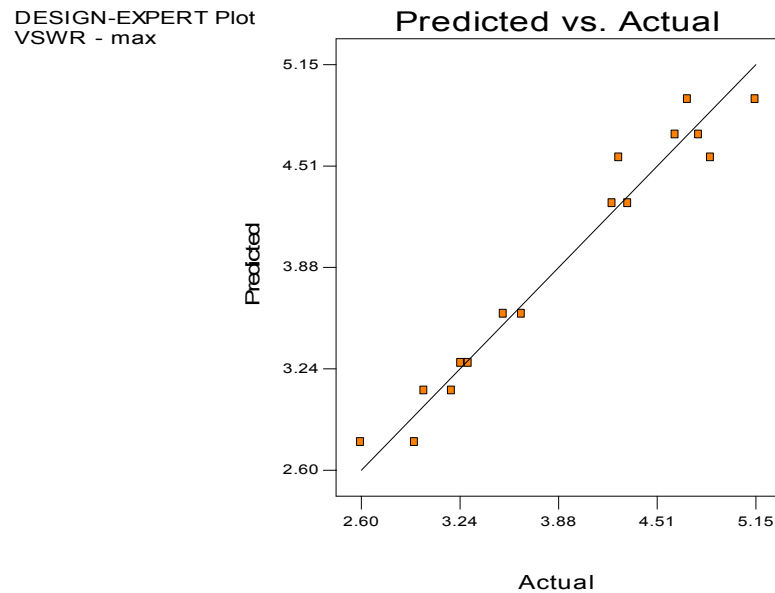


**Figure 2.12.4.** Predicted versus Actual values.

There is a very special category of experiments called factorial experiments. They have two or more factors of interest. Factorial experiments are conducted in random order to try to cancel out the effect of a factor that has not been considered in the experiment (not an input factor). Factorial designs are more efficient than to vary one factor at once because the interactions between factors are evaluated. The number of runs needed for a particular experiment is determined by the levels used to evaluate each factor and the factors to be studied. Then for a particular experiment the number of runs is given by  $n^k$  where  $n$  is the number of levels for each factor and  $k$  is the number of factors.  $2^k$  experiments are very typical where a low level and a high level are considered for each factor. It is assumed that the behavior to be analyzed with  $2^k$  experiments is linear. Central points are used to detect if the assumption of linearity is reasonable.

There are two ways to calculate the model for factorial designs that predicts the behavior of a response under study. The first one is using analysis of variance (ANOVA). One or more repetitions of the experiments are needed to estimate the error with ANOVA. Analysis of variance is used for experiments with qualitative input factors.

The other approach is a linear regression model. Regression is used with quantitative input factors. In this approach, the model of the process is obtained by the operation  $\bar{b} = (X'X)^{-1}X^{-1}y$ , where  $\bar{b}$  is a vector with the model coefficients,  $y$  is the experiment's result and  $X$  is the design matrix. The design matrix columns are determined by the number of coefficients to be estimated and its rows by the number of results. For example for a  $2^2$  factorial experiment, the design matrix dimensions would be 4 by 4. A factorial design is structured in a way that guarantees that when  $(X'X)^{-1}$  is calculated the result obtained is a diagonal matrix with zeros everywhere except on the diagonal. The design matrix for a  $2^2$  factorial experiment is presented below, along with the  $(X'X)^{-1}$  matrix. Note that the  $(X'X)^{-1}$  is a diagonal matrix as predicted.

$$X = \begin{bmatrix} 1 & -1 & -1 & 1 \\ 1 & 1 & -1 & -1 \\ 1 & -1 & 1 & -1 \\ 1 & 1 & 1 & 1 \end{bmatrix} \quad (X'X)^{-1} = \begin{bmatrix} 1/4 & 0 & 0 & 0 \\ 0 & 1/4 & 0 & 0 \\ 0 & 0 & 1/4 & 0 \\ 0 & 0 & 0 & 1/4 \end{bmatrix}$$

The matrix  $X$  presented above is filled with -1 and 1 because coded factors are being used. For example, if factor A is a dimension of an antenna where:

$$A_{low} = 0.9 \text{ mm}$$

$$A_{high} = 1.4 \text{ mm}$$

$$\bar{A} = 1.15 \text{ mm}$$

Then,

$$X_{A_{low}} = \frac{A_{low} - \bar{A}}{\frac{range\{A\}}{2}} = \frac{.9 - 1.15}{\frac{.5}{2}} = -1 \quad (2.14)$$

$$X_{A_{high}} = \frac{A_{high} - \bar{A}}{\frac{range\{A\}}{2}} = \frac{1.4 - 1.15}{\frac{.5}{2}} = 1 \quad (2.15)$$

The factor has been codified and now the low level of A is known as -1 and the high level is associated with 1. All the factors in the experiment are codified with -1 for the low level and 1 for the high level.

An example of a model calculated by the linear regression method is presented below. The design of experiment consists of a  $2^3$  factorial experiment for a total of 8 runs. In this case, a process is being evaluated where factors A, B, C are believed to describe the output response of the process. The factors A, B, C are evaluated along with their interactions. The table below establishes the state of each factor for a particular run. Factors A, B, C could be anything. In the case of an antenna, factor A could be dimension in mm and factor B the characteristics of the substrate. It is then important to code the factors uniformly, -1 when the factor is set to the low level and 1 when it is set to the high level. In this way, the contributions that the factor and interactions make to the output of the process can be evaluated easily. While working with factors uniformly coded, the magnitude of the coefficients helps to easily identify which factors or combination of factors that affect the response positively or negatively.

**Table 2.1.**  $2^3$  factorial experiment design table.

Experiment	A	B	C
1 (000)	1	1	1
c (001)	1	1	1
B (010)	1	1	1
bc (011)	1	1	1
a (100)	1	1	1
ac (101)	1	1	1
ab (110)	1	1	1
abc (111)	1	1	1

The linear regression model for a  $2^3$  design is presented below.

$$y = b_0 + b_1X_A + b_2X_B + b_3X_AX_B + b_4X_C + b_5X_AX_C + b_6X_BX_C + b_7X_AX_BX_C + \varepsilon \quad (2.16)$$

This model describes the observed response with 100% accuracy. But not all the factors and interactions affect the response with the same weight. To establish which factors affect the response the most, a half normal probability plot is used. A normal probability plot is presented in Figure 2.12.5.

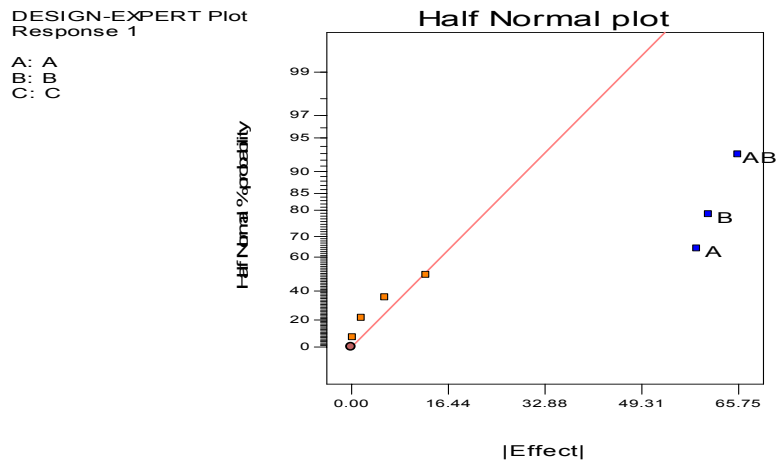


**Figure 2.12.5.** Half Normal Plot of Example.

Note that in this case factors A, B and the interaction of AB appear separated from the rest of the runs. The other runs all fall on a straight line with a normal

distribution of mean equal to zero and constant variance. This is the case because factors A, B and AB are the ones that affect the output of the process the most.

Therefore, the regression model could be reduced to just a few terms. This is presented below.

$$y = 40 + 6X_A - 4X_B + 8X_A X_B \quad (2.17)$$

The model is simplified and to check the consistency of the simplified model, one must be certain that the values predicted by the simplified model are similar to the observed values of the process. The equation presented above shows that factor A affects the output response more than factor B does. It also shows that the interaction between factors A and B is more important than the contributions from factors A or B alone because the magnitude of the coefficient before the term  $X_A X_B$  is larger than the magnitude of the coefficients before terms  $X_A$  or  $X_B$ . Simply put, the simplified model presented above allows us to understand the way that the input factors should be manipulated to get the desired output response. It also allows us to understand the effects that the input factors have on the output of the process.

Design of Experiments involves many other things that were not presented here. A good reference on the DOE Topic is Design and Analysis of Experiments, 5<sup>th</sup> Edition by D.C. Montgomery [27].

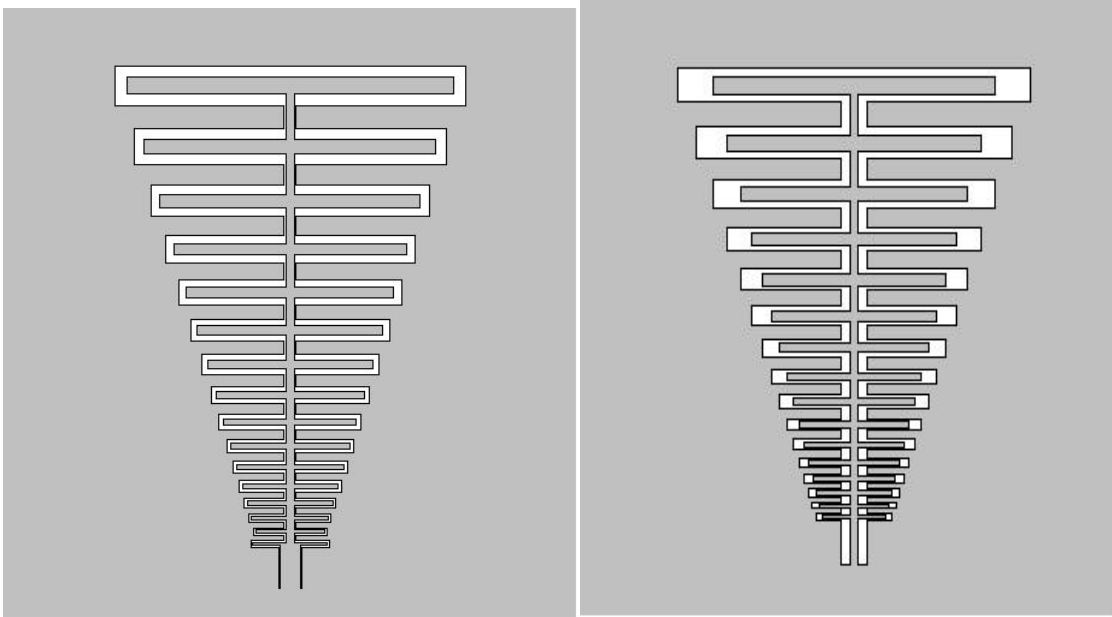
## 3 Methodology

### 3.1 Purpose

It is of great interest to model and experimentally verify the performance of different LPFSA configurations. It is desirable to identify the factors that affect the frequency response and radiation pattern of the antenna and ways to improve them. This will be achieved using Design of Experiments techniques. Also, the antennas will be analyzed on the time domain to verify the fidelity of short pulse transmission.

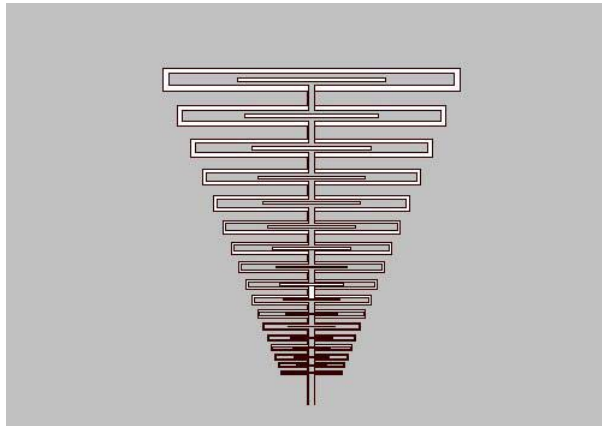
The structures to be analyzed are presented in Figure 3.1. The baseline configuration is the original LPFSA presented in [14] and shown in Figure 3.1.1. The configurations with wider side slots and phasing slot are presented in Figure 3.1.2 and 3.1.3 respectively. The antennas are fed using a CPW line and deposited on top of a substrate layer. The substrates used are: RO 5880 with permittivity  $\epsilon_r = 2.2$  and thickness  $h = 0.787$  mm, RO 4350 with permittivity  $\epsilon_r = 3.48$  and thickness  $h = 0.762$  mm and RO 3006 with permittivity  $\epsilon_r = 6.15$  and thickness  $h = 0.635$  mm.

The dimensions of the LPFSA are shown in Figures Figure 3.1.2 and Figure 3.1.3. Figure 3.1.2 presents the dimensions for the largest element only. The dimensions of the other elements in the antenna are scaled down by the scaling factor ( $\tau$ ). These dimensions are: the element's length ( $L$ ), the slot width ( $W$ ), the side slot width ( $W_s$ ), the length of the phasing slot ( $L_p$ ), the width of the phasing slot ( $W_p$ ), the spacing between the slots ( $S$ ), the spacing between antenna elements (BOOM). Figure 3.1.3 shows dimensions from the CPW line that connects all the elements with characteristic impedance  $Z$  and of the feed line.



(1)

(2)



(3)

**Figure 3.1.1.** Top View of LPFSAs. (1) Baseline Configuration. (2) LPFSA with wider side slots. (3) LPFSA with phasing slot.

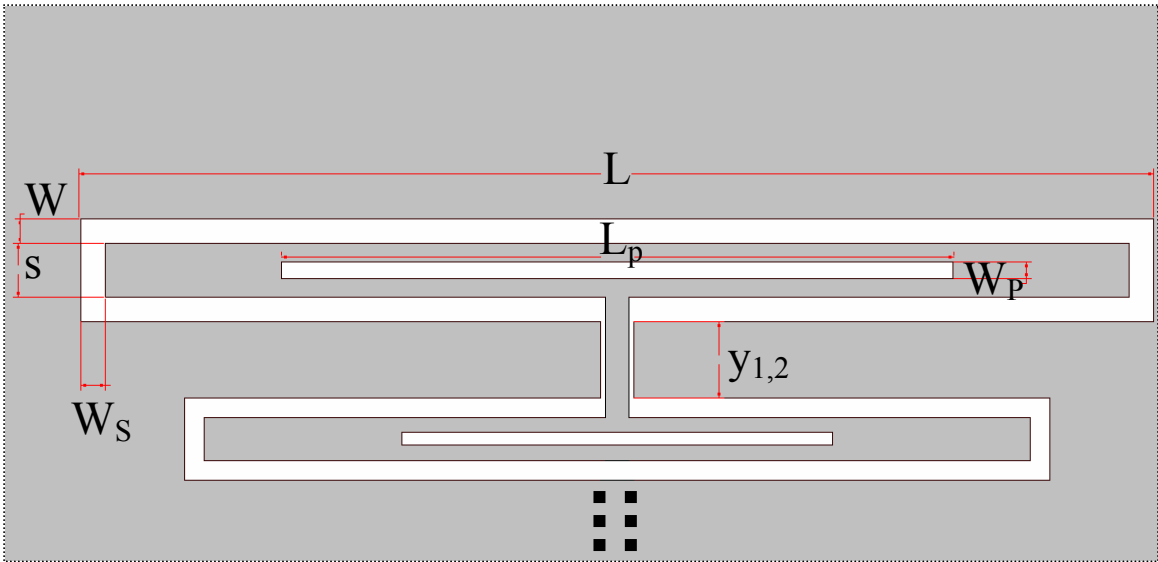


**Figure 3.1.2.** Log Periodic Folded Slot Antenna Dimensions.

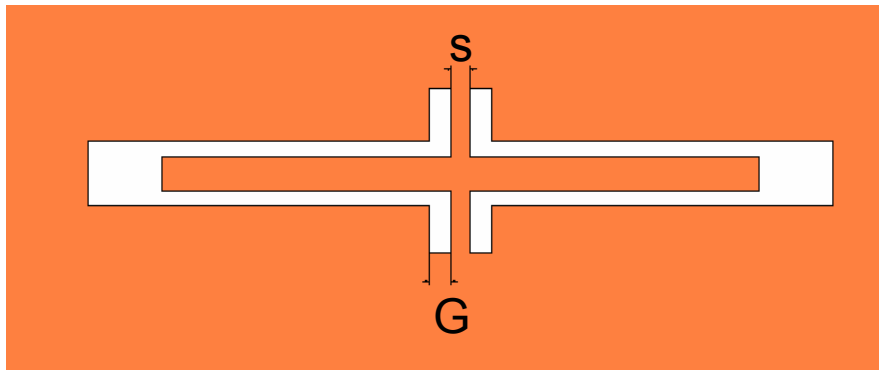


**Figure 3.1.3.** Elements Connecting Line Dimensions.

### 3.2 Procedure

The first step is data collection. After simulating a number of LPFSAs varying some of its factors, levels that guaranteed linear response were chosen for the DOE study. After all the experiments were completed for a particular DOE, the results were analyzed. The analysis helps to identify the factors that affect the antenna negatively. Modifications to the design were proposed to improve the antenna performance based on the results. The next step was data collection for the solution proposed after examining

the data of the DOE. The cycle repeated itself until the design goals were satisfied. The final step was to fabricate the antennas to verify the simulated results. A diagram showing the procedure is presented below.

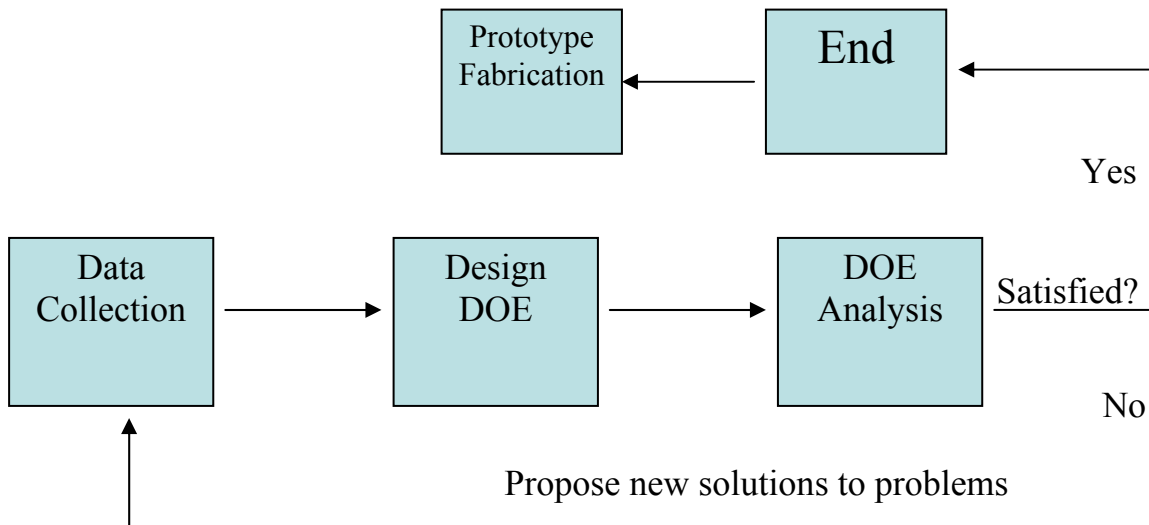


**Figure 3.2.1.** Procedure Involved in the design of LPFSA.

### 3.3 Simulation Software

#### 3.3.1 Electromagnetic Simulator

The antennas were analyzed and simulated using Ansoft Designer. The software has an electromagnetic simulator based on the Method of Moments. The method of moments is the best choice for the simulation of slot type structures. Other simulation software was available including Agilent’s Momentum and Ansoft HFSS. Momentum is also an EM simulator based on the method of moments but it was discarded as an option because the simulation times were between 3 to 4 days on just a handful of frequency points. Ansoft HFSS was another choice but it was slower than Ansoft Designer with similar results using the finite element method. The simulation time using Designer was between 4 and 12 hours for each simulation depending on the complexity of the structure. The original simulation time was between 12 and 36 hours on 300 frequency points

between 3 and 11 GHz for each simulation. It was discovered that the simulation time could be reduced if the simulation was broken into parts, each part simulating a different part of the frequency band. This was the only way that the simulation time could be reduced to between 4 and 12 hours. Several computers were used to simulate the antennas with Ansoft Designer 1.1. One of them had a Intel Xeon 3.06 GHz processor with 3 GB of RAM. The remaining machines were Pentium IV PCs with 1 GB of RAM. The difference in simulation time was about 40 minutes between the Xeon machine and the slowest Pentium IV 2 GHz machine.

### **3.3.2 Design Expert Software**

The Design Expert was used to analyze the data for the DOEs. The software allows us to analyze all types of experimental designs including multilevel factorials.

## **3.4 Design Equations for LPFSA**

A handful of equations are necessary to design a LPFSA. Generally, the band of operation and the scaling factor are the input variables to the design. In this case, the boom length is also specified beforehand. If the boom is set, then the separation between antenna elements is also set. One could also specify the number of elements in the antenna as an input factor. The number of elements and the scaling factor are dependent on each other and only one of them can be used as an input factor. In the next few paragraphs, the design equations are presented.

The first step is to determine the band of operation of the antenna. Once this parameter is known, the length of the folded slot elements can be determined. The  $f_{low}$  sets the length of the largest element as shown by Equation 3.1. The elements in the antenna resonate when their length is nearly  $\lambda/2$ . In [20 – 22], it is shown that the length of a folded slot antenna is equivalent to Equation 3.1. For folded slot antennas, the length is critical because it determines the resonant frequency.

In the case of a LPFSA, the length of each folded slot element is not as critical as the case where just one folded slot antenna element is used as the antenna. The lengths of the folded slot elements still needs to be nearly  $\lambda/2$  but they do not need to resonate at a specific frequency because the effects of all of them joined together create a broadband antenna. The length of the smallest element is set by  $f_{high}$ . This frequency is not necessarily the highest frequency of the desired band of operation. In [14],  $f_{high}=1.5f_N$ ,  $f_N$  is the highest frequency of the desired band of operation. This is done to ensure good response at high frequencies. In this work, the same rule is used. Also, to improve the low frequency characteristics, the length of the longest element is designed to be a little longer than  $\lambda/2$  to ensure that that particular element resonates at a frequency lower than  $f_{low}$ .

$$C = 2(L_a + S_a + W_{a2} - W_{a1}) \quad (3.1)$$

Once the scaling factor ( $\tau$ ) is chosen, the number of antenna elements needed in the antenna is determined (equation 3.3). Also, the dimensions of the biggest element are scaled down with  $\tau$  for the other elements to ensure broadband operation. Note that the scaling factor (equation 3.2) relates the lengths of two adjacent folded slot elements. The sum of all the interspacing between antenna elements, the boom length, is determined by setting  $d_{1,2}$  to a specific value. The operation is shown in equations 3.4 and 3.5. Parameters sigma and alpha (equations 3.6 and 3.7) are related to the interspacing between antenna elements. The spacing between antenna elements is a factor that impacts the frequency response of the antenna depending also on other input factors. This point will be explained in Chapter 4.

Scaling Factor:

$$\tau = \frac{l_{i+1}}{l_i} = \frac{d_{i,i+1}}{d_{i-1,i}} \quad (3.2)$$

Number of Elements:

$$N = \frac{\log\left(\frac{f_1}{f_N}\right)}{\log \tau} + 1 \quad (3.3)$$

Boom Length:

$$Boom = d_{1,2} \left[ \frac{\tau^{N-1} - 1}{\tau - 1} \right] \quad (3.4)$$

$$Boom = d_{1,2} \sum_{i=0}^{N-2} \tau^i \quad (3.5)$$

Spacing Factor:

$$\sigma = \frac{d_{i,i+1}}{2l_i} = \frac{1 - \tau}{4 \tan \alpha} \quad (3.6)$$

Angle:

$$\alpha = \tan^{-1} \left( \frac{1 - \tau}{4\sigma} \right) \quad (3.7)$$

The gain in the antenna is not an input factor. However, the gain of the antenna increases as the number of elements increases. When the number of elements increases,  $\tau$  also increases.

### 3.5 Log Periodic Folded Slot Antenna Design Example

A LPFSA is designed and analyzed in this section. The same procedure is repeated over and over again until all the experiments of a particular DOE are completed. The responses of all the experiments then are analyzed using the software Design Expert to identify the factors that affect the response and develop models to estimate different antenna parameters based on input factors.

### 3.5.1 Input Factors

**Table 3.1.** LPFSA Design Example Input Factors. (Set Parameters, Fixed in the Test)

Band of Operation (GHz)	3.1 – 10.6
Scaling Factor	0.89
Substrate Used	RO 4350
Boom length	51 mm

Since  $f_N = 10.6$  GHz ,  $f_{high} = 15.9$  GHz.

### 3.5.2 Feed line Dimensions

The dimensions for a 50 ohm feed line are presented below. (Check Figure 2.9.1 for reference.)

**Table 3.2.** 50 ohm line Dimensions.

S (mm)	2.5
G (mm)	0.15
Z (ohm)	50
h (mm)	0.76

### 3.5.3 Elements Connecting Line Dimensions

One of the critical parts of the design is the impedance of the line that connects all the antenna elements. For this example, a 65 ohm line is used. The dimensions are presented below. (Check Figure 2.9.1 for reference.)

**Table 3.3.** Elements Connecting Line Dimensions.

S (mm)	1.0000
G (mm)	0.2051
Z (ohm)	65
h (mm)	.76

### 3.5.4 Calculated Parameters

**Table 3.4.** Calculated Parameters of LPFSA Example

N	16
$\alpha$	17.46°
$\Sigma$	0.087
$d_{1,2}$	4.79 mm
$\lambda_g$	66.92 mm

The value of  $\lambda_g$  is used to calculate the dimensions of the first element as established by equation 3.1. The dimensions are depicted in Figure 3.2. Then, the scaling factor is used to calculate the dimensions of the remaining elements. The length of the first element is adjusted to make it resonate before 3.1 GHz. In reality, the first element resonates at around 2.5 GHz to ensure good low frequency characteristics. Therefore, the last element resonates at around 14.25 GHz instead of 15.9 GHz.

The dimensions for all the elements as well as the spacing between antenna elements is calculated with the scaling factor and presented below.

**Table 3.5.** Element Dimensions.

Element	L (mm)	W (mm)	S (mm)	Spacing (mm)
1	42.06223	1.4000	2.0000	2.8199
2	37.43538	1.2460	1.7800	2.5097
3	33.31749	1.1089	1.5842	2.2336
4	29.65257	0.9870	1.4099	1.9879
5	26.39078	0.8784	1.2548	1.7693
6	23.48780	0.7818	1.1168	1.5746
7	20.90414	0.6958	0.9940	1.4014
8	18.60468	0.6192	0.8846	1.2473
9	16.55817	0.5511	0.7873	1.1101
10	14.73677	0.4905	0.7007	0.9880
11	13.11573	0.4365	0.6236	0.8793
12	11.67300	0.3885	0.5550	0.7826
13	10.38897	0.3458	0.4940	0.6965
14	9.24618	0.3078	0.4396	0.6199
15	8.22910	0.2739	0.3913	0.5517
16	7.32390	0.2438	0.3482	0.4910

The remaining dimensions necessary to draw the complete structure are calculated based on the values presented in Table 3.5 and the dimensions of the coplanar waveguide line that connects all the elements. The calculation of all the dimensions could be a tedious process but is calculated instantly using a spreadsheet in Microsoft Excel that calculates all the dimensions based on input parameters. These dimensions are needed to draw the structures presented in Figure 3.1. The design example is simulated using Ansoft Designer and the response is analyzed. The same procedure is repeated over and over again for each experiment of a particular DOE.

### 3.5.5 Results

One of the design goals of the antenna is that the VSWR needs to be less than 2. This is equivalent to say that the return loss needs to be less than -10 dB. The return loss graph of the design example is presented below. The return loss is always below the -10 dB line. Note that in many places the return loss dips to -25 dB and then rebounds to -13 dB and then same pattern repeat itself. This is the expected behavior of a log periodic antenna.

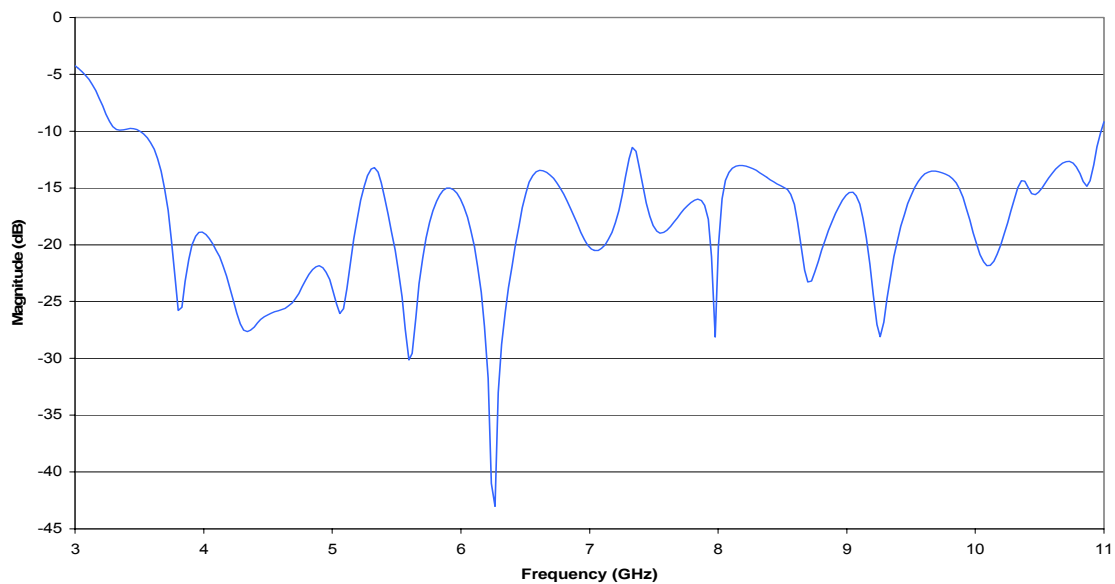


**Figure 3.5.1.** Return Loss Response of Example.

Another design goal is to make the variations in the input resistance of the antenna to be as small as possible for the entire frequency band to maintain a VSWR  $< 2$ . In Figure 3.5.2, the real resistance of the antenna is presented. Since it was established on the previous graph that VSWR was less than 2 for the entire frequency band it is no surprise to see that the real part input impedance is close to 50 ohms. The real part of input impedance varies between 40 and 60 ohms for the most part of the frequency band. Wild variations in the input resistance are associated with a VSWR  $> 2$ . Variations in the input resistance can be made smaller by adding more elements and therefore increasing the scaling factor.

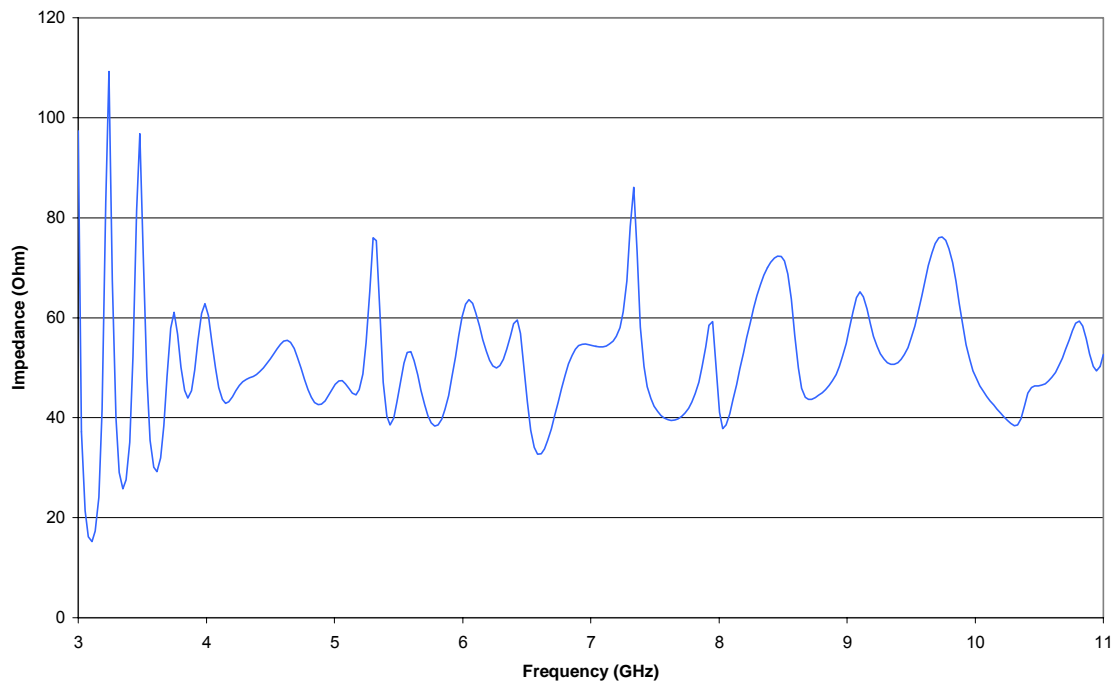


**Figure 3.5.2.** Input Resistance of Example.

Another design goal of a log periodic folded slot antenna is to maintain as flat as possible the gain of the antenna. Typical behavior of a log periodic antenna implies that the variations in gain are minimal within a period and the same pattern should repeat itself for the entire band of operation. The gain at the angle of maximum radiation is presented in Figure 3.5.3. It is observed that the gain varies wildly in the band of

operation. This implies that sidelobes, backlobes and even end fire radiation will appear when the radiation pattern is swept against frequency. This can be verified with Ansoft Designer and Chapter 4 presents solutions to this problem.

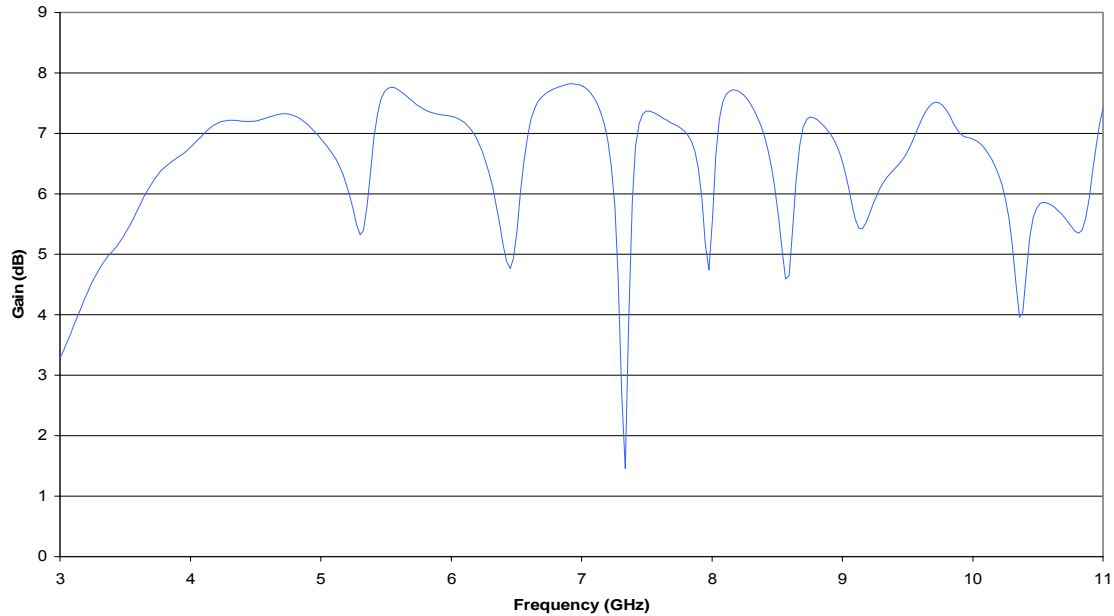


**Figure 3.5.3.** Gain in the direction of maximum radiation ( $\theta=85^\circ$ ,  $\phi=90^\circ$ ) of Example.

Many other things can be verified to evaluate the performance of the LPFSA. One of them is the phase of the reflection coefficient that can be used to determine the existence of an end effect. According to [5], the end effect could be present if jumps of  $360^\circ$  are observed in the plot as presented in Figure 2.4.2. Also, the radiation characteristics need to be verified at closely spaced frequencies to ensure broadband operation. The 3 dB beamwidth and the performance in the time domain can also be verified.

### 3.6 Simulation Results From Preliminary Designs – Data Collection

The next few paragraphs explain and present the results of various simulations that helped to set the levels for the different DOEs. Before setting the levels for the different DOEs, one needs to be certain that the values chosen meet the required design

goals. One of the critical factors of log periodic antennas is the scaling factor. One of the very early steps in the data collection process was to simulate log periodic folded slot antennas by varying the scaling factor. When the scaling factor ( $\tau$ ) is 0.8 just 9 folded slot elements are needed in the antenna build on top of a Rogers 5880 substrate with permittivity  $\epsilon_r = 2.2$  and thickness  $h = 0.787$  mm. On the other hand, when the scaling factor ( $\tau$ ) is near 1 and equal to 0.95, 33 elements are needed. The purpose of this is to evaluate the performance of the different antenna designs to use the information to set the levels for the different DOEs. The designs are based on the baseline configuration presented in Figure 3.1.

In Figure 3.6.1, the return loss of designs with different scaling factors is presented. The antennas are simulated using Ansoft Designer on Rogers RT Duroid 5880 substrate. For a scaling factor of 0.85, 12 elements are needed in the antenna. Meanwhile, 17 elements are needed for a scaling factor of 0.9. Note that the best performance in terms of return loss is given by the design with a scaling factor of 0.9.

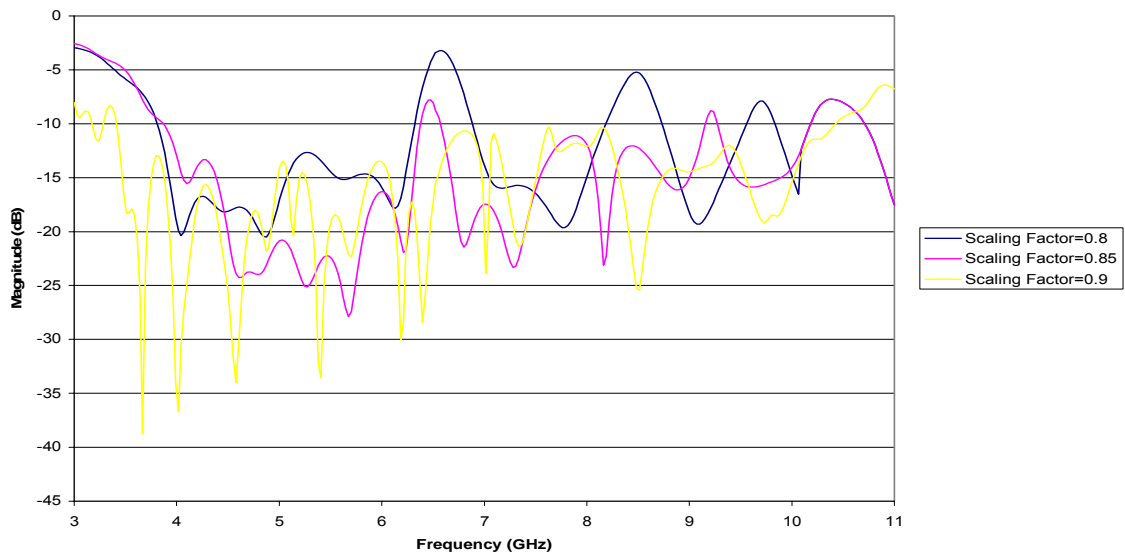


**Figure 3.6.1.** Return Loss Response of designs with different scaling factors.

The designs are also evaluated in terms of their radiation patterns. Figure 3.6.2 shows the gain in the direction of maximum radiation ( $\theta=85^\circ$ ,  $\phi=90^\circ$ ) This is the place

where the gain reaches the maximum. The graph shows that the gain is larger for the design with a scaling factor of 0.9. Also, the drops in gain are smaller for the design with the largest scaling factor. Careful analysis showed that the radiation pattern is unstable for all the cases but worst for the cases of scaling factors of 0.8 and 0.85. Based on this, it was decided that one of the levels for the scaling should be near 0.9.

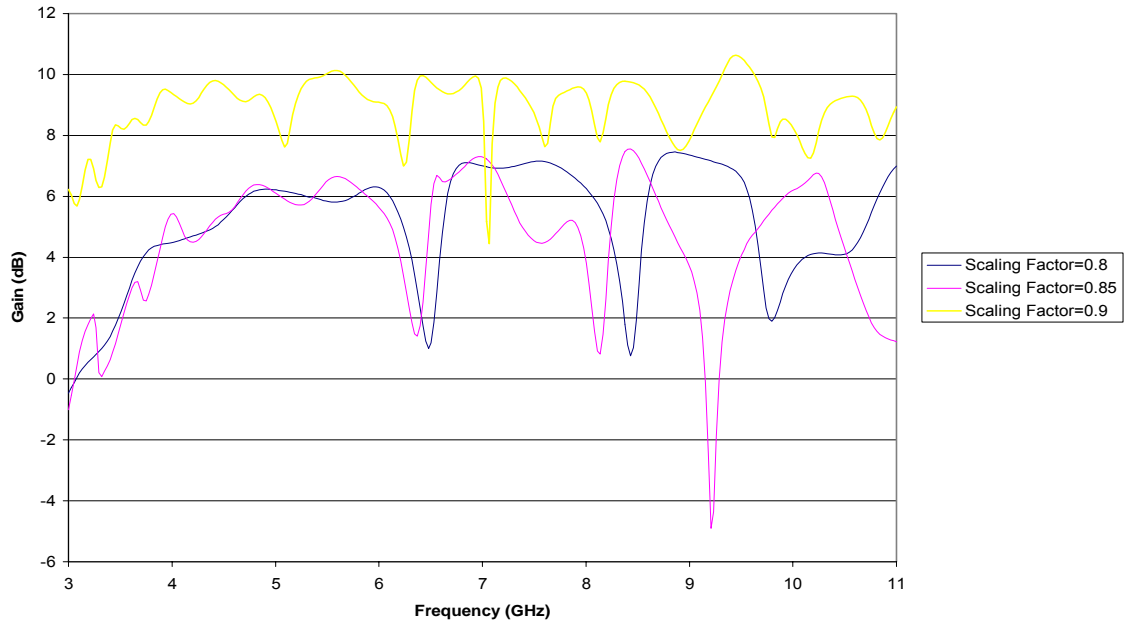


**Figure 3.6.2.** Gain ( $\theta=85^\circ$ ) of designs with different scaling factors.

As part of the data collection process, the antennas were simulated by keeping the scaling factor constant (0.89) but changing the relative permittivity of the substrate. The dimensions of the antennas were reduced as the relative permittivity increased. The antennas worked within acceptable levels for substrates with relative permittivity equal to 2.2 and 3.48. But it was not possible to match the antenna to 50 ohms using the substrate with relative permittivity equal to 6.15. The return loss for the designs presented in Figure 3.6.3 indicates that the  $VSWR > 3$  for the designs with a scaling factor equal to .89. The return loss for the design with a scaling factor of 0.95 presents a  $VSWR < 2.5$  for the majority of the operating band. A similar case is presented in Figure 3.6.4,  $VSWR > 3$  even though the boom length and the impedance of the elements connecting line are varied. It was then decided that the substrate Rogers RO 3006 ( $\epsilon_r=6.15$ ) could not be used for the DOEs if one of the levels for the scaling factor was near 0.9.

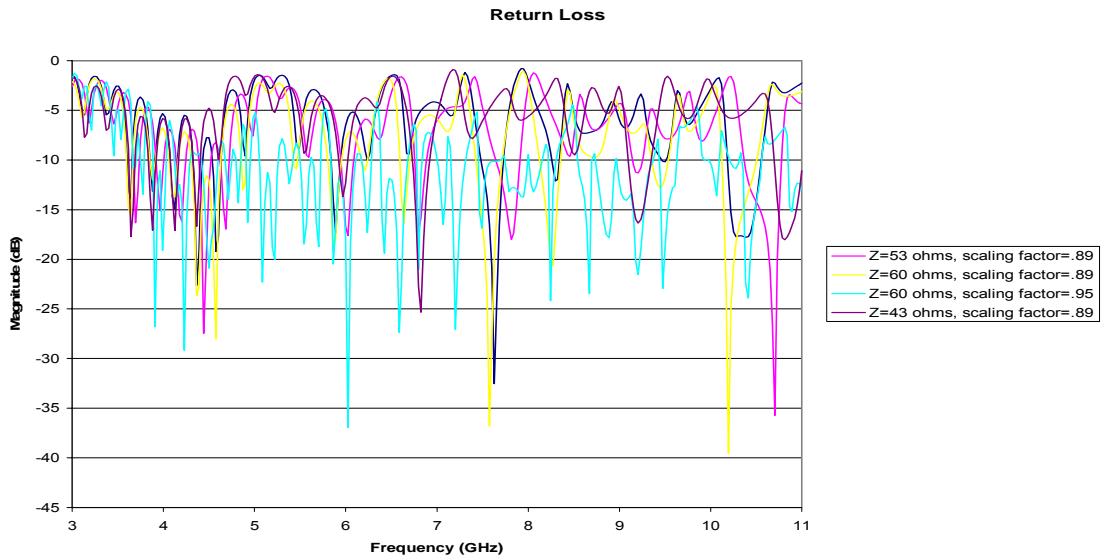


**Figure 3.6.3.** Return Loss Response of designs with  $\epsilon_r=6.15$ .

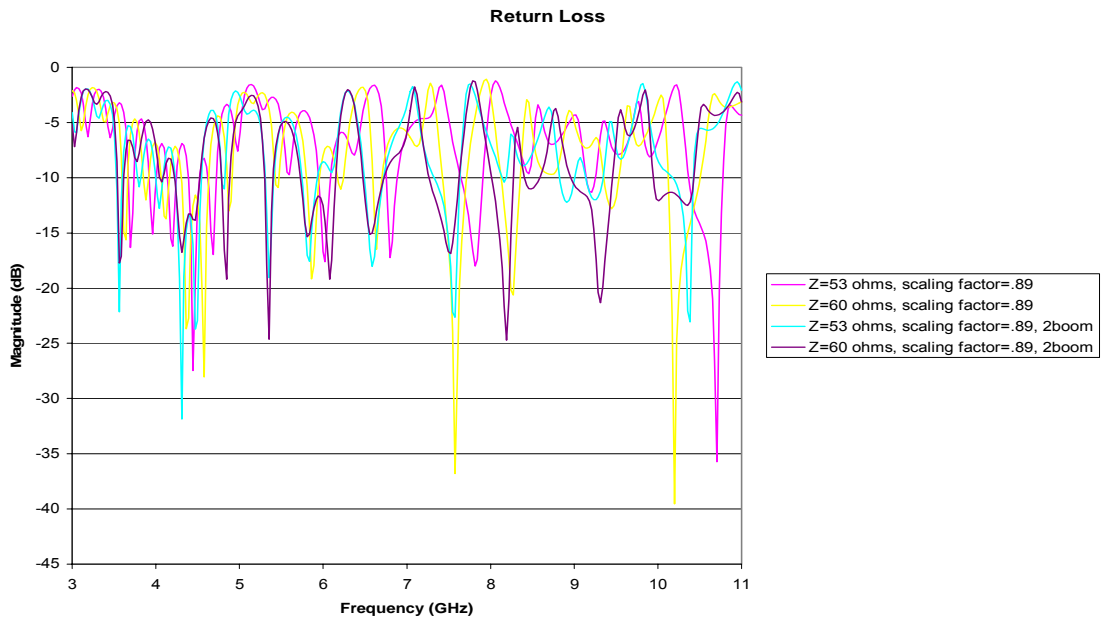


**Figure 3.6.4.** Return Loss Response of designs with  $\epsilon_r=6.15$ .

The spacing between antenna elements was varied to see if it had an impact on the response of the antenna. The response of the antenna is degraded if the spacing is set too small or too big. Figure 3.6.5 shows the return loss response of several designs where the

boom length was varied. The results show that if the spacing is too small, the response will be affected. Based on these results, the spacing for the designs of the DOE were set within acceptable levels.

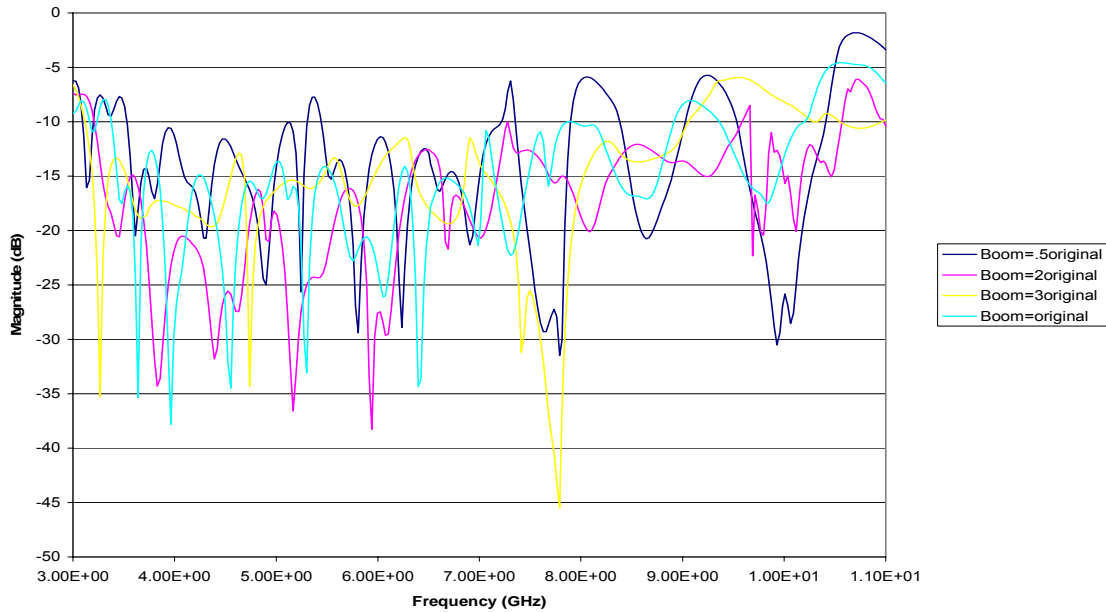


**Figure 3.6.5.** Return Loss Response of designs where the boom length was varied.

### 3.7 Design of Experiments

This section presents the different DOEs that were performed and the factors and levels on each one. The results from the DOEs will be presented in Chapter 4.

#### 3.7.1 DOE I

Initially, the DOE tried to identify the factors that affect the impedance bandwidth of the antenna. It consisted of five main factors over two levels. The factors were: W (width of the slots of the biggest element), S (spacing between the slots of the biggest element), Boom (spacing between folded slots),  $\tau$  (scaling factor) and Z (impedance of the line that interconnects all the elements). The remaining antenna dimensions are scaled down from the dimensions of the biggest element using the scaling factor. These

antennas were simulated on top of a substrate with permittivity  $\epsilon_r = 3.48$  and thickness  $h = 0.762$  mm. The factors and the levels where they were varied are presented in Table 3.6. Table 3.7 shows the design matrix of a  $2^5$  full factorial. As explained in Chapter 2, the design matrix of the experiment shows the state of each factor for a particular run. The results of this DOE will be presented in Chapter 4. The baseline configuration (Figure 3.1) is analyzed with this DOE.

**Table 3.6.** Factors and Levels for DOE1.

Factor	Low level	High level
W (mm)	0.9	1.4
S (mm)	2	4
Boom	2.82	5.64
T	0.89	0.95
Z (ohm)	74	150

**Table 3.7.** Design Matrix for DOE1.

Design name	Alternate name	W (mm)	S (mm)	Boom (mm)	$\tau$	Z (ohm)
00000	1	.9	2	Y	.89	74
00001	A	.9	2	Y	.89	150
00010	B	.9	2	Y	.95	74
00011	Ba	.9	2	Y	.95	150
00100	C	.9	2	2y	.89	74
00101	Ca	.9	2	2y	.89	150
00110	Cb	.9	2	2y	.95	74
00111	Cba	.9	2	2y	.95	150
01000	D	.9	4	Y	.89	74
01001	Da	.9	4	Y	.89	150
01010	Db	.9	4	Y	.95	74
01011	DbA	.9	4	Y	.95	150
01100	Dc	.9	4	2y	.89	74
01101	Dca	.9	4	2y	.89	150
01110	Dcb	.9	4	2y	.95	74
01111	Dcba	.9	4	2y	.95	150
10000	E	1.4	2	Y	.89	74
10001	Ea	1.4	2	Y	.89	150
10010	Eb	1.4	2	Y	.95	74
10011	Eba	1.4	2	Y	.95	150
10100	Ec	1.4	2	2y	.89	74
10101	Eca	1.4	2	2y	.89	150
10110	Ecb	1.4	2	2y	.95	74
10111	Ecba	1.4	2	2y	.95	150
11000	Ed	1.4	4	Y	.89	74

11001	Eda	1.4	4	Y	.89	150
11010	Edb	1.4	4	Y	.95	74
11011	Edba	1.4	4	Y	.95	150
11100	Edc	1.4	4	2y	.89	74
11101	Edca	1.4	4	2y	.89	150
11110	Edcb	1.4	4	2y	.95	74
11111	Edcba	1.4	4	2y	.95	150

### 3.7.2 DOE II

The second DOE is similar to the first one; the only difference is the  $Z$  level. In this case,  $Z$  is varied between 65 and 85 ohms. The new level for  $Z$  was chosen because the old level of  $Z$  did not provide a linear region to analyze the responses and develop statistical models. The antennas were simulated on top of a substrate with permittivity  $\epsilon_r = 3.48$  and thickness  $h = 0.762$  mm. The factors and the levels where they were varied are presented in Table 3.8. The design matrix of this DOE is very similar to the one on Table 3.7, the only change is the range where  $Z$  is varied.

**Table 3.8.** Factors and Levels for DOE 2.

Factor	Low level	High level
W (mm)	0.9	1.4
S (mm)	2	4
Boom	2.82	5.64
T	0.89	0.95
Z (ohm)	65	85

### 3.7.3 DOE III

This DOE considers the effect of widening the side slots on the radiation characteristic and impedance bandwidth (Figure 3.1.2). The width of the side slots is an input factor as well as the impedance of the line that connects all the antenna elements. The boom length and the scaling factor are also input factors for a total of 16 runs.

**Table 3.9.** Factors and Levels for DOE3.

Factor	Low level	High level
Z (ohm)	115	145
Boom	1.41	2.82
Side Slots	2.7	4.5
Scaling	.89	.92

### 3.7.4 DOE IV

The objective of this DOE is to find out the effects of the phasing slot in the radiation characteristics and impedance bandwidth of the antenna (Figure 3.1.3). In this case, the scaling factor ( $\tau$ ) is kept constant. It is known that as  $\tau$  increases the abnormalities in the radiation pattern disappear. From previous DOEs, it is known that a scaling factor  $\tau = 0.89$  produces abnormalities in the radiation pattern. The length and width of the phasing slot are input factors of the experiment because the optimal values for these parameters are not known. The boom length and the characteristic impedance of the line are the remaining input factors for a total of 16 runs.

**Table 3.10.** Factors and Levels for DOE4.

Factor	Low level	High level
Z (ohm)	65	85
Boom	2.82	5.64
Length	$0.75\alpha$	$1.15\alpha$
Width	$\frac{1}{5}S$	$\frac{1}{3}S$
Phasing	$\frac{1}{5}S$	$\frac{1}{3}S$

## 3.8 Time Domain Analysis

The transfer function of an antenna can be used to determine the feasibility of the antenna to transmit clean short pulses. New communication standards for home networks such as UWB wireless technology is based on the transmission of clean short pulses. Two basic conditions are needed for the transmission of clean short pulses: the transfer function must be flat in amplitude and its phase should be linear. Specifically, it is of great interest to calculate the antenna transfer function for the different log periodic

folded slot antenna configurations studied on this work. The objective is to obtain the response of the antenna in the time domain to decide if the structure can be used for UWB communications.

The following derivation calculates the antenna transfer function with the software tools available. One could use the far-field data from Ansoft Designer to calculate the transfer function if the experimental far-field data is not available. It is important to point out that the transfer function is dependent on direction. And in this case the transfer function will be calculated at the direction of maximum radiation.

The circuit depicted below presents an antenna connected to a load resistance  $R_L$ . The transfer function to be calculated is the ratio of the voltage at the terminals of the transmitting antenna and the voltage across the load resistance  $R_L$ . This quantity allows us to determine the shape of the transmitted pulse at the receiving circuit. In this section, the transfer function of the antenna will be calculated as a function of the incident field intensity at the receiving antenna, the effective height and the input impedance.

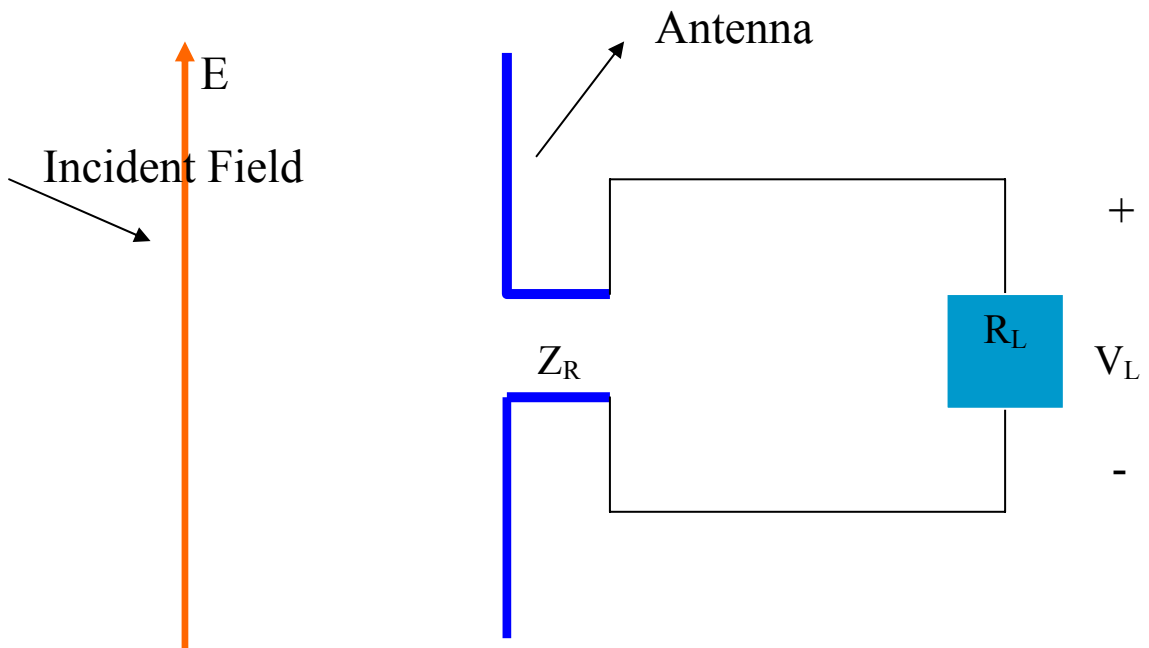


**Figure 3.8.1.** Receiving circuit depiction.

The load voltage across resistance  $R_L$  can be expressed using a voltage divider knowing that there is an open circuit voltage in the receiving antenna terminals  $V_{oc}(\omega)$ . Using  $Z_r(\omega)$  to denote the impedance of the antenna and  $R_L$  as the load resistor, the load voltage can be expressed as:

$$V_L(\omega) = \frac{V_{oc}(\omega)Z_L(\omega)}{Z_L(\omega) + Z_R(\omega)}$$

The impedance of the antenna is a known quantity. But, how the open circuit voltage in the receiving antenna terminals can be determined? Using basic antenna definitions [29], one realizes that the open circuit antenna voltage is the dot product of the effective height and incident electric field.

$$V_{oc}(\omega) = \bar{h}(\omega) \bullet \bar{E}(\omega)$$

The effective height can be expressed in terms of the power radiated by the antenna.

The power radiated can be expressed by:

$$P(\omega) = \frac{E_a^2(\omega)A_e(\omega)}{Z_0}$$

$$P(\omega) = S(\omega)A_e(\omega)$$

By combining both equations, we get:

$$h(\omega) = 2\sqrt{\frac{R_R(\omega)A_e(\omega)}{Z_0}}$$

Now to find the effective aperture  $A_e$ , the definition of Directivity is used:

$$D(\omega) = \frac{4\pi A_e(\omega)}{\lambda^2(\omega)}$$

where  $D(\omega)$  refers to Directivity.

Then,

$$A_e(\omega) = \frac{D(\omega)\lambda^2(\omega)}{4\pi}$$

The transfer function as function of frequency and direction can be expressed as:

$$H(\omega, \theta, \phi) = \frac{V_L(\omega)}{V_T(\omega)}$$

Where:  $V_L(\omega)$  is the voltage across  $R_L$  in the receiving circuit.

$V_T(\omega)$  is the voltage across the antenna terminals in the transmitting circuit.

Rearranging, the received voltage can be expressed as the product of the transfer function times the voltage waveform at the input of the receiving antenna.

$$V_L(\omega) = H(\omega, \theta, \phi)V_{GM}(\omega)$$

Knowing that

$$V_L(\omega) = \frac{V_{oc}(\omega)Z_L(\omega)}{Z_L(\omega) + Z_R(\omega)}$$

where :  $Z_L(\omega)$  is the input impedance of the receiving antenna.  
 $Z_R(\omega)$  is the load resistance

It is assumed that  $V_T(\omega) = 1$  for all frequencies because this is the excitation at the input port that uses Ansoft Designer. Now, the received voltage expression can be computed since the transfer function will be equal to  $V_L(\omega)$  and the shape of the input waveform is known.

The received voltage expression is transformed into the time domain using the inverse Fourier transform.

$$V_L(t) = \mathfrak{F}^{-1}\{H(\omega, \theta, \phi)V_{GM}(\omega)\} \quad (3.8)$$

Finally, the received voltage waveform in the time domain can be compared to the voltage waveform at the transmitting antenna to determine if the pulse was transmitted faithfully. It is expected that the amplitude of the received pulse to be smaller much smaller than the amplitude of the transmitted pulse. The antenna might not work for time domain applications if it is difficult to identify the transmitted pulse in the received waveform.

### **3.9 Prototype Fabrication**

Some antenna designs were fabricated using a Proto Mat H100 milling machine and also using the etching technique in order to validate the simulations. Then the measurements were taken at the UPRM Radiation Laboratory. The results were compared in cases where the prototype was fabricated using the milling machine and also using the etching technique. The Agilent 8510C S-parameter network analyzer was used to take the measurement of return loss, VSWR and input impedance of each prototype that was fabricated. The antennas were fabricated on top of a Rogers RO 4350 substrate with permittivity  $\epsilon_r = 3.48$  and thickness  $h = 0.762$  mm.

## 4 Results and Discussion

This chapter discusses the results from all the Design of Experiments described in Chapter 3. Results and comparisons based on the time domain analysis procedure outlined in Chapter 3 are also presented. Finally, results on simulations based on the modulated impedance feeder are presented.

### 4.1 DOE I Results

The following tables present the results from DOE I. The simulations were performed with Ansoft Designer between 3 GHz and 11 GHz. Although each simulation consists of 300 frequency points, the following tables present the mean, minimum and maximum of the most important parameters. The statistical models were based on these responses and these results are explained later on. Finally, a comparison between designs establishes the effects that the variation in the level of each main factor has on the impedance bandwidth and the radiation characteristics of the antenna.

**Table 4.1.** Mean and Minimum Values of the Reflection Coefficient of DOE I.

<i>Experiment</i>	<i>Alternate Name</i>	<i>S11_mean(dB)</i>	<i>S11_min(dB)</i>	<i>S11_min(mag)</i>	<i>S11_mean(mag)</i>
1	0	-15.4590	-43.7526	0.0065	0.1985
A	1	-3.2913	-9.6122	0.3307	0.6953
B	10	-16.7711	-32.6927	0.0232	0.1716
Ba	11	-2.0747	-6.4941	0.4735	0.7883
C	100	-10.5463	-22.8366	0.0721	0.3127
Ca	101	-1.2907	-6.7017	0.4623	0.8480
Cb	110	-9.2651	-26.1851	0.0491	0.3621
Cba	111	-1.0340	-3.2082	0.6912	0.8883
D	1000	-16.4275	-43.2215	0.0069	0.1840
Da	1001	-3.3927	-9.4328	0.3376	0.6802
Db	1010	-17.1881	-41.2562	0.0087	0.1707
DbA	1011	-14.8215	-7.2095	0.4360	0.7750
Dc	1100	-10.4832	-28.3334	0.0383	0.3161
Dca	1101	-1.3261	-4.3974	0.6027	0.8593
Dcb	1110	-8.8830	-27.7440	0.0410	0.3780
Dcba	1111	-0.9684	-2.9377	0.7130	0.8962

<i>Experiment</i>	<i>Alternate Name</i>	<i>S11_mean(dB)</i>	<i>S11_min(dB)</i>	<i>S11_min(mag)</i>	<i>S11_mean(mag)</i>
E	10000	-17.9056	-41.9886	0.0080	0.1539
Ea	10001	-5.9457	-19.0893	0.1111	0.5218
Eb	10010	-18.8494	-39.9508	0.0101	0.1478
Eba	10011	-2.7906	-7.4876	0.4223	0.7327
Ec	10100	-15.6020	-39.2025	0.0110	0.1867
Eca	10101	-3.1077	-12.2411	0.2443	0.6848
Ecb	10110	-15.8810	-43.2175	0.0069	0.1795
Ecba	10111	-1.2435	-3.5217	0.6667	0.8663
Ed	11000	-18.7361	-39.0344	0.0112	0.1440
Eda	11001	-5.7827	-13.5727	0.2096	0.5227
Edb	11010	-19.8678	-41.8250	0.0081	0.1296
Edba	11011	-2.9518	-7.1938	0.4368	0.7208
Edc	11100	-14.6955	-39.0068	0.0112	0.2000
Edca	11101	-3.3073	-12.9134	0.2261	0.6766
Edeb	11110	-13.8553	-37.1369	0.0139	0.2184
Edcba	11111	-1.2797	-4.1379	0.6210	0.8658

**Table 4.2.** Mean, Minimum and Maximum Values of VSWR and Input Resistance of DOE I.

<i>Experiment</i>	<i>Alternate Name</i>	<i>VSWR(max)</i>	<i>VSWR(mean)</i>	<i>VSWR(min)</i>	<i>Rmin</i>	<i>Rmax</i>
1	0	3.3415	1.5491	1.0131	14.9677	118.6237
A	1	32.5065	7.8562	1.9880	2.3494	292.9400
B	10	4.3774	1.4739	1.0475	12.0209	181.5473
Ba	11	50.5323	12.7981	2.7985	1.0342	535.1500
C	100	4.0560	1.9774	1.1555	13.1485	160.1357
Ca	101	48.0714	16.5671	2.7195	1.0487	666.8000
Cb	110	6.0176	2.2275	1.1032	9.7942	142.9546
Cba	111	68.7717	23.5000	5.4762	0.8252	808.5000
D	1000	3.0506	1.5050	1.0139	16.8570	121.2695
Da	1001	28.9274	7.5207	2.0192	2.3073	286.6800
Db	1010	3.5643	1.4636	1.0175	14.2028	149.3886
DbA	1011	2.5964	12.9910	2.5463	0.9192	563.8200
Dc	1100	4.2010	1.9974	1.0797	13.6023	170.5279
Dca	1101	52.8754	18.1588	4.0345	0.9523	695.2000
Dcb	1110	3.7848	2.2818	1.0855	16.7729	140.5401
Dcba	1111	71.4286	25.7769	5.9697	0.7584	975.2900
E	10000	4.1760	1.4087	1.0160	15.2235	109.2507
Ea	10001	16.3291	3.9346	1.2499	4.8358	163.9500
Eb	10010	3.2041	1.3964	1.0203	16.4559	130.1192
Eba	10011	18.8323	7.9448	2.4620	0.0021	671.1100
Ec	10100	2.7965	1.4920	1.0222	20.9089	139.1743
Eca	10101	20.0607	6.5680	1.6466	2.7628	269.3700

<i>Experiment</i>	<i>Alternate Name</i>	<i>VSWR(max)</i>	<i>VSWR(mean)</i>	<i>VSWR(min)</i>	<i>Rmin</i>	<i>Rmax</i>
Ecb	10110	4.0484	1.4691	1.0139	20.4627	121.2456
Ecba	10111	53.4772	18.4363	5.0002	1.3771	1847.5400
Ed	11000	4.2594	1.3811	1.0226	12.5562	128.4271
Eda	11001	14.3471	3.9773	1.5303	4.6514	168.6000
Edb	11010	2.9687	1.3346	1.0163	17.4909	116.9627
Edba	11011	22.8995	7.6533	2.5513	2.5334	490.6200
Edc	11100	2.8013	1.5275	1.0227	20.5700	135.3322
Edca	11101	15.1902	6.3296	1.5844	7.0226	672.4800
Edcb	11110	2.6503	1.5841	1.0282	25.0024	108.9144
Edcba	11111	56.8616	18.4700	4.2774	1.0721	795.6800

**Table 4.3.** Mean Value of the Gain of DOE I.

<i>Experiment</i>	<i>Alternate Name</i>	<i>Gain_mean(dB)</i>
1	0	3.5515
A	1	1.5095
B	10	5.7898
Ba	11	0.9189
C	100	3.722
Ca	101	-0.9673
Cb	110	8.3601
Cba	111	-5.9781
D	1000	6.3677
Da	1001	2.6511
Db	1010	8.832
DbA	1011	1.5725
Dc	1100	6.6631
Dca	1101	-0.4277
Dcb	1110	8.5925
Dcba	1111	-6.3957
E	10000	3.9811
Ea	10001	4.9969
Eb	10010	8.7813
Eba	10011	3.9736
Ec	10100	6.9674
Eca	10101	3.8176
Ecb	10110	9.2503
Ecba	10111	-1.5227
Ed	11000	6.8493
Eda	11001	5.3539
Edb	11010	9.1655
Edba	11011	4.5413
Edc	11100	7.1393
Edca	11101	3.5866

Edbc	11110	9.4403
Edcba	11111	-3.0532

**Table 4.4.** Standard Deviation and Variance of the Gain and Input Resistance of DOE I.

<i>Experiment</i>	<i>Alternate Name</i>	<i>Gain dB Std Deviation</i>	<i>Gain (dB) Variance</i>	<i>Input Resistance Variance</i>	<i>Input Resistance Std Deviation</i>
1	0	1.4136	1.9983	221.83	14.89
A	1	1.1701	1.3690	353.88	18.81
B	10	1.3607	1.8516	108.51	10.42
Ba	11	1.0731	1.1516	459.29	21.43
C	100	1.7342	3.0074	262.40	16.20
Ca	101	1.0850	1.1772	744.15	27.28
Cb	110	0.8859	0.7848	224.45	14.98
Cba	111	0.9253	0.8561	1789.06	42.30
D	1000	1.0054	1.0109	133.90	11.57
Da	1001	0.8911	0.7941	285.22	16.89
Db	1010	0.9255	0.8566	110.74	10.52
DbA	1011	0.8947	0.8005	442.71	21.04
Dc	1100	0.8675	0.7525	176.42	13.28
Dca	1101	0.8179	0.6690	650.99	25.51
Dcb	1110	0.6988	0.4883	178.38	13.36
Dcba	1111	0.7243	0.5246	1632.74	40.41
E	10000	1.0623	1.1285	150.53	12.27
Ea	10001	0.9783	0.9570	217.02	14.73
Eb	10010	0.9684	0.9377	386.57	19.66
Eba	10011	0.9044	0.8179	260.58	16.14
Ec	10100	1.0979	1.2055	176.01	13.27
Eca	10101	0.8353	0.6977	662.84	25.75
Ecb	10110	0.7701	0.5930	122.63	11.07
Ecba	10111	0.7488	0.5607	972.51	31.19
Ed	11000	0.8705	0.7579	228.49	15.12
Eda	11001	0.7263	0.5275	198.87	14.10
Edb	11010	0.8307	0.6901	386.84	19.67
Edba	11011	0.7578	0.5743	244.43	15.63
Edc	11100	0.7794	0.6075	249.47	15.79
Edca	11101	0.6097	0.3717	629.31	25.09
Edbc	11110	0.6726	1.0109	98.28	9.91
Edcba	11111	0.6377	0.4067	965.91	31.08

### 4.1.1 Model for the Mean of the Gain

The first model tries to predict the mean of the gain. The model shows that the boom length, the impedance of the line that connects all of the antenna elements and the scaling factor are significant factors in the behavior of the LPFSA. The two way interactions of the boom length and the impedance of the central line ( $Z$ ) and also the scaling factor and the impedance of central line are the remaining significant factors in the model. This can be observed in Figure 4.1.1. A Normal plot presented in Figure 4.1.1 shows that the aforementioned effects are the ones that affect the antenna response the most while the rest of the terms follow a normal distribution and have little effect on the response.

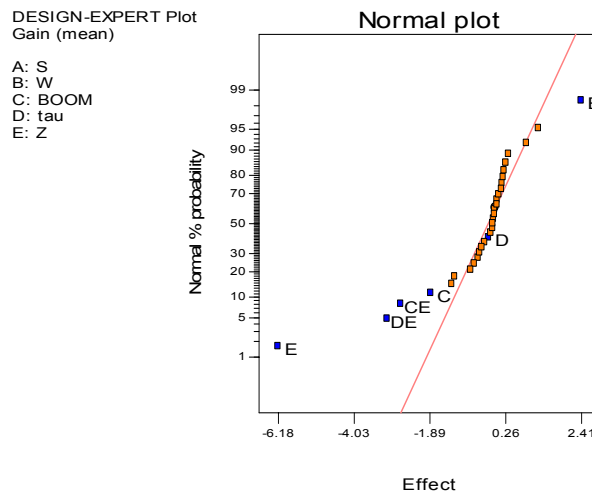


**Figure 4.1.1.** Graphical method for determining the parameters that affect the mean of the gain using DOE I data.

Equation 4.1.1 presents the model itself. The equation presented using coded factors show that  $Z$  must be kept at the lower level to obtain higher gain. The effect of keeping  $Z$  at the high level ( $Z=150$  ohms) is very costly because the gain is significantly lower than in traditional log periodic antennas. The model predicts that if  $Z$  is increased to 150 ohms, the gain decreases 3 dB. It is also saying that if the boom length is increased from the lower level the gain drops by 1 dB. This is indicative that the other antennas responses will also be affected by these factors. The gain is expressed in dB.

$$\text{Gain (mean)} = 4.00095 + 1.20B - 0.93C - 0.11D - 3.09E - 1.35CE - 1.54DE \quad (4.1.1)$$

Table 4.5 shows the values predicted by the model as well as the actual values. There is very good agreement between the predicted and actual values. Figure 4.1.2 shows that the residuals follow a normal distribution and also shows that the residuals present a random behavior. These are good signs that the model is accurate.

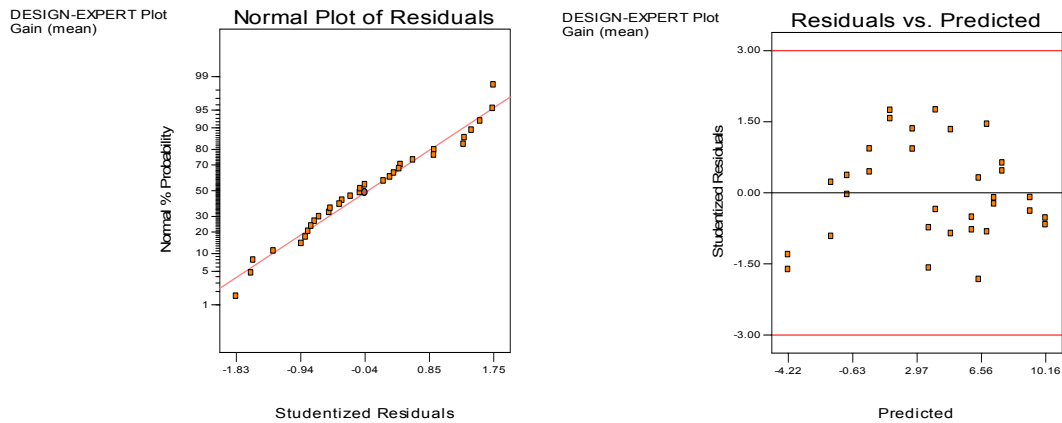


**Figure 4.1.2.** Normal Plot of Residuals and Residuals versus Predicted Values Plot for Gain (mean) model for DOE I.

**Table 4.5.** Actual and Predicted Values of the Model.

Diagnostics Case Statistics					
Experiment	Actual	Predicted			
Number	Value	Value			
00000	3.55	4.03	00001	1.51	3.64
01000	6.37	4.03	01001	2.65	3.64
10000	3.98	6.43	10001	5.00	6.05
11000	6.85	6.43	11001	5.35	6.05
00100	3.72	4.88	00101	-0.97	-0.92
01100	6.66	4.88	01101	-0.43	-0.92
10100	6.97	7.28	10101	3.82	1.49
11100	7.14	7.28	11101	3.59	1.49
00010	5.79	6.90	00011	0.92	0.33
01010	8.83	6.90	01011	1.57	0.33
10010	8.78	9.30	10011	3.97	2.74
11010	9.17	9.30	11011	4.54	2.74
00110	8.36	7.75	00111	-5.98	-4.22
01110	8.59	7.75	01111	-6.40	-4.22
10110	9.25	10.16	10111	-1.52	-1.82
11110	9.44	10.16	11111	-3.05	-1.82

### 4.1.2 Model for the Mean of the Reflection Coefficient

The following model tries to predict the mean of the magnitude of the reflection coefficient. The log periodic properties of the antenna are taken into consideration when the objective is to predict the behavior of the reflection coefficient with one value. The mean of the reflection coefficient allows us to evaluate the performance of the design. It is expected that the magnitude of the reflection coefficient should be below .33 for the entire frequency band since one of the design goals is to keep the VSWR < 2. A value that is near or above .33 tells us that the VSWR > 2 for most part of the frequency band.

The Normal plot (Figure 4.1.3) for the model shows that again the impedance of central connecting line ( $Z$ ) and the boom length are the most important factors in the performance of the antenna. It also shows that the scaling factor, the width of the slots and the interaction of the scaling factor with  $Z$  also affect the performance of the antenna. Note that the width of the slots ( $W$ ) factor is on the left side of the graph. When  $W$  is set to high level, it actually helps the antenna response because it helps to reduce the mean of the reflection coefficient. The model that predicts the mean of the reflection coefficient is presented in Equation 4.1.2.

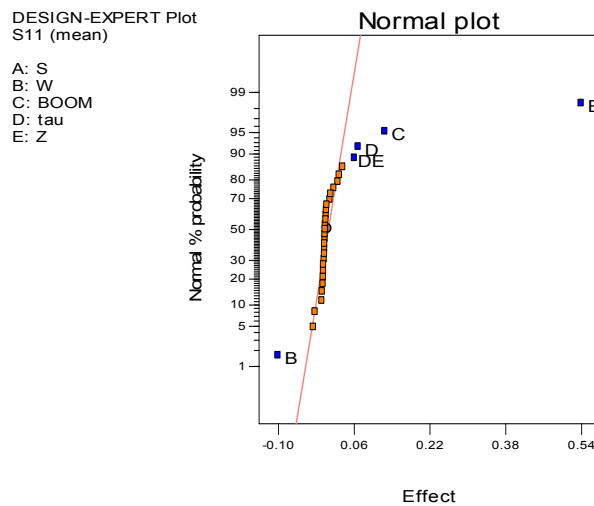


**Figure 4.1.3.** Graphical method for determining the parameters that affect the mean of the reflection coefficient using DOE I data.

$$S_{11} (\text{mean}) = 0.48 - 0.05B + 0.06C + 0.03D + 0.27E + 0.03DE \quad (4.1.2)$$

The model presented above using coded factors says that in order to reduce the mean of the magnitude of the reflection coefficient  $Z$  and the boom length must be set to the lower level and the width of the slots ( $W$ ) needs to be set to the higher level. Just by doing those three things the mean of the magnitude of the reflection coefficient is reduced considerably and guarantees that the VSWR will be less than 2 for the entire frequency band. By setting  $Z=74$  ohms, boom=59 mm and  $W=1.4$  mm a good frequency response is guaranteed.

Figure A.1 strengthens the accuracy of the model because it shows the desirable characteristics of the residuals following a normal distribution and that the residuals present a random behavior. Table A.1 presents the predicted values using the model and the actual values. These results are located in the appendix section.

#### **4.1.3 Model for the Minimum of Reflection Coefficient**

This model tries to predict the minimum of the magnitude of the reflection coefficient. The parameter is important because if the value is too large, even if it is not above .33 (VSWR > 2), the reflections could become very large if the value is above .20. Then, the impedance bandwidth goals will not be accomplished. The model could also be calculated using the dB scale. The problem with that model is that it fails to take into account factor  $Z$ , the most critical factor in the design of log periodic antennas.  $Z$  is the feeder characteristic impedance.

The normal plot presented in Figure 4.1.4 shows again the same factors that influenced the mean of the gain and the mean of the magnitude of the reflection coefficient also influences the minimum of the reflection coefficient. The factors that affect the response negatively the most include the impedance of the central line ( $Z$ ), the boom length and the interactions of the scaling factor and  $Z$ . Meanwhile,  $W$  affects the

response positively. The model is presented in Equation 4.1.3. The model is presented in coded factors and the model presented is the square of the minimum of the reflection coefficient. The Design Expert Software recommended this transformation because the ratio between maximum and minimum values was greater than 3.

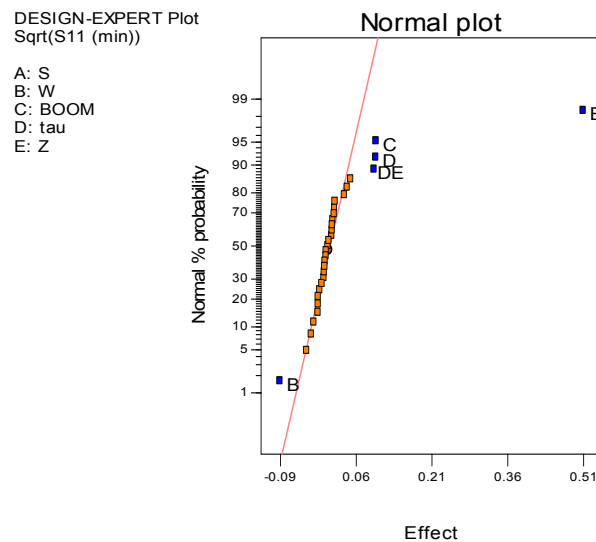


**Figure 4.1.4.** Graphical method for determining the parameters that affect the minimum of the reflection coefficient using DOE I data.

$$\text{Sqrt}(S11 (\text{min})) = 0.39 - 0.046B + 0.05C + 0.049D + 0.26E + 0.048DE \quad (4.1.3)$$

According to the model, the minimum of the magnitude of the reflection coefficient is achieved by setting the boom length and Z to the lower level and W to the higher level. In Figure A.2, it is shown that the residuals follow a normal distribution and the also present a random behavior against the predicted values. The predicted values by the model are compared to the actual values in table A.2. These results are located in the appendix section.

#### 4.1.4 Model for the Input Resistance

One of the critical factors in the design of log periodic antennas is how much the input resistance varies in the band of interest. It will be shown later on that the variations can be reduced by adding more elements to antenna by increasing the scaling factor. The next model tries to predict the maximum of the input resistance. The model helps us to discriminate between good and bad designs by evaluating the maximum of the input resistance. The oscillations in input impedance throughout the band of interest should be minimal and not surpass 30 ohms above or below the 50 ohm level. If the maximum of the input resistance is above 150 ohms, then that is indicative that values similar to that one will be appearing throughout the frequency band. This is due to the fact that log periodic antennas exhibit the same antenna characteristics in each period. The number of periods in a log periodic antenna is related to the number of elements.

Figure 4.1.5 shows the Normal plot for the model. It includes more terms than previous models and even three way interactions. A power transform was used because the ratio between the minimum and the maximum value for  $R_{\max}$  was very large. The Normal plot shows that the width of the slots ( $W$ ) and the two way interaction between the boom length and the scaling factor are the only ones that affect the response positively by keeping  $W$  and the scaling factor to the high level and the boom length set to the lower level. The most influential factor that affects the response negatively is again the impedance of the central line ( $Z$ ). Other factors that affect the response negatively include the boom length, the scaling factor and interactions between the scaling factor, the boom length and the impedance of the central line ( $Z$ ). One surprising result is that it indicates that the scaling factor should be set to the lower level to maintain the maximum of the input resistance as low as possible. This is the case because there is a big difference between the minimum and maximum value for  $R_{\max}$  across all the designs. The model will be more effective and will not identify the scaling factor as one of the negative factors, if the variability of  $Z$  between the low level and the high level is reduced. The model is presented in Equation 4.1.4.

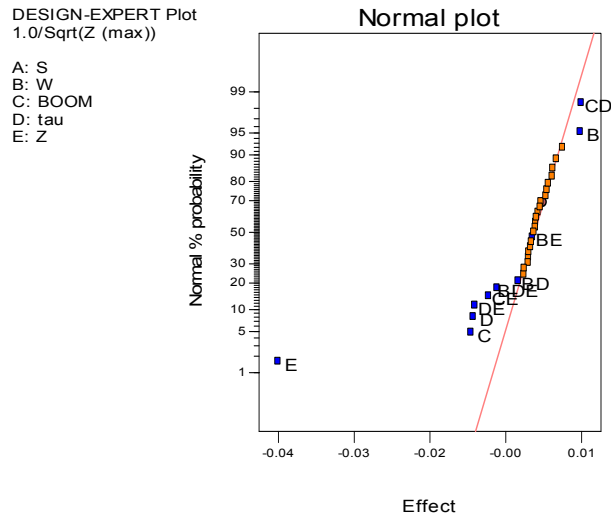


**Figure 4.1.5.** Graphical method for determining the parameters that affect the maximum of the input resistance using DOE I data.

$$1.0/\text{sqrt}(R(\max)) = 0.066 - 0.003B - 0.005C - 0.00487D - 0.02E - 0.00138BD - 0.00027BE + 0.003498CD - 0.00368CE - 0.00474DE - 0.00303BDE \quad (4.1.4)$$

Table A.3 shows the values predicted by the model as well as the actual values. There is very good agreement between the predicted and actual values. Figure A.3 shows that the residuals follow a normal distribution and also shows that the residuals present a random behavior. These are good signs that the model is accurate. These results are located in the appendix section.

The designs that exhibit large values for  $R_{\max}$  are the ones that also exhibit very small values when the minimum of the input resistance is evaluated. Those designs have the impedance of the central line (Z) and the boom length set to the high level. The model to predict the minimum of the input resistance is shown below.

$$R(\min) = 9.21 + 1.61B + 0.55C - 0.408D - 7.049E + 1.037BC + 0.149088BD - 0.7263BE - 0.7281CE - 0.6805DE - 0.8347BCE - 0.847BDE \quad (4.1.5)$$

The model shows that the slot width ( $W$ ) and the boom length affect the response positively along with their interactions. It again shows that the impedance of the central line ( $Z$ ) affect the response of the antenna negatively when it set to the high level. The scaling factor along with the two and three way interactions of the scaling factor, the boom length and  $Z$  also affect the response negatively. Although in this case the minimum of the input resistance is slightly increased by keeping the boom length set to the high level, other models have shown that the antenna response looks better while keeping the boom length set to the higher level.

#### **4.1.5 Effects in the Antenna Parameters**

The DOE consisted of 32 runs. One way to evaluate the effects that each level has on the frequency response of the designs is to compare the frequency response of two designs at a time. This helps us to confirm the findings from the different statistical models based on one response for each design. In this case, the frequency response consists of 300 frequency points equally spaced between 3 and 11 GHz.

##### **4.1.5.1 Effects of the Impedance of the Central Line in the Return Loss Response**

In Figure 4.1.6, the return loss response is evaluated between two different designs. It is observed that the return loss shifts toward the -5 dB line when the impedance of the central line increases from 74 ohms (design 00000) to 150 ohms (design00001) (a). This is very bad because the VSWR is less than 2 for design 00000 but is greater than 5 and even reaching 30 for design 00001 (a). This confirm the findings of all the statistical models based on one point responses that stated that the impedance of the central line ( $Z$ ) was the factor that affected the response of the antenna the most. All the designs can be compared by keeping the other factors (width of the slots, spacing between the slots, scaling factor and boom length) equal and changing just the impedance of the line. A total of 16 comparisons concluded that when  $Z$  is set to 150

ohms the return loss of the antenna worsens. This is the case for figures 4.1.7 and 4.1.8. In Figure 4.1.7, design 00100 (c) and design 00101 (ca) are compared.

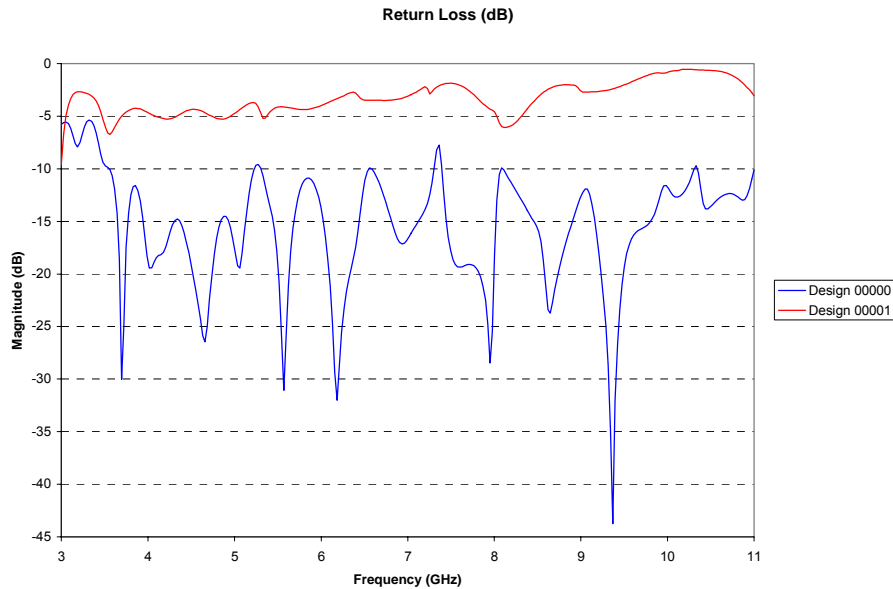


**Figure 4.1.6.** Return Loss Response for DOE I Design 00000 and Design 00001.

Design 00100 (c) has the boom length set to the high level while design 00101 (ca) has both the boom length and the impedance of the central line set to the high level. Note that the boom length is set to the high level on both designs. The return loss of the antenna increases if the boom is set to high if the response of design 00000 and design 00100 (c) are compared side by side (see Figure 4.1.6 versus Figure 4.1.7). The statistical models also established that setting the boom length to the level would impact the antenna response negatively. Again, the return loss is above -3 dB (VSWR > 10) for design 00101 (ca). The return loss response of design 00100 (c) is above the -10 dB line (VSWR > 2) in some parts of the frequency band. This is due to the fact that increasing the boom length to an antenna with just 16 antenna elements (scaling factor = .89) has a negative impact on the response. Figure 4.1.11 shows that even if the scaling factor is increased (design 00010 (b) versus design 00011 (ba)) the return loss worsens if Z is set to the high level. The same behavior is observed if Z is increased to 150 ohms no matter the levels of the rest of the factors are set.

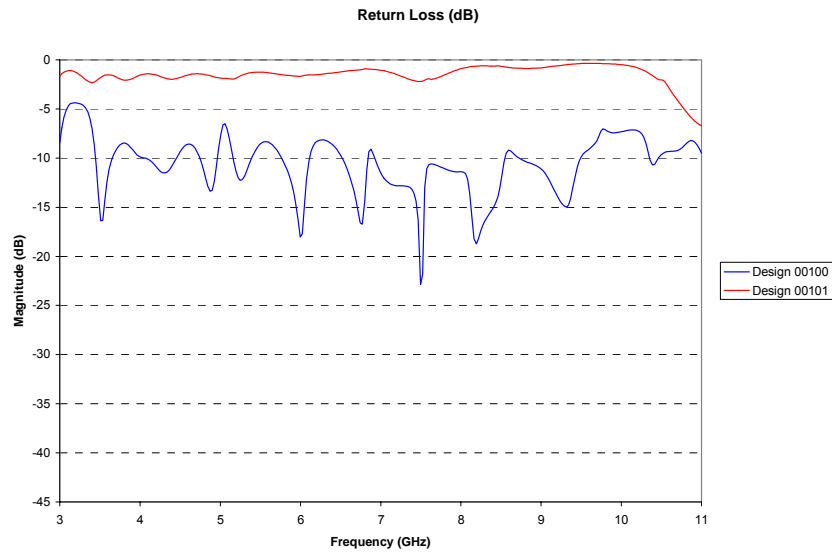


**Figure 4.1.7.** Return Loss Response for DOE I Design 00100 and Design 00101.

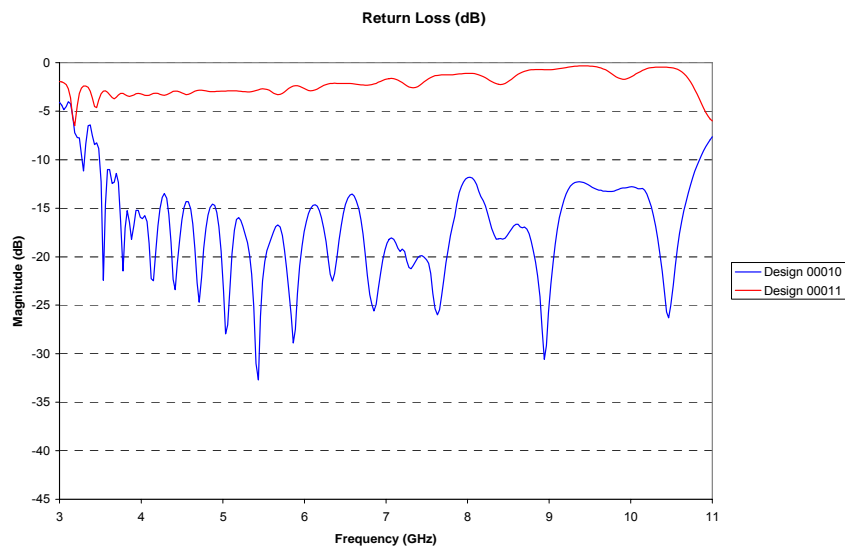
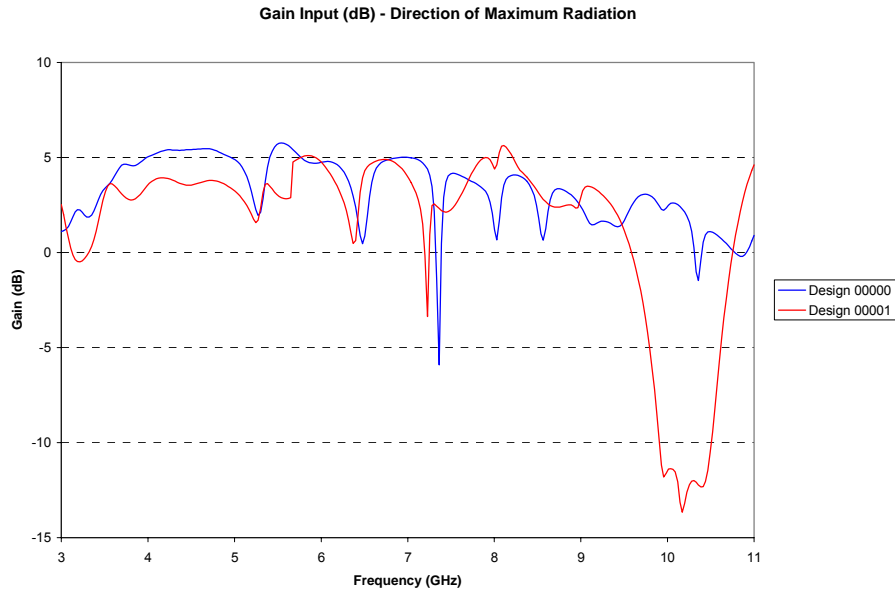


**Figure 4.1.8.** Return Loss Response for DOE I Design 00010 and Design 00011.

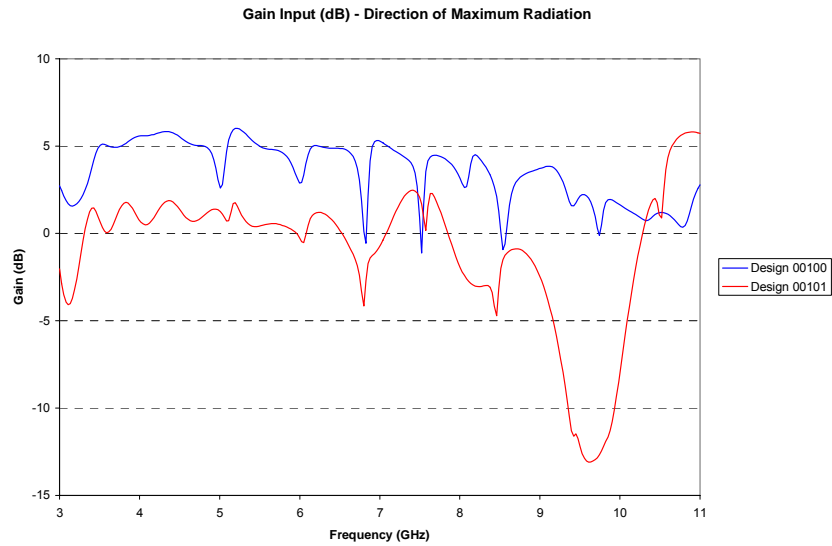
#### 4.1.5.2 Effects of the Impedance of the Central Line in the Radiation Pattern

Figure 4.1.9 compares the gain (theta = 85 degrees) between designs 00000 and 00001 (a). When  $Z$  is increased to the high level, the radiation characteristics of the antenna also worsen especially in the high frequencies when the gain drops to a negative

value. The same behavior is observed in Figures 4.1.10 and 4.1.11. In Figure 4.1.9, the scaling factor is set to the high level while  $Z$  is varied and the remaining factors are set to the low level. Meanwhile, in Figure 4.1.10, the boom length is set to the high level while  $Z$  is varied and the remaining factors are set to the low level.



**Figure 4.1.9.** Gain in the Direction of Maximum Radiation for DOE I Design 00000 and Design 00001.



**Figure 4.1.10.** Gain in the Direction of Maximum Radiation for DOE I Design 00100 and Design 00101.

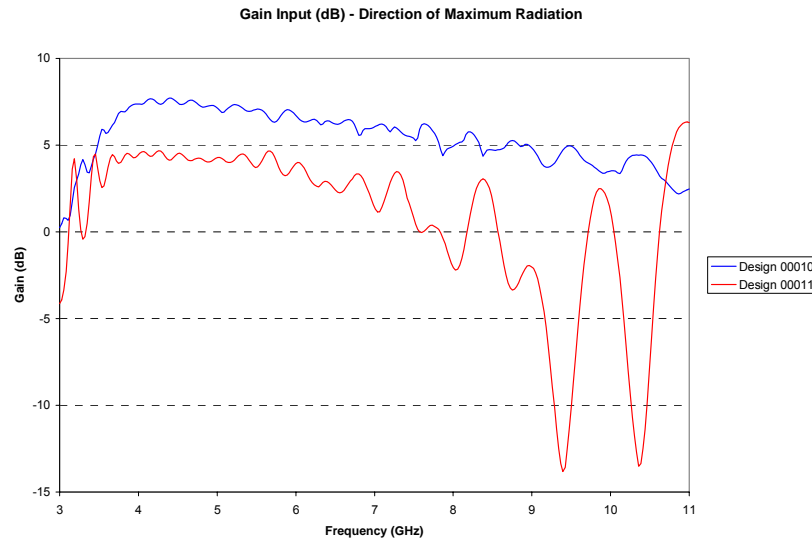


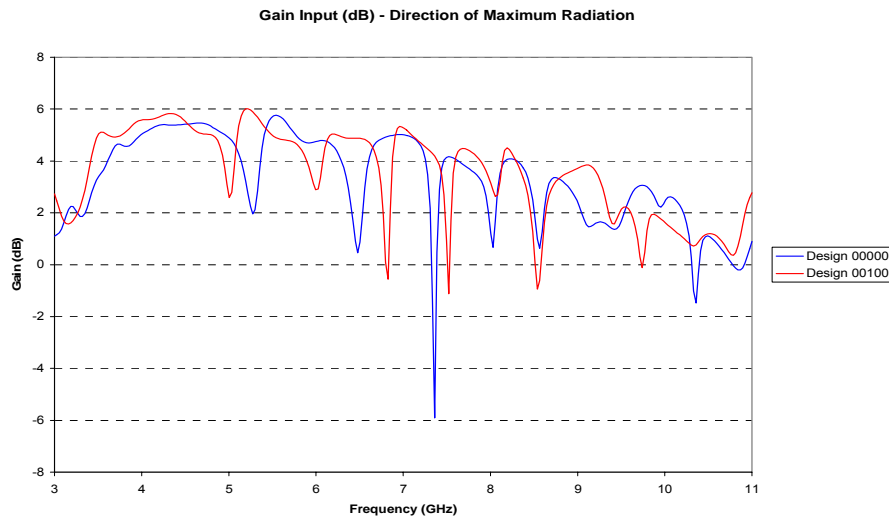
**Figure 4.1.11.** Gain in the Direction of Maximum Radiation for DOE I Design 00010 and Design 00011.

#### 4.1.5.3 Effects of the Boom Length in the Radiation Pattern

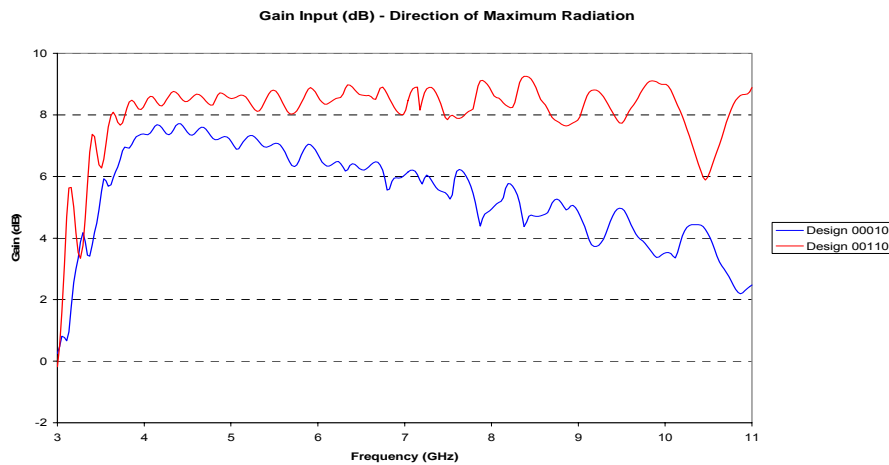
It has been stated in previous sections that if the boom length is set to the high level the return loss and the impedance bandwidth worsens. In this section, the role of increasing the boom length and its effects on the radiation characteristics of the antenna are examined.

Figure 4.1.12 shows that the radiation characteristics are not affected by increasing the boom length (design 00000 versus design 00100 (c)). However, the return loss worsens if the boom length is increased. However, when the boom length is increased and the scaling factor is set to the high level (antenna with 33 folded slot elements) the radiation characteristics improve. This is observed in Figure 4.1.13 where designs 00010 (b) and 00110 (cb) are compared. The maximum gain for design 00010 (b) starts at 6 dB and decreases until reaching a minimum of 3 dB at 11 GHz. When the boom length is increased and the other factors are kept equal (design 00110 (cb)) the maximum of the gain is very stable and above 8 dB for the entire frequency band. The price to pay is that the VSWR increases in most cases above two. A simpler solution is

to make the slot width wider without increasing the boom length (Figure 3.1.1.3). This works great for the case where a scaling factor of .95 is used. For the case of a scaling factor of .89 (16 elements) the radiation pattern characteristics are not greatly improved by increasing just the width of the slots. A solution to the problem is presented later in this chapter.



**Figure 4.1.12.** Gain in the Direction of Maximum Radiation for DOE I Design 00000 and Design 00100.



**Figure 4.1.13.** Gain in the Direction of Maximum Radiation for DOE I Design 00010 and Design 00110.

Figure 4.1.14 compares the variations in the maximum gain using designs 01010 (db) and 01110 (dcb). Note that the variations in gain are little when the width of the slots is increased and the scaling factor is equal to .95 (33 elements). The variations in gain increases at high frequencies if the boom length is increased (design 01110 (dcb)). Also the return loss worsens when the boom length is increased between the two designs as shown in Figure 4.1.15. Then, it is recommended that the boom length should remain in the low level while keeping the width of the slots ( $W$ ) at the high level.

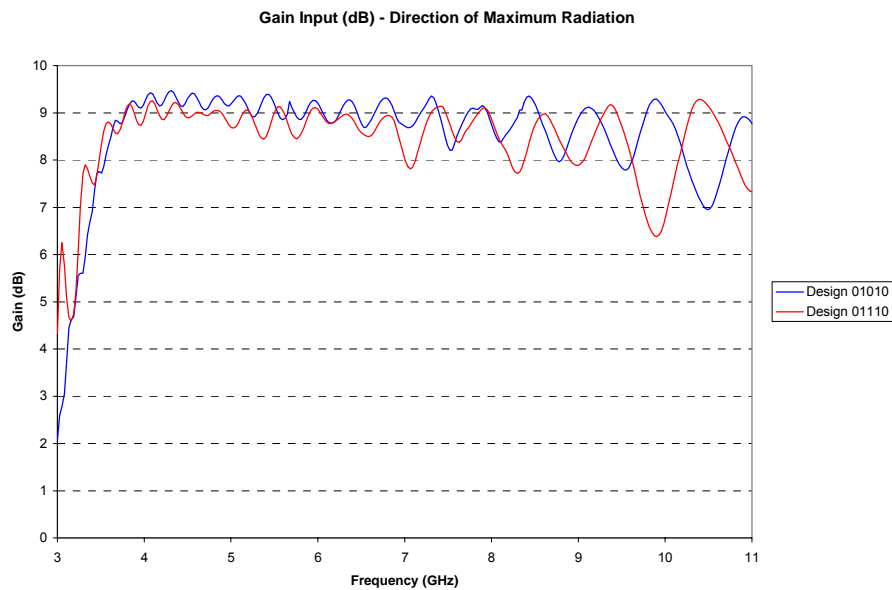


**Figure 4.1.14.** Gain in the Direction of Maximum Radiation for DOE I Design 01010 and Design 01110.

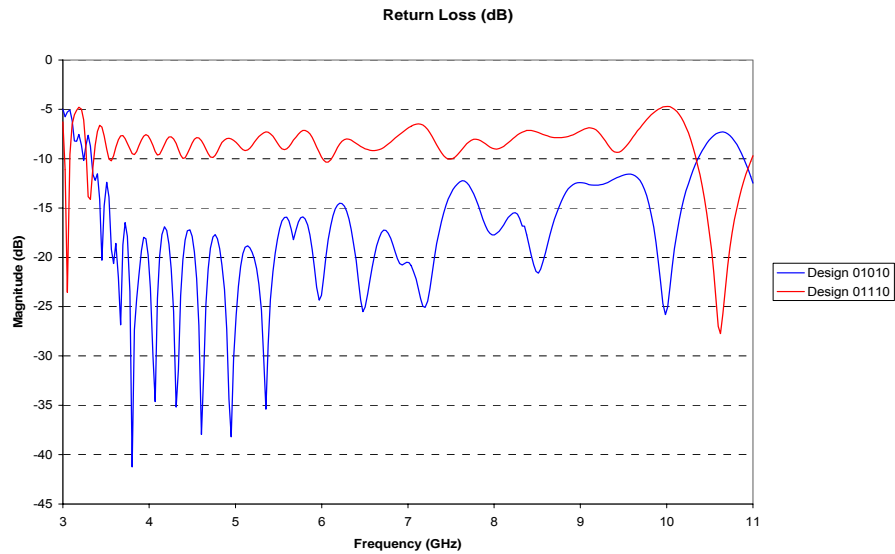


**Figure 4.1.15.** Return Loss Response for DOE I Design 01010 and Design 01110.

## 4.2 DOE II Results

The following tables present the results from DOE II. The simulations were performed with Ansoft Designer between 3 GHz and 11 GHz. Although each simulation consists of 300 frequency points, the following tables present the mean, minimum and maximum of the most important parameters. The statistical models were based on these responses and these results are explained later on. Finally, a comparison between designs establishes the effects that the variation in the level of each main factor has on the impedance bandwidth and the radiation characteristics of the antenna.

**Table 4.6.** Mean and Minimum Values of the Reflection Coefficient of DOE II.

<i>Experiment</i>	<i>Alternate Name</i>	<i>S11_mean(dB)</i>	<i>S11_min(dB)</i>	<i>S11_min(mag)</i>	<i>S11_mean(mag)</i>
1	0	-14.9625	-37.6157	0.0132	0.2076
A	1	-12.4373	-29.1182	0.0350	0.2666
B	10	-18.8768	-38.9755	0.0113	0.1391
Ba	11	-10.8015	-20.4376	0.0951	0.3021
C	100	-14.5173	-34.6736	0.0185	0.2150
Ca	101	-8.5997	-14.7940	0.1821	0.3839
Cb	110	-14.0363	-22.6920	0.0734	0.2140
Cba	111	-5.4184	-17.2834	0.1367	0.5474

<i>Experiment</i>	<i>Alternate Name</i>	<i>S11_mean(dB)</i>	<i>S11_min(dB)</i>	<i>S11_min(mag)</i>	<i>S11_mean(mag)</i>
D	1000	-16.6850	-37.6918	0.0130	0.1720
Da	1001	-12.3025	-35.6344	0.0165	0.2682
Db	1010	-18.7342	-45.5156	0.0053	0.1435
Dba	1011	-11.0935	-23.2383	0.0689	0.2973
Dc	1100	-15.2610	-38.7599	0.0115	0.1952
Dca	1101	-8.5536	-18.3743	0.1206	0.3871
Dcb	1110	-14.8218	-44.5066	0.0060	0.1995
Dcba	1111	-5.3278	-14.1762	0.1955	0.5538
E	10000	-17.9031	-43.0261	0.0071	0.1539
Ea	10001	-16.1201	-35.9752	0.0159	0.1812
Eb	10010	-14.1266	-27.5918	0.0417	0.2208
Eba	10011	-16.9184	-30.0383	0.0315	0.1738
Ec	10100	-18.0006	-40.5206	0.0094	0.1530
Eca	10101	-10.4189	-20.5671	0.0937	0.3114
Ecb	10110	-20.9390	-39.6893	0.0104	0.1172
Ecba	10111	-8.7293	-23.1344	0.0697	0.3796
Ed	11000	-15.6050	-34.6515	0.0185	0.1920
Eda	11001	-16.0466	-26.6812	0.0463	0.1808
Edb	11010	-13.2519	-30.7667	0.0290	0.2375
Edba	11011	-16.6503	-36.4975	0.0150	0.1748
Edc	11100	-14.6953	-39.0276	0.0112	0.2000
Edca	11101	-10.1734	-23.0390	0.0705	0.3233
Edcb	11110	-20.5208	-38.4615	0.0119	0.1089
Edcba	11111	-8.0478	-22.7511	0.0729	0.4076

**Table 4.7.** Mean, Minimum and Maximum Values of VSWR and Input Resistance of DOE II.

<i>Experiment</i>	<i>Alternate Name</i>	<i>VSWR(mean)</i>	<i>VSWR(min)</i>	<i>VSWR(max)</i>	<i>Rmin</i>	<i>Rmax</i>
1	0	1.5812	1.0267	3.7977	13.2868	108.1504
A	1	1.8029	1.0725	3.8605	12.9558	131.0147
B	10	1.3686	1.0228	3.8593	13.3496	101.5752
Ba	11	1.9445	1.2102	4.9695	10.0725	137.0300
C	100	1.6036	1.0376	3.5674	14.1539	119.5395
Ca	101	2.3383	1.4453	4.5673	11.3662	197.2516
Cb	110	1.5837	1.1583	4.1909	17.2410	105.0504
Cba	111	3.5693	1.3167	7.6011	8.9331	198.5992
D	1000	1.4583	1.0264	4.3927	14.9389	133.4927
Da	1001	1.8165	1.0336	3.2164	15.8520	111.5991
Db	1010	1.3772	1.0107	3.9783	12.7192	97.7794
Dba	1011	1.9253	1.1479	3.8866	14.7814	114.7766
Dc	1100	1.5267	1.0233	3.2200	15.7197	123.6209
Dca	1101	2.3701	1.2742	4.2519	12.6227	191.6301

Decb	1110	1.5265	1.0120	2.5962	19.6407	88.7977
Dcba	1111	3.6858	1.4861	6.9473	8.8727	210.3387
E	10000	1.4084	1.0142	4.1670	15.2255	109.2340
Ea	10001	1.4789	1.0323	3.3493	19.2939	112.8572
Eb	10010	1.6222	1.0871	3.7073	14.8762	174.6458
Eba	10011	1.4809	1.0650	3.2757	16.7802	143.0066
Ec	10100	1.3978	1.0190	3.8313	24.1022	132.7312
Eca	10101	1.9435	1.2067	3.5258	18.1482	174.7667
Ecb	10110	1.2987	1.0209	3.1675	17.5929	157.3724
Ecba	10111	2.2835	1.1499	5.4163	16.9469	184.4627
Ed	11000	1.5295	1.0377	5.4936	9.2843	141.4225
Eda	11001	1.4777	1.0972	2.9162	23.3483	114.2988
Edb	11010	1.6698	1.0596	4.4402	11.8454	144.3697
Edba	11011	1.4754	1.0304	2.9413	19.2257	110.6118
Edc	11100	1.5274	1.0226	2.7915	20.5851	135.3587
Edca	11101	2.0040	1.1516	3.5856	17.8694	151.2473
Edcb	11110	1.2656	1.0242	3.3751	15.6834	120.3769
Edcba	11111	2.4421	1.1572	4.0835	14.0494	160.7210

**Table 4.8.** Mean, Maximum and Minimum Values of the Gain of DOE II.

<i>Experiment</i>	<i>Alternate Name</i>	<i>Gain_mean(dB)</i>	<i>Gain_max(dB)</i>	<i>Gain_min(dB)</i>
I	0	5.988847	7.68885	-4.72891
A	1	6.205893	7.732541	-0.62734
B	10	5.584287	7.694683	2.501151
Ba	11	8.221644	9.072595	2.84845
C	100	3.835187	6.394258	-2.55763
Ca	101	6.632941	7.937467	1.35414
Cb	110	8.82368	9.670665	3.652689
Cba	111	8.575949	9.450543	2.376739
D	1000	6.474403	7.95716	2.313652
Da	1001	6.673201	7.808821	3.389631
Db	1010	8.692015	9.437544	4.090733
DbA	1011	8.770938	9.471281	3.602535
Dc	1100	6.986364	8.353245	3.451357
Dca	1101	7.016155	8.096535	4.301817
Dcb	1110	9.265867	9.909912	5.264973
Dcba	1111	8.951273	9.690528	5.716281
E	10000	6.509762	7.821066	1.460405
Ea	10001	6.630534	7.822027	1.824518
Eb	10010	8.504031	9.294476	3.325818
Eba	10011	8.690585	9.390084	4.10949
Ec	10100	6.792116	8.536224	2.233314
Eca	10101	7.121746	8.302927	3.771917
Ecb	10110	9.095939	9.84573	5.140773

Ecba	10111	9.162772	9.787128	4.528844
Ed	11000	6.807941	8.070095	3.6847
Eda	11001	7.044726	7.940134	4.248464
Edb	11010	8.983143	9.692923	5.024636
Edba	11011	9.131402	9.8161	4.955738
Edc	11100	7.23822	8.348199	4.668632
Edca	11101	7.480602	8.437486	5.067042
Edcb	11110	9.514127	10.16932	5.781602
Edcba	11111	9.469001	10.11486	6.515995

**Table 4.9.** Standard Deviation and Variance of the Gain and Real part of Input Resistance of DOE II.

<i>Experiment</i>	<i>Alternate Name</i>	<i>Gain dB Std Deviation</i>	<i>Gain (dB) Variance</i>	<i>Input Resistance Variance</i>	<i>Input Resistance Std Deviation</i>
I	0	1.4136	1.9983	221.83	14.89
A	1	1.1701	1.3690	353.88	18.81
B	10	1.3607	1.8516	108.51	10.42
Ba	11	1.0731	1.1516	459.29	21.43
C	100	1.7342	3.0074	262.40	16.20
Ca	101	1.0850	1.1772	744.15	27.28
Cb	110	0.8859	0.7848	224.45	14.98
Cba	111	0.9253	0.8561	1789.06	42.30
D	1000	1.0054	1.0109	133.90	11.57
Da	1001	0.8911	0.7941	285.22	16.89
Db	1010	0.9255	0.8566	110.74	10.52
DbA	1011	0.8947	0.8005	442.71	21.04
Dc	1100	0.8675	0.7525	176.42	13.28
Dca	1101	0.8179	0.6690	650.99	25.51
Dcb	1110	0.6988	0.4883	178.38	13.36
Dcba	1111	0.7243	0.5246	1632.74	40.41
E	10000	1.0623	1.1285	150.53	12.27
Ea	10001	0.9783	0.9570	217.02	14.73
Eb	10010	0.9684	0.9377	386.57	19.66
Eba	10011	0.9044	0.8179	260.58	16.14
Ec	10100	1.0979	1.2055	176.01	13.27
Eca	10101	0.8353	0.6977	662.84	25.75
Ecb	10110	0.7701	0.5930	122.63	11.07
Ecba	10111	0.7488	0.5607	972.51	31.19
Ed	11000	0.8705	0.7579	228.49	15.12
Eda	11001	0.7263	0.5275	198.87	14.10
Edb	11010	0.8307	0.6901	386.84	19.67
Edba	11011	0.7578	0.5743	244.43	15.63
Edc	11100	0.7794	0.6075	249.47	15.79

Edca	11101	0.6097	0.3717	629.31	25.09
Edcb	11110	0.6726	1.0109	98.28	9.91
Edcba	11111	0.6377	0.4067	965.91	31.08

#### 4.2.1 Model for the Minimum of the Gain

The model tries to predict the minimum of the gain using the results from DOE II. The Normal plot presented in Figure 4.2.1 shows that for the gain the most influential factors are the scaling factor, the width of the slots (W) and the spacing between the slots (S). The other factors influencing the response are: the boom length, the impedance of the central line (Z) and two and three way interactions between the scaling factor and Z, the spacing between the slots (S) and Z and the width of the slots (W) and the scaling factor. The statistical model is presented in Equation 4.2.1.

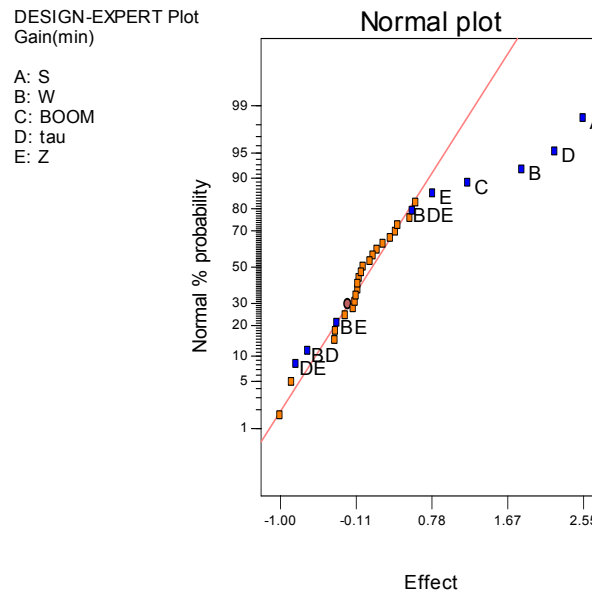


**Figure 4.2.1.** Graphical method for determining the parameters that affect the minimum of the gain using DOE II data.

$$\begin{aligned}
 \text{Gain (min)} = & 3.2279 + 1.0931A + 0.9185B + 0.6014C + 1.1119D + 0.5799E - \\
 & 0.3354BD - 0.3486BE - 0.5880DE + 0.4612BDE
 \end{aligned}
 \tag{4.2.1}$$

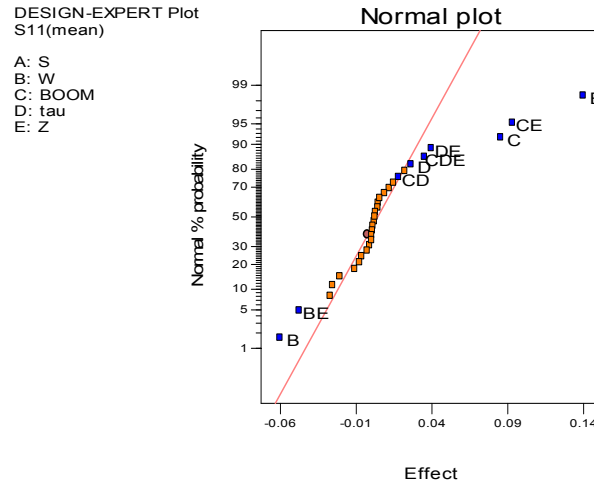
The model indicates that to obtain the maximum of the minimum gain it is necessary to set the levels of the main factors to high. The DOE II was performed with the idea in mind of identifying influential factors in the response other than the impedance of the central line where DOE I demonstrated that it is the most influential factor in the response. Setting the impedance to the high level helps to increase the minimum of the gain but it also causes the antenna to have a higher VSWR. This comes from the observations of DOE I and therefore it is not recommended to set  $Z$  to the high level. It is recommended to set the width of the slots and the scaling factor to the high level because they would increase the minimum by 2 dB. This tells us that by adding more elements the antenna is likely to exhibit an increase in gain.

Table A.4 shows the values predicted by the model as well as the actual values. There is very good agreement between the predicted and actual values. Figure A.4 shows that the residuals follow a normal distribution and also shows that the residuals present a random behavior. These are good signs that the model is accurate. However, Figure A.4 shows that there is an outlier, design 01100. From DOE I analysis, it was established that setting the boom length to the high level as in design 01100 causes the antenna to exhibit a high VSWR which is not desirable. Table A.4 shows that three designs have negative values in the minimum of the gain. This indicates that the designs have strange radiation characteristics. These results are located in the appendix section.

#### **4.2.2 Model for the Mean of the Reflection Coefficient**

This model tries to estimate the mean of the reflection coefficient. This was also attempted with DOE I. The differences between DOE I and DOE II are the values used for the impedance of the central lines. In DOE I, it was observed that the mean for almost all the designs that had  $Z$  set to the high level was above 0.33 (VSWR > 2). In this DOE, the level of variation was reduced. Like all the models presented previously, the most influential factors are the impedance of the central line ( $Z$ ) and the boom length (see Figure 4.2.2). The two way interaction between the boom length and the impedance

of the central line ( $Z$ ) is also important. Also, the width of the slots affects the response positively by setting  $W$  to the high level. The model is presented in Equation 4.2.2.



**Figure 4.2.2.** Graphical method for determining the parameters that affect the mean of the reflection coefficient using DOE II data.

$$S11(\text{mean}) = 0.2503 - 0.0305B + 0.0433C + 0.0133D + 0.0650E + 0.0531CE + 0.02598DE \quad (4.2.2)$$

The model is similar to the one proposed from the DOE I data. The main difference is that the values obtained for DOE II are smaller and therefore the intercept and the contributions of the factors are smaller. The important thing is that they have the same proportion as before. The two way interactions also play an important part. The model for the mean of the reflection coefficient has been improved from the model obtained from DOE I. The impedance of the central line ( $Z$ ) and the boom length along with their interactions affect negatively the response the most.

In Figure A.5, it is shown that the residuals follow a normal distribution and they also present a random behavior against the predicted values. The predicted values by the model are compared to the actual values in table A.5. These results are located in the appendix section.

### 4.2.3 Model for the Minimum of the Reflection Coefficient

The following model tries to estimate the minimum of the reflection coefficient. As shown by Figure 4.2.3, the most influential factors are the impedance of the central line ( $Z$ ), the boom length and the two way interaction between them. The model is presented in Equation 4.2.3. It establishes that the impedance of the central and the boom length are the factors that contribute a negative effect to the response. As in previous cases, it is recommended to set both factors to the low level to reduce the reflections to a minimum.

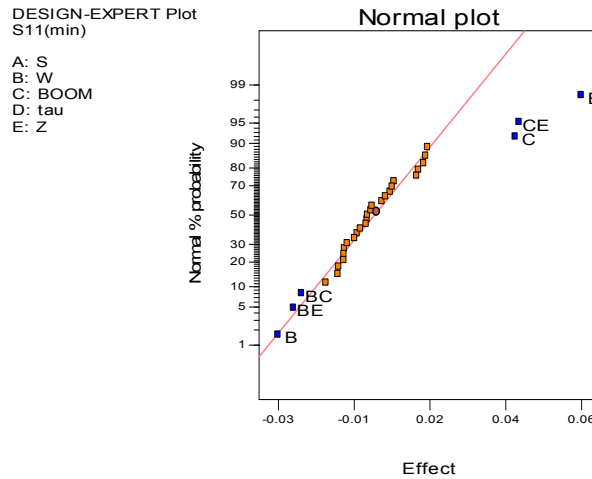


**Figure 4.2.3.** Graphical method for determining the parameters that affect the minimum of the reflection coefficient using DOE II data.

$$S11(\min) = 0.0487 - 0.014B + 0.0197C + 0.0291E - 0.0107BC - 0.0118BE + 0.0203CE \quad (4.2.3)$$

The residuals follow a normal distribution and show random behavior in the residuals versus predicted plot as presented in Figure A.6. These are good signs that the model can be trusted. The calculated and predicted values are presented in Table A.6. These results are located in the appendix section.

#### 4.2.4 Model for the Minimum of the VSWR

The following model tries to predict the minimum of the VSWR with the data from DOE II. This was attempted with the data from DOE I but it was not possible to obtain a statistical model with the data due to the fact that the high level of  $Z$  from DOE I ( $Z=150$  ohm) caused some designs to report a maximum of 50 for the VSWR and a minimum of 10 for some cases. Half of the designs reported a VSWR near 1 and the other half near 10. The model required nearly all the terms to predict the values.

For DOE II, the high level of  $Z$  was reduced to 85 ohms. This caused most designs to exhibit a minimum between 1 and 1.5. Now, the factors that affected the VSWR response of the antenna could be identified. It is no surprise to see again in the Normal plot (Figure 4.2.4) that the most influential factors affecting negatively the minimum of the VSWR are the boom length, the impedance of the central line ( $Z$ ) and their two way interaction. The width of the slots ( $W$ ) and the two way interactions of  $W$  with the impedance of the central line and the boom length affect the response positively. The model is presented in Equation 4.2.4. There is an additional consideration for this model. The VSWR quantity is always greater than 1. Fortunately, all the predicted values calculated with the model are greater than 1.

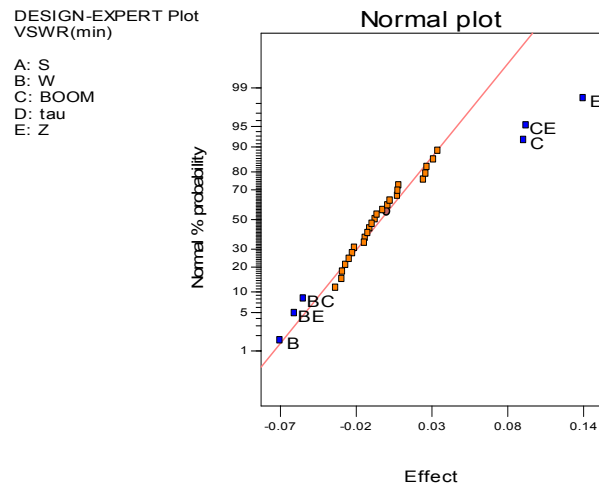


**Figure 4.2.4.** Graphical method for determining the parameters that affect the minimum of the VSWR using DOE II data.

$$VSWR (min) = 1.1088 - 0.0353B + 0.0479C + 0.0681E - 0.0273BC - 0.0303BE + 0.0487CE \quad (4.2.4)$$

The model suggest like all previous model on different antenna parameters that the boom length and the impedance of the central line ( $Z$ ) should be kept at the low level while keeping the width of the slots ( $W$ ) at the high level. The two way interactions play an important role in the model because their contributions do not allow the predicted values to fall below 1.

The normal plot of residuals follows a normal distribution. The residuals versus predicted values plot exhibit random behavior as expected in Figure A.7. The actual and predicted values are in very good agreement. These values are presented in Table A.7. These results are located in the appendix section.

#### **4.2.5 Model for the Minimum of the Input Resistance**

The remaining model estimates the minimum of the input resistance. According to the effects plot in Figure 4.2.5, the most influential factor to obtain the minimum of the input impedance is the width of the slots and two way interactions between the boom length and the impedance of the central line ( $Z$ ). It is highly desirable to obtain a minimum of the input resistance as close as possible to 50 ohms. If the value is very small, then the VSWR could be high and that is not desirable.

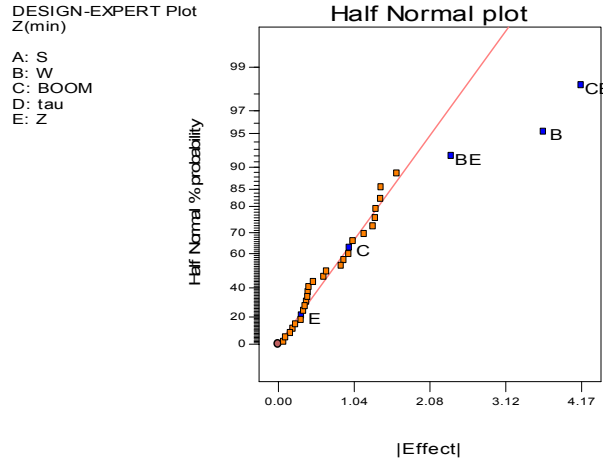


**Figure 4.2.5.** Graphical method for determining the parameters that affect the minimum of the real part of the input impedance using DOE II data.

$$R (min) = 15.36 + 1.82B + 0.49C - 0.16E + 1.19BE - 2.08CE \quad (4.2.5)$$

Table A.8 shows the values predicted by the model as well as the actual values. There is very good agreement between the predicted and actual values. Figure A.8 shows that the residuals follow a normal distribution and also shows that the residuals present a random behavior. These are good signs that the model is accurate.

#### 4.2.6 Effects in the Antenna Parameters

The DOE consisted of 32 runs. One way to evaluate the effects that each level has on the frequency response of the designs is to compare the frequency response of two designs at a time. This helps us to confirm the findings from the different statistical models based on one response for each design. In this case, the frequency response consists of 300 frequency points equally spaced between 3 and 11 GHz.

##### 4.2.6.1 Effects of the Scaling Factor in the Radiation Pattern

One of the main advantages of making the scaling factor larger is that the gain will increase by 2 dB. Another advantage is that anomalies present in the radiation

pattern on antennas with smaller scaling factors disappears. The following section compares the radiation characteristics between designs from DOE II where the scaling factor is varied.

In figure 4.2.6, the gain at maximum radiation between designs 10010 (eb) and 10000 (e) is presented. Design 10000 (e) shows drops of nearly 5 dB in some cases. This is not acceptable because the log periodic principle establishes that the radiation characteristics and the response of other antenna parameters should present the same behavior period after period. The big drops in gain when analyzed from a 3-D view perspective indicate that the radiation pattern exhibits sidelobes, backlobes and even a  $180^\circ$  main beam reversal appear in the radiation pattern. A 3-D view of design 10000 (e) at one of the frequency points where a huge drop is present is presented in Figure 4.2.7. The radiation pattern in Figure 4.2.8 is not what should be expected for log periodic antennas. The antenna with a scaling factor 0.89 with just 16 folded slot elements fails to maintain broadband backfire radiation mainly because the magnetic currents in the folded slot arms are not parallel. Two conditions are needed to maintain broadband backfire radiation; a  $180^\circ$  phase difference between the successive elements, and equal phases of the electric field (magnetic currents) on each arm of the folded slot. The first condition is easily accomplished since the CPW feed line provides the  $180^\circ$  phase difference between the elements. However, it is difficult to achieve the second condition with the baseline configuration (no phasing slot in Figure 3.1.1).

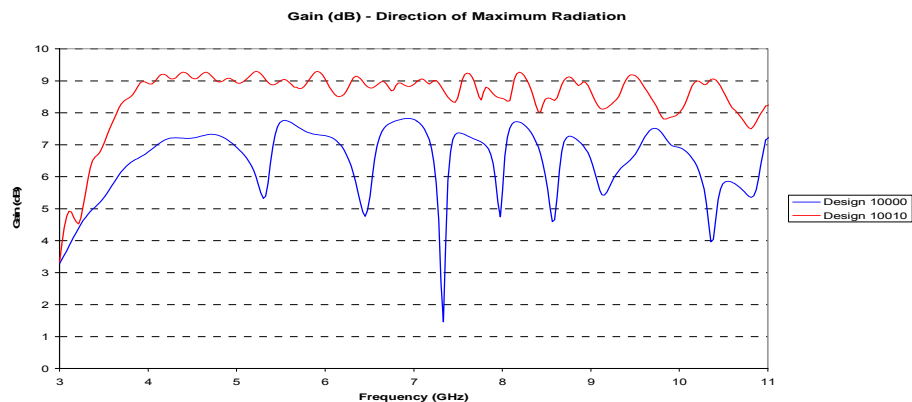


**Figure 4.2.6.** Gain in the Direction of Maximum Radiation for DOE II Design 10000 and Design 10010.

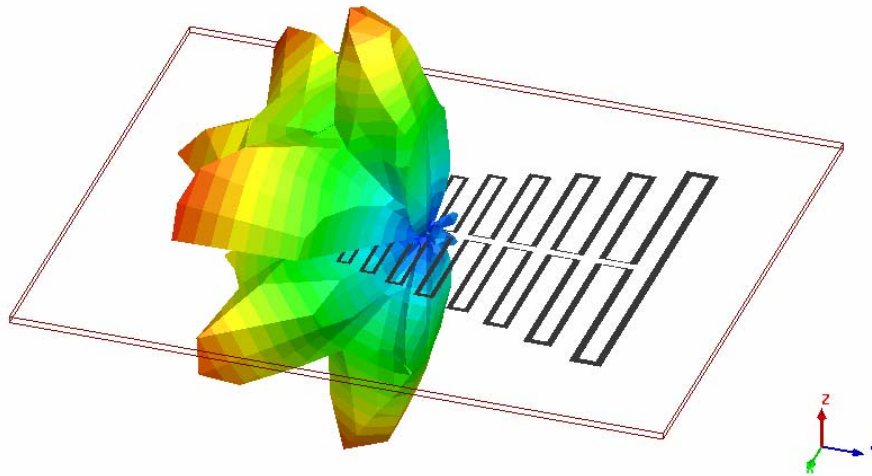


**Figure 4.2.7.** 3-D View of Radiation Pattern for DOE II Design 10000 ( $f = 10.86$  GHz)

The radiation pattern of design 10000 (e) ( $\phi=90^\circ$  and  $f=10.86$  GHz) shows a poor 15 dB front to back ratio. This is very bad because the 3-D representation shows major sidelobes and backlobes that should not be there.

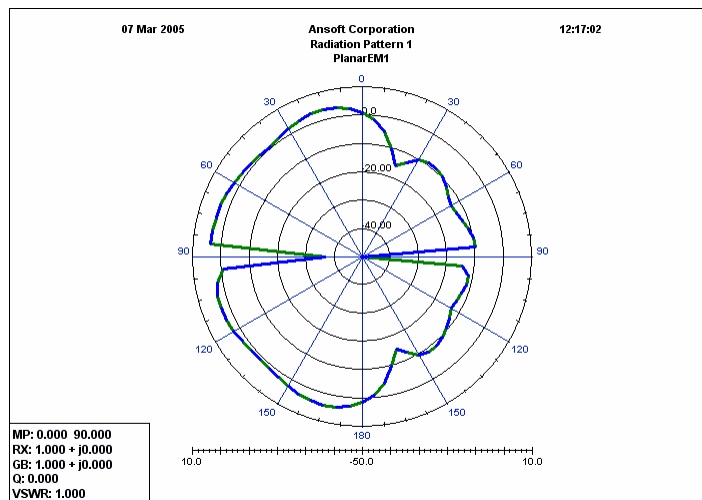


**Figure 4.2.8.** Radiation Pattern ( $\phi=90^\circ$ ) for DOE II Design 10000 ( $f = 10.86$  GHz).

On the other hand, the 3-D view of the radiation pattern at  $f=7.70$  GHz for Design 10010 (eb) (Figure 4.2.9) shows no anomalies. Note that there are no sidelobes and the beam is directed in the right direction. When the scaling factor is increased from 0.89 to 0.95 more folded slot elements will be added to the antenna. Thus, more folded slot

elements will reside in the active region, consequently improving not only the efficiency of the antenna, but also the stability of its far-field pattern.

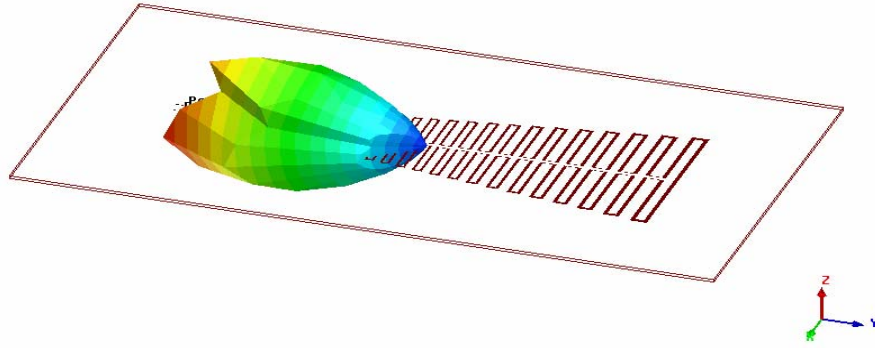


**Figure 4.2.9.** 3-D View of Radiation Pattern for DOE II Design 10010 ( $f = 7.70$  GHz).

Note that the backlobes in this case are small and there are no sidelobes. Also, the front to back ratio yields more than 30 dB.

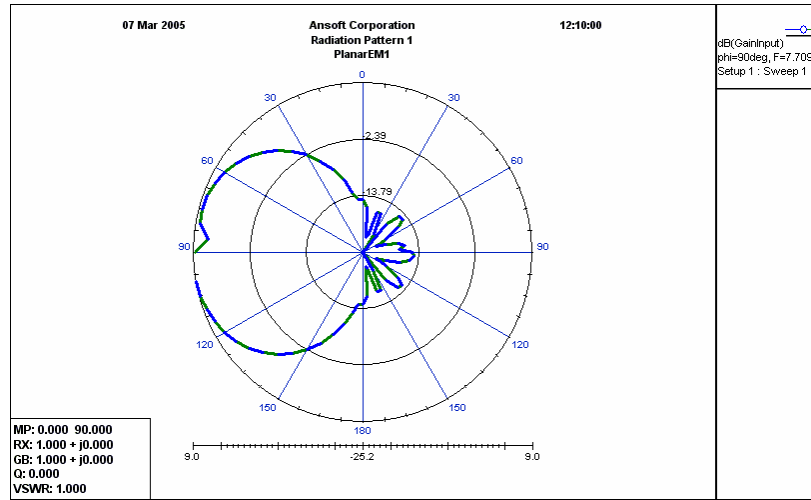


**Figure 4.2.10.** Radiation Pattern ( $\phi = 90^\circ$ ) for DOE II Design 10000 ( $f = 10.70$  GHz).

#### 4.2.6.2 Effects of the Scaling Factor in the Input Resistance

The scaling factor has little effect in the input resistance of a log periodic folded slot antenna. Data from DOE II show that the range of variation of the input resistance shrinks when the scaling factor goes from 0.89 to 0.95 (design 00000 versus 00010 (b)). This is the only case when the phenomenon occurs (see Figure 4.2.11). When other factors are set to high level increasing the scaling from 0.89 to 0.95, it makes no difference in the input impedance of the antenna. This can be observed in Figures 4.2.12 and 4.2.13 where designs 00101 (ca) and 00111 (cba) and also designs 10000 (e) and 10010 (eb) are compared.

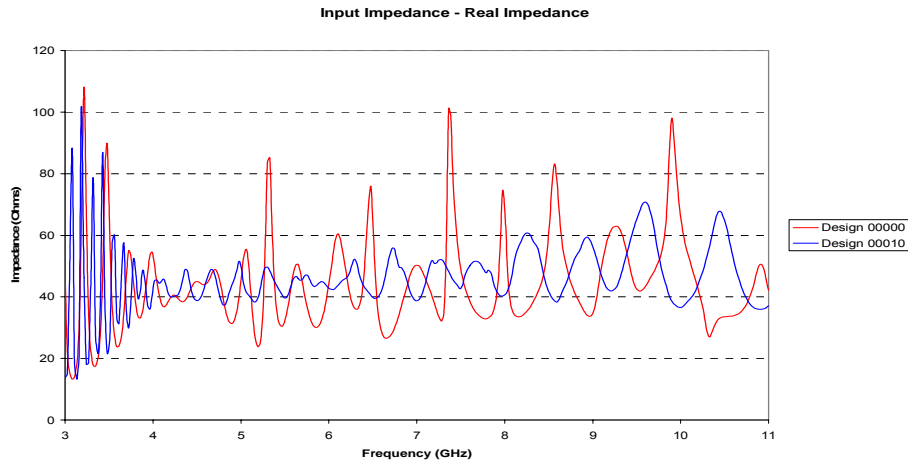


**Figure 4.2.11.** Input Resistance for DOE II Design 00000 and Design 00010.

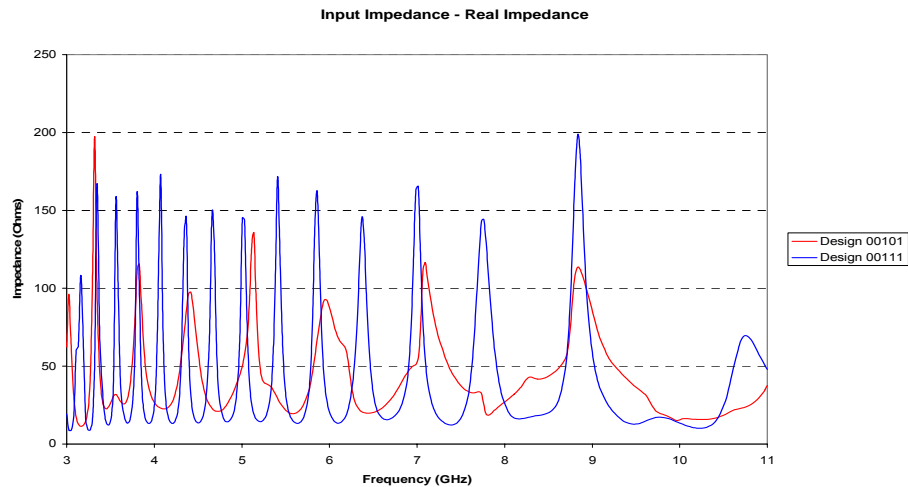


**Figure 4.2.12.** Input Resistance for DOE II Design 00101 and Design 00111.

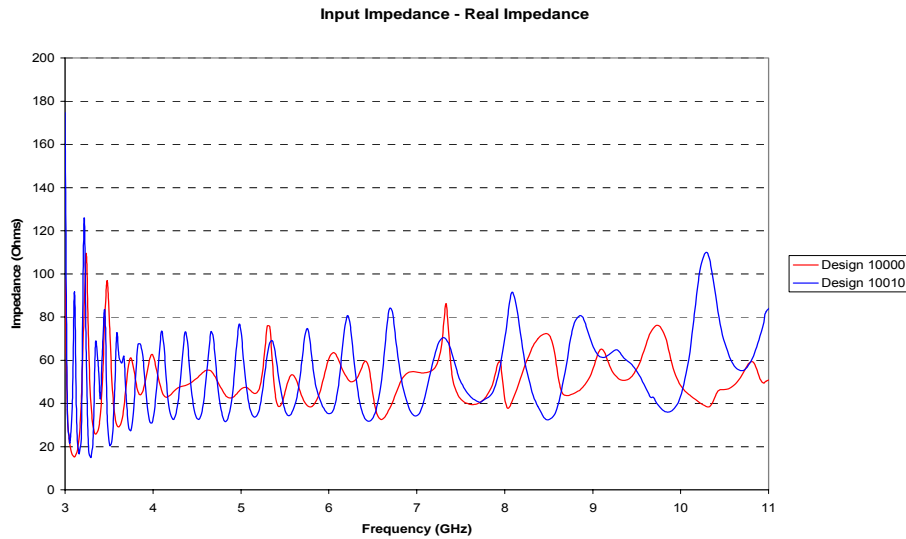


**Figure 4.2.13.** Input Resistance for DOE II Design 10000 and Design 10010.

#### 4.2.6.3 Effects of the Spacing between Slots in the Input Resistance

The spacing between the slots of the biggest element was varied between 2 mm and 4 mm. The scaling factor reduces these values for each subsequent element in the antenna. The effect is similar to the effect observed when the width of the slots was increased. When the spacing between the slots is increased the range where the input resistance varies shrinks. Although the shrinking effect is not as dramatic as the effect observed after increasing the width of the slots. One effect that was observed is that the peaks in the input resistance are shifted between the designs. This effect is observed in Figure 4.2.14 where a comparison between the input resistance of designs 00011 (ba) and 01011 (dba) is presented. Note that the red line (design 01011) (dba) is shrunk and shifted from the blue line (design 00011) (ba). The effect was observed in all the comparisons.

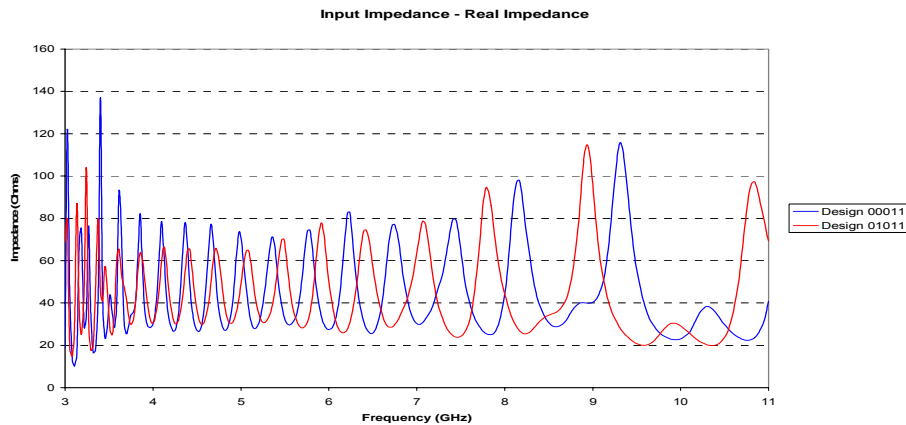


**Figure 4.2.14.** Input Resistance for DOE II Design 00011 and Design 01011.

#### 4.2.6.4 Effects of the Width of the Slots in the Input Resistance

In DOE II, the width of the largest slot on the biggest element was varied between 0.9 mm and 1.4 mm. The scaling factor reduces these values for each subsequent element in the antenna. The effect on the input resistance of the antenna when the width of the slots is set at the high level (1.4 mm) is very positive in most cases. It helps to reduce the range of variation of the input resistance which in turn reduces the VSWR. Figure 4.2.15 shows the input resistance plot of designs 00110 (cb) and 10110 (ecb). The range of variation of the input resistance shrunk with design 10110 (ecb) and also reduced the VSWR of the antenna with respect to design 00110 (cb).

In other cases, the input resistance response deteriorates when the width of the slots is set to the high level. This is the case between designs 00010 (b) and 10010 (eb) where the scaling factor is set to the high level and the remaining factors set to their lower level. The input resistance response of design 00010 (b) versus 10010 (eb) is presented in Figure 4.2.16. In this case, the range of variation of the input impedance increases when  $W$  is set to 1.4 mm. For DOE II, the phenomenon occurred also when designs 01010 (db) and 11010 (edb) were compared against each other. Interesting enough, the boom length is set to the low level in those designs. The problem is not present when the boom length is set to the high level. A total of 16 comparisons between all the designs in DOE II lead to the conclusion that the input impedance improves when

the width of the biggest slot is set to the high level at 1.4 mm with only two exceptions explained above.

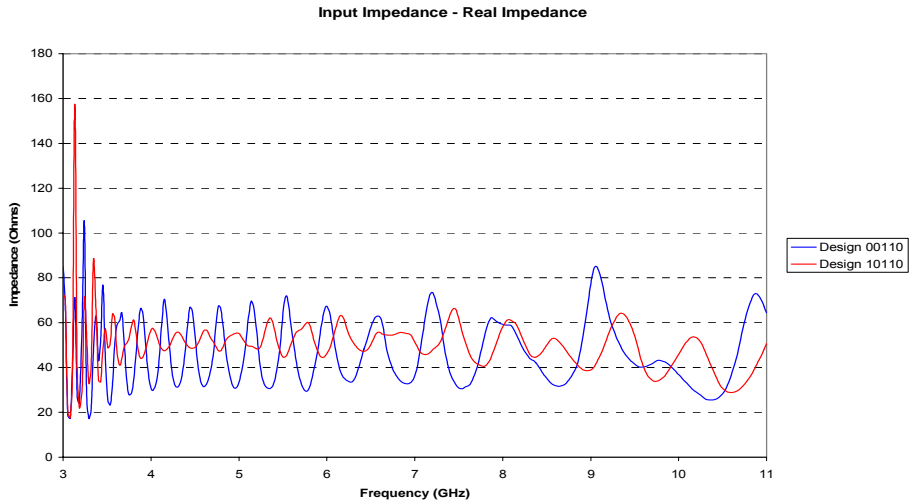


**Figure 4.2.15.** Input Resistance for DOE II Design 00110 and Design 10110.

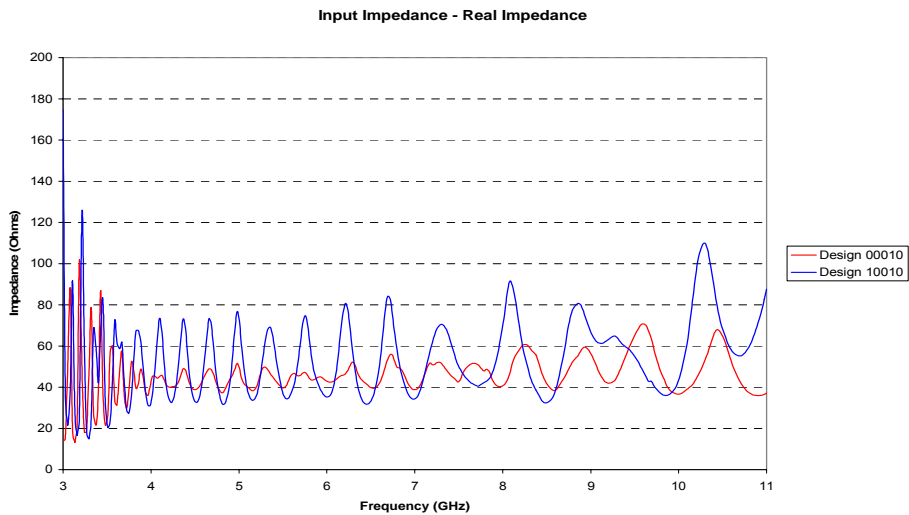


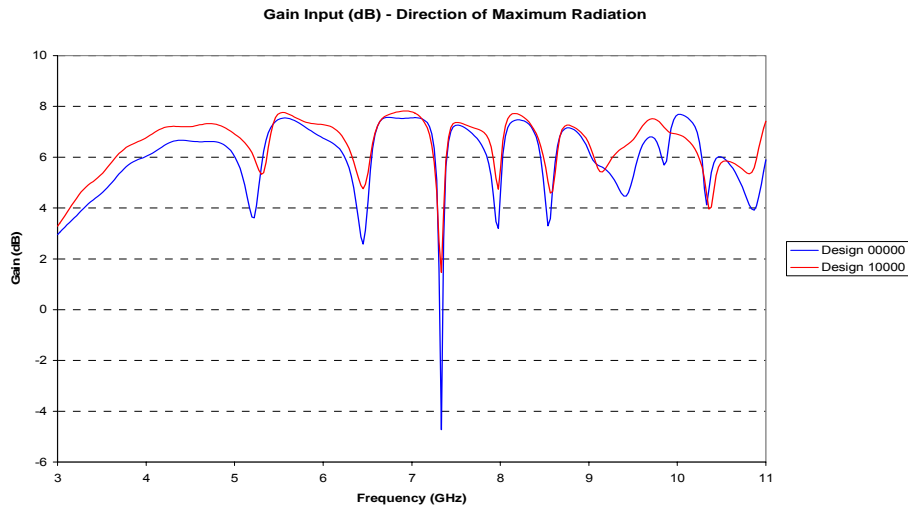
**Figure 4.2.16.** Input Resistance for DOE II Design 00010 and Design 10010.

#### 4.2.6.5 Effects of the Width of the Slots in the Radiation Pattern

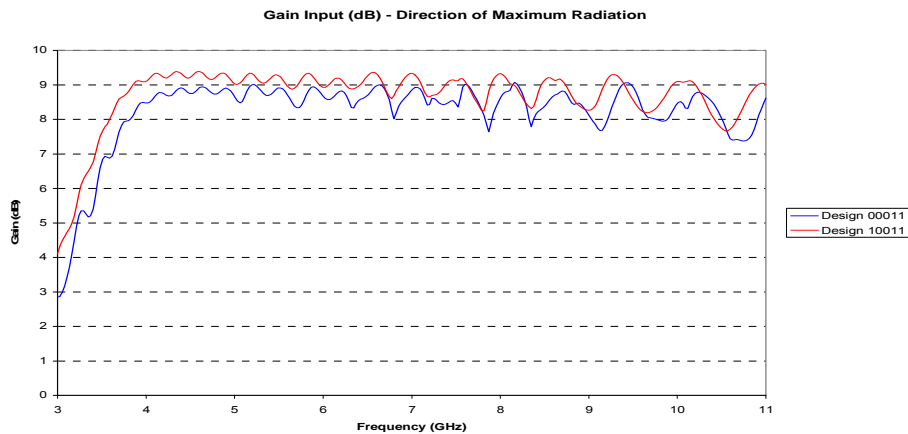
The gain of the log periodic antenna designs examined from the DOE II data increases slightly when the width of the slot of the largest element is increased from 0.9 mm to 1.4 mm. The phenomenon can be observed in Figures 4.2.17 and 4.2.18. In

Figure 4.2.17, the gain increases slightly when the width of the slots is increased to 1.4 mm. More important is the fact that the gain drops though still present in design 10000 (e), are reduced when the width of the slots is increased. The gain drops are still big and the problem in the radiation pattern still exists for design 10000 (e) with a scaling of 0.89.

In Figure 4.2.18, the comparison of the gain in the direction of maximum radiation is presented between designs 00011 (ba) and 10011 (eba). These designs have a scaling factor set to 0.95. This means that there are 33 folded slot elements in the antenna. It has been established before that by increasing the scaling from 0.89 to 0.95 the problems in the radiation pattern disappear. This is evident in Figure 4.2.18 where no large drops in gain are present. Here, the gain of the antenna increases slightly when the width of the slots is increased to 1.4 mm. The same phenomenon occurs in all the comparisons possible between the designs. Therefore, the effect of increasing the width of the largest slot to 1.4 mm is positive to the radiation characteristics of the antenna.



**Figure 4.2.17.** Gain in the Direction of Maximum Radiation for DOE II Design 00000 and Design 10000.



**Figure 4.2.18.** Gain in the Direction of Maximum Radiation for DOE II Design 00011 and Design 10011.

#### 4.2.6.6 Effects of the Spacing between Slots in the Radiation Pattern

The effect of increasing the spacing between the slots from 2 mm to 4 mm in the largest element is similar to the effect experienced in the radiation pattern when the width of the slots is increased. The gain increases slightly when the spacing between the slots in each folded slot element.

### 4.3 DOE III Results

The following tables present the results from DOE III. The simulations were performed with Ansoft Designer between 3 GHz and 11 GHz. Although each simulation consists of 300 frequency points, the following tables present the mean, minimum and maximum of the most important parameters. The statistical models were based on these responses and these results are explained later on. Finally, a comparison between designs establishes the effects that the variation in the level of each main factor has on the impedance bandwidth and the radiation characteristics of the antenna.

The purpose of this DOE is to find a solution to the problems in the radiation pattern of LPFSA with a scaling of 0.89 or less. Specifically, the proposed solution

includes the widening of the side slots of each folded slot element to correct the phase of the Electric Field between the folded slot arms.

**Table 4.10.** Mean and Minimum Values of the Reflection Coefficient for DOE III.

<i>Experiment</i>	<i>Alternate Name</i>	<i>S11_mean(dB)</i>	<i>S11_mean(mag)</i>	<i>S11_min(dB)</i>	<i>S11_min(mag)</i>
1	0	-8.1505	0.4326	-20.3278	0.0963
A	1	-6.9558	0.5127	-22.4467	0.0755
B	10	-14.0151	0.2520	-34.8006	0.0182
Ba	11	-10.1042	0.3569	-34.4957	0.0188
C	100	-4.8869	0.5850	-15.0349	0.1771
Ca	101	-3.6298	0.6767	-10.9350	0.2840
Cb	110	-11.4655	0.3251	-33.8731	0.0202
Cba	111	-10.4005	0.3804	-35.1103	0.0176
D	1000	-5.6794	0.5496	-14.3886	0.1908
Da	1001	-4.3677	0.6268	-12.5303	0.2363
Db	1010	-12.2960	0.3232	-31.9806	0.0252
DbA	1011	-11.8451	0.3331	-52.4355	0.0024
Dc	1100	-3.6459	0.6762	-23.5822	0.0662
Dca	1101	-2.1113	0.7959	-10.2030	0.3089
Dcb	1110	-8.0119	0.4468	-27.2204	0.0435
dcbA	1111	-5.0081	0.5911	-16.9300	0.1424

**Table 4.11.** Mean, Minimum and Maximum Values of VSWR and Input Resistance of DOE III.

<i>Experiment</i>	<i>Alternate Name</i>	<i>VSWR(mean)</i>	<i>VSWR(min)</i>	<i>VSWR(max)</i>	<i>Rmean</i>	<i>Rmin</i>	<i>Rmax</i>
1	0	2.8727	1.2131	5.7039	54.9058	15.4968	190.6814
A	1	4.2311	1.1632	10.3651	50.8244	5.2687	325.9517
B	10	1.8195	1.0371	5.9664	62.7108	15.7403	265.6272
Ba	11	2.3792	1.0384	8.0537	57.5554	6.9981	323.6344
C	100	4.3011	1.4305	8.7029	54.2251	10.0747	284.2881
Ca	101	6.7134	1.7931	14.8152	49.9439	3.3924	472.8879
Cb	110	2.1761	1.0413	4.0506	57.2071	17.8800	150.1582
Cba	111	2.7602	1.0357	6.1210	56.5515	8.1938	181.8373
D	1000	4.1805	1.4716	9.7771	54.1909	8.1461	282.6484
Da	1001	5.5842	1.6189	14.9117	50.7854	5.0743	416.5383
Db	1010	2.3724	1.0517	5.4718	59.1646	12.7285	210.4767
DbA	1011	2.4132	1.0048	7.6387	55.6043	13.5103	310.0836
Dc	1100	6.2800	1.1418	14.1068	53.0321	5.8579	438.3075
Dca	1101	11.9989	1.8940	34.0514	43.3779	1.7783	778.8137
Dcb	1110	3.2182	1.0911	7.8795	59.2902	12.4500	232.2392
DcbA	1111	5.1383	1.3321	17.0802	53.5987	3.0555	285.2502

**Table 4.12.** Mean, Maximum and Minimum Values of the Gain of DOE III.

<i>Experiment</i>	<i>Alternate Name</i>	<i>Gain_max(dB)</i>	<i>Gain_min(dB)</i>	<i>Gain_mean(Db)</i>
1	0	7.7288	3.4367	6.5521
A	1	8.7768	4.8179	7.9569
B	10	7.6812	3.4072	6.8885
Ba	11	8.9307	2.8593	8.2945
C	100	7.9350	4.3298	6.9094
Ca	101	9.0359	5.5929	8.2027
Cb	110	7.9343	4.4443	7.2475
Cba	111	9.4478	5.3903	8.8541
D	1000	7.6926	2.5753	6.3956
Da	1001	8.5882	4.9671	7.6488
Db	1010	7.6839	3.1494	6.7853
DbA	1011	8.8561	4.1710	8.1830
Dc	1100	7.8119	3.9456	6.7138
Dca	1101	8.4159	0.3420	6.8629
Dcb	1110	7.9302	4.0924	7.1720
Dcba	1111	9.2570	4.4635	8.3086

**Table 4.13.** Mean, Minimum and Maximum Values of VSWR and Input Resistance.

<i>Experiment</i>	<i>Alternate Name</i>	<i>Gain dB Std Deviation</i>	<i>Gain (dB) Variance</i>	<i>Input Resistance Variance</i>	<i>Input Resistance Std Deviation</i>
1	0	0.8590	0.7379	1822.255	42.68788
A	1	0.7291	0.5316	2914.496	53.98608
B	10	0.7782	0.6056	630.2244	25.10427
Ba	11	0.9444	0.8920	1203.368	34.6896
C	100	0.6994	0.4891	3576.805	59.8064
Ca	101	0.6356	0.4040	5574.427	74.66209
Cb	110	0.5872	0.3448	939.9965	30.65936
Cba	111	0.6437	0.4143	1367.265	36.97655
D	1000	1.0016	1.0033	3094.268	55.62614
Da	1001	0.8104	0.6567	4311.36	65.66095
Db	1010	0.8874	0.7875	1139.843	33.76157
DbA	1011	0.8488	0.7205	1673.4	40.90721
Dc	1100	0.8180	0.6691	5789.389	76.08804
Dca	1101	1.6647	2.7713	9124.099	95.52015
Dcb	1110	0.6972	0.4861	2162.271	46.50023
dcba	1111	1.0804	0.7379	3353.304	57.90772

### 4.3.1 Model for the Mean of the Gain

The following model tries to estimate the mean of the gain. The Normal plot presented in Figure 4.3.1 indicates that the influential factors in the mean of the gain are the impedance of the central line ( $Z$ ), the scaling factor and the width of the side slots. The two way interaction between the impedance of the central line ( $Z$ ) and the scaling factor play also an important role in the gain response of the antenna. The model is presented in Equation 4.3.1.

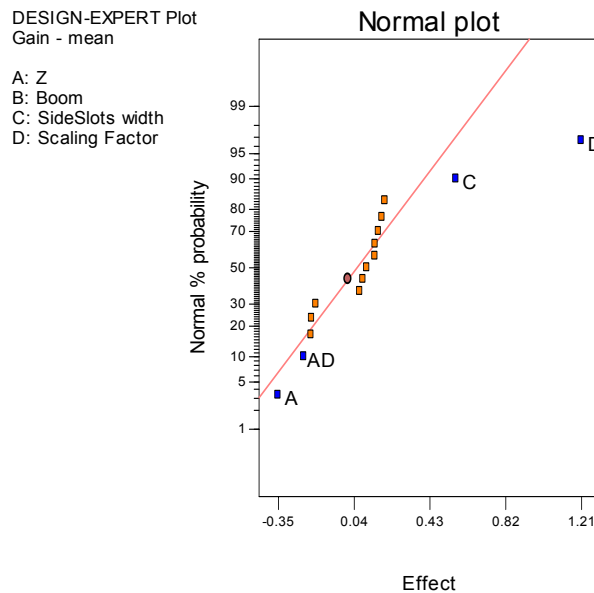


**Figure 4.3.1.** Graphical method for determining the parameters that affect the mean of the gain using DOE III data.

$$Gain (mean) dB = 7.4360 - 0.1772A + 0.2807C + 0.6030D - 0.1109AD \quad (4.3.1)$$

To obtain the maximum value for the equation above is recommended to set the width of the side slots to the high level and set the impedance of the central line ( $Z$ ) to the low level. The model failed to point out the big influence that the boom length has on the response of the antenna. When the boom length is set to the high level, big dropouts are experienced especially at high frequencies. The model failed to pick this mainly because just one point is used in the model for each experiment.

The Normal plot of residuals (Figure A.9) follows a normal distribution. The residuals versus predicted values plot show random behavior in Figure A.9. This is what is expected of a good prediction model. The actual and predicted values are in very good agreement. They are presented in Table A.9. These results are located in the appendix section.

### 4.3.2 Model for the Mean of the Reflection Coefficient

The following model estimates the mean of the reflection coefficient. Even though one point is used for each experiment it is enough to determine the influential factors in the response. The Normal plot in Figure 4.3.2 shows that the most influential factors are the side slots width and the boom length. The impedance of the central line ( $Z$ ) and the three way interaction between  $Z$ , the boom length and the side slots width play a smaller role in the response of the antenna. It is important to point out that the side slots width have a serious impact on the return loss response of the antenna. The equation describing the model is presented in Equation 4.3.2.

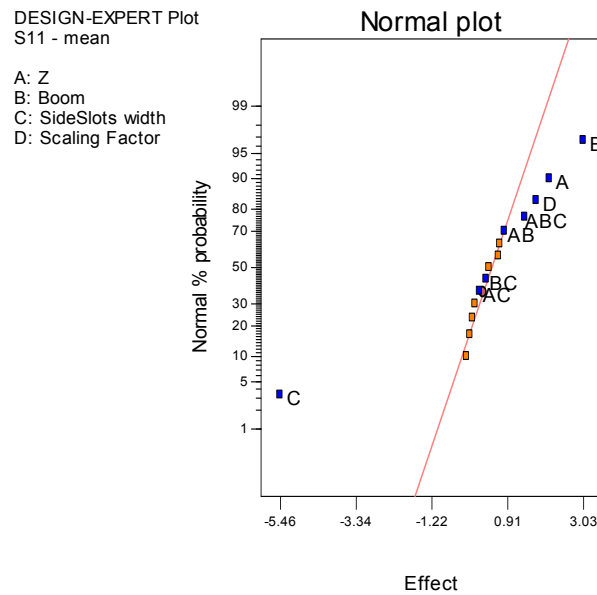


**Figure 4.3.2.** Graphical method for determining the parameters that affect the mean of the reflection coefficient using DOE III data.

$$S_{11} \text{ (mean) dB} = -7.6609 + 1.0402A + 1.5159B - 2.7324C + 0.8580D + 0.4105AB + 0.0628AC + 0.1559BC + 0.6979ABC \quad (4.3.2)$$

The objective with the model is to obtain the smallest value as possible. The ideal goal is to obtain a value less than -10 dB (VSWR < 2). The best way to achieve this is to set the side slots width to the high level and the boom length to the low level.

Table A.10 shows the values predicted by the model as well as the actual values. There is very good agreement between the predicted and actual values. Figure A.10 shows that the residuals follow a normal distribution and also shows that the residuals present a random behavior. These are good signs that the model is accurate. These results are located in the appendix section.

### **4.3.3 Model for the Minimum of the Input Resistance**

The remaining model estimates the minimum of the input resistance. The value should be as large as possible but less than 50 ohms to prevent a VSWR>2. The Normal plot shows (Figure 4.3.3) that the influential factors in the response are the side slots width, the impedance of the central line and the scaling factor. The proposed model is presented in Equation 4.3.3.

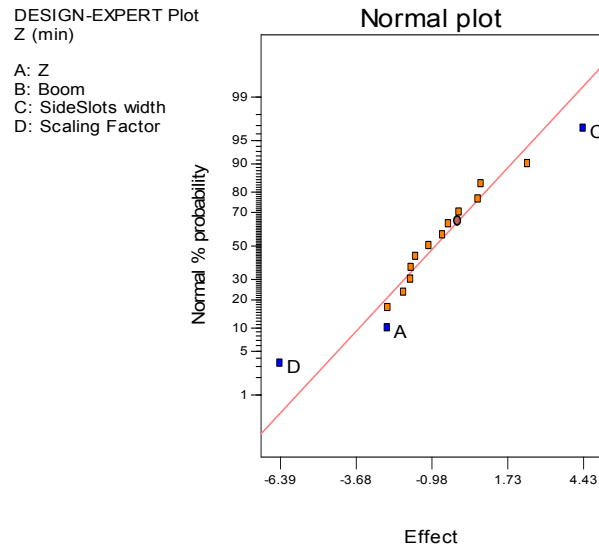


**Figure 4.3.3.** Graphical method for determining the parameters that affect the minimum of the input resistance using DOE III data.

$$R (\min) = 9.1028 - 1.2778A + 2.2167C - 3.1939D \quad (4.3.3)$$

To increase the minimum value of the input resistance, the width of the side slots must be set to the low level and the impedance of the central line and the scaling factor should be set to the high level. The width of the side slots has a positive impact on the response when they are set to the high level.

Table A.11 shows the values predicted by the model as well as the actual values. There is very good agreement between the predicted and actual values. Figure A.11 shows that the residuals follow a normal distribution and also shows that the residuals present a random behavior. These are good signs that the model is accurate. These results are located in the appendix section.

#### **4.3.4 Effects in the Antenna Parameters**

The DOE consisted of 16 runs. One way to evaluate the effects that each level has on the frequency response of the designs is to compare the frequency response of two designs at a time. This helps us to confirm the findings from the different statistical models based on one response for each design. In this case, the frequency response consists of 300 frequency points equally spaced between 3 and 11 GHz.

##### **4.3.4.1 Effects of the Widening of the Side Slots in the Return Loss Response and Radiation Pattern**

The width of the side slots was varied between 2.7 mm and 4.5 mm for the largest folded slot element for DOE III. The objective was to analyze the impact of the widening of the side slots in the impedance bandwidth and the radiation characteristics of the antenna. The return loss response between designs 0000 and 0010 (b) is presented in Figure 4.3.4. There is a big difference in the return loss response between the two designs. When the side slots width is increased the return loss response improves considerably. One negative effect of the technique devised to help improve the radiation characteristics of the antenna is that the bandwidth is reduced. In Figure 4.3.4 is shown that the  $VSWR < 2$  until 8.5 GHz. It is important to point out that the scaling factor is varied in this DOE and designs 0000 and 0010 (b) have a scaling factor of 0.85 with just 12 folded slot elements. The bandwidth of the antenna is reduced by 28% when this technique is used. But if the VSWR constraints are relaxed the antenna works for the entire range of operation for a  $VSWR < 2.5$ . All the possible comparisons between all the designs concluded that if the widening of the side slots is kept at the low level it will destroy the impedance bandwidth of the antenna as shown in Figure 4.3.4 with design 0010 (b).

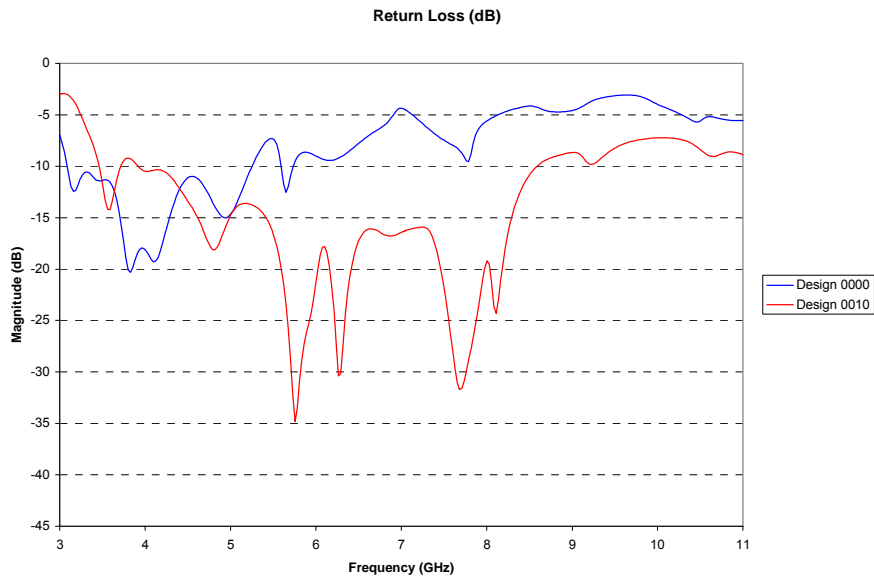


**Figure 4.3.4.** Return Loss Response for DOE III Design 0000 and Design 0010.

The radiation characteristics of the antenna configuration change dramatically when the width of the side slots is varied between the two levels. When the width of the side slots of the biggest element is set to 2.7 mm (low level), the radiation pattern is not stable and drops in gain are still experienced. However, when the width of the side slots of the biggest element is set to 4.5 mm (high level), the radiation pattern is stable. Therefore, the phase of the electric field on the slots are in phase when the width of the side slots is increased to the high level since no dropouts in gain or backlobes are experienced. The radiation pattern of some designs is presented in Figure 4.3.5 and 4.3.6. Note that the gain becomes stable when the width of the side slots is increased to the high level (designs 0000 and 0011 (ba)). However, the radiation pattern becomes unstable at high frequencies when the scaling factor and the boom length are both set to the high level mainly because having these factors simultaneously set to the high level destroys the impedance bandwidth of the antenna configuration. This effect can be observed in Figure 4.3.6.

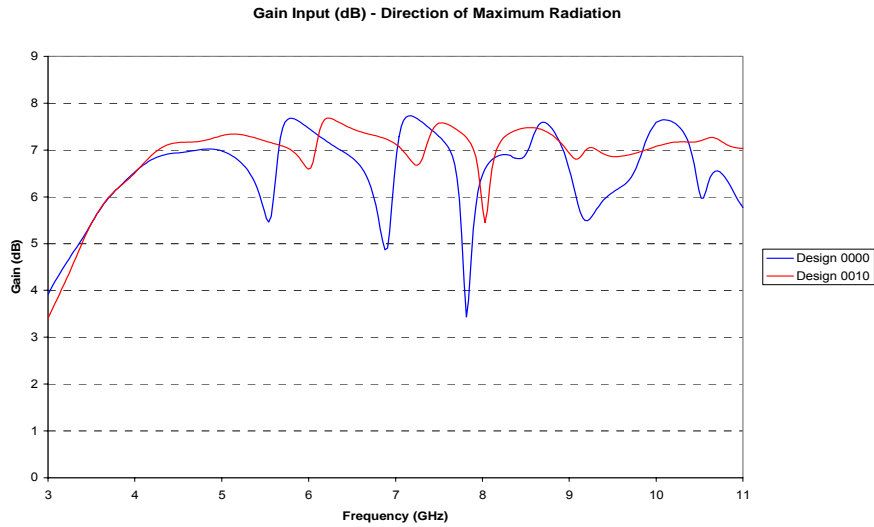


**Figure 4.3.5.** Gain in the Direction of Maximum Radiation for DOE III Design 0000 and Design 0010.

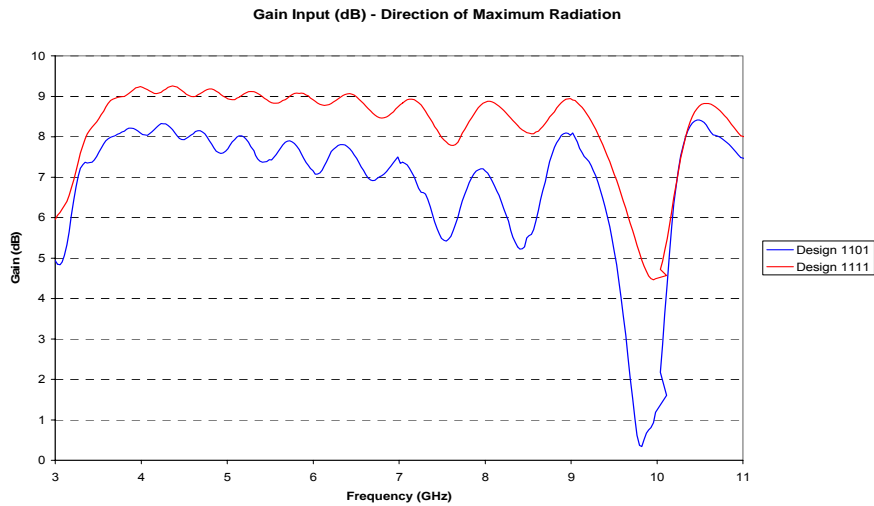


**Figure 4.3.6.** Gain in the Direction of Maximum Radiation for DOE III Design 1101 and Design 1111.

#### 4.3.4.2 Effects of the Scaling Factor in the Return Loss Response and Radiation Pattern

For this DOE, the scaling factor was varied between 0.85 and 0.92. An antenna with a scaling factor of 0.85 consists of 12 folded slot elements. Meanwhile, an antenna with a scaling factor consists of 21 folded slot elements. In general, the VSWR increases

when the scaling factor is increased to 0.92. The return loss response between designs 0010 (b) and 0011 (ba) is presented in Figure 4.4.7. The plot shows that the return loss increases when the scaling factor is increased. This behavior could be explained by the fact that the impedance of the feeder line for these designs is now 115 ohms. The same behavior was observed for all the designs. On the other hand, the radiation characteristics are improved when the scaling factor increases from 0.85 to 0.92.

The fact that the radiation pattern characteristics improve when the scaling factor increases is not a surprise because it was established since the first DOE that when the scaling factor increases it helps to improve the radiation characteristics. A comparison between the gain of designs 0000 and 0001 (a) at the direction of maximum radiation is presented in Figure 4.4.8. The huge drops in gain that are related to the instability of the radiation pattern disappear when the scaling factor is increased. Now, the drops in gain are less than 1 dB for the entire frequency range.

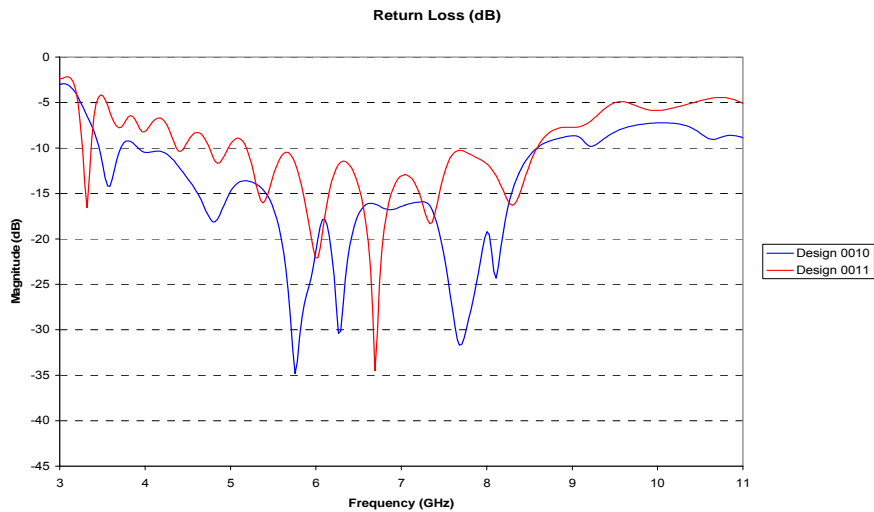


**Figure 4.3.7.** Return Loss Response for DOE III Design 0010 and Design 0011.

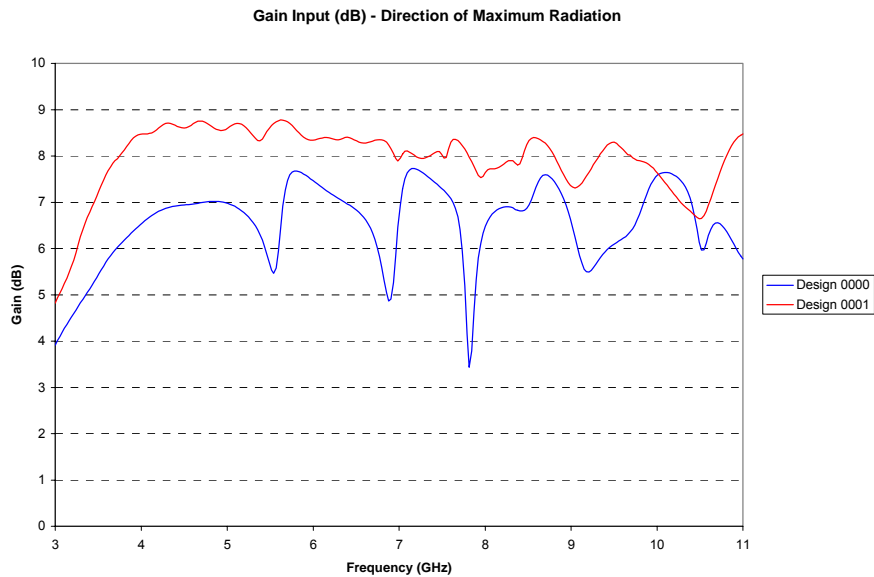


**Figure 4.3.8.** Gain in the Direction of Maximum Radiation for DOE III Design 0000 and Design 0001.

#### 4.3.4.3 Effects of the Boom Length in the Return Loss Response and Radiation Pattern

The boom length has been identified as one of the factors that affect the frequency response of log periodic folded slot antennas the most. The effect of increasing the boom length is evaluated now that the side slots are wider than the top and bottom slots to improve the radiation characteristics of the antenna. In Figure 4.3.9, the return loss responses of designs 0100 (c ) and 0000 is presented. It is observed that the VSWR increases when the boom length is set to the high level. The same behavior was observed in all the comparisons made between the different designs.



**Figure 4.3.9.** Return Loss Response for DOE III Design 0000 and Design 0100.

The radiation characteristics are not affected greatly when the boom length is set to the high level. The comparison of the gain between designs 0010 (b) and 0110 (cb) indicates that the radiation characteristics do not change much when the boom length is increased. This can be explained by the fact that the impedance of the feeder line is now between 115 and 145 ohms and the input impedance of each folded slot element is now different from DOE I and II because the side slots are now wider. The same behavior was observed on the other designs.

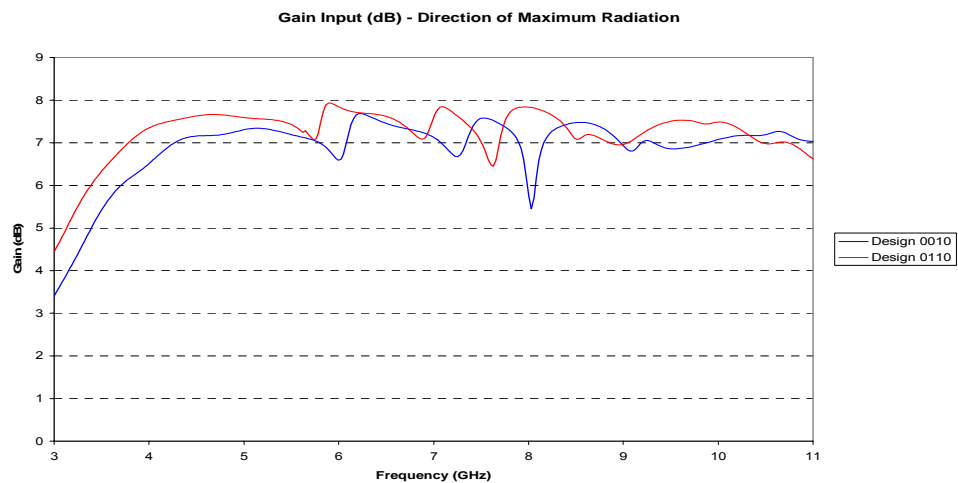


**Figure 4.3.10.** Gain in the Direction of Maximum Radiation for DOE III Design 0010 and Design 0110.

#### 4.3.4.4 Effects of the Impedance of the Central Line in the Return Loss Response and Radiation Pattern

All the statistical models agree on the fact that the most important factor in the design of log periodic folded slot antennas is the impedance of the central line ( $Z$ ). In this DOE, the same behavior is observed, that is, the return loss response worsens when the impedance of the central line is increased to the high level. This behavior can be observed in Figure 4.3.11. Only one exception occurs and is observed in Figure 4.3.12. This is the case when the antenna has  $Z$  set to 145 ohms and the scaling factor to 0.92 along with the widest side slots possible.

The radiation characteristics of the antenna are affected when the impedance of the line is increased to 145 ohms and the scaling factor is set to the high level especially at high frequencies. This can be observed in Figure 4.3.13. The comparison between designs with a scaling factor of 0.85 indicated that the radiation characteristics are not affected greatly when the scaling factor is set to the low level independent of the level chosen for the impedance of the feeder line.

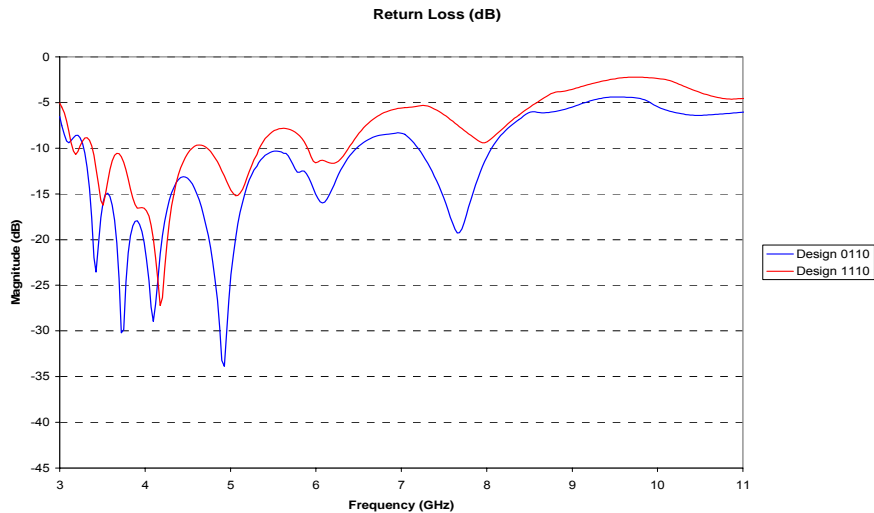


**Figure 4.3.11.** Return Loss Response for DOE III Design 0110 and Design 1110.

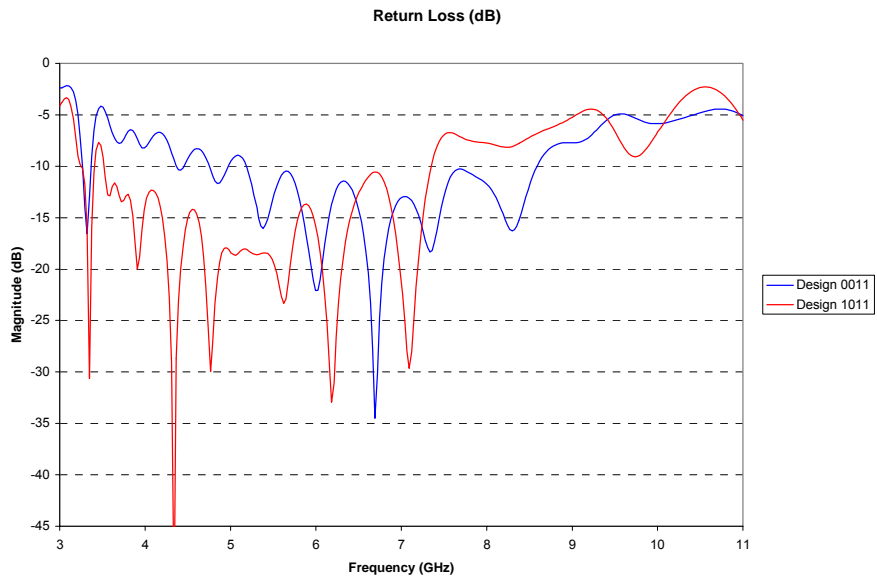


**Figure 4.3.12.** Return Loss Response for DOE III Design 0011 and Design 1011.

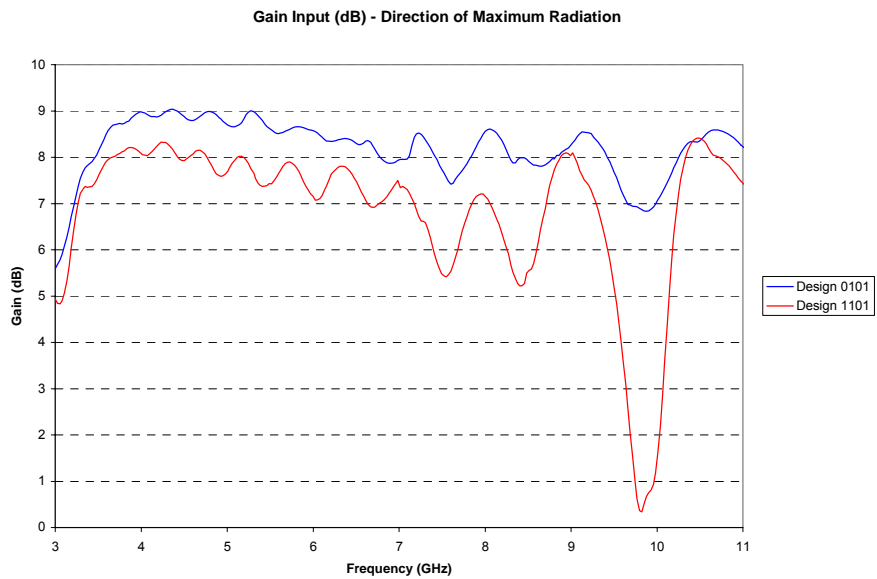


**Figure 4.3.13.** Gain in the Direction of Maximum Radiation for DOE III Design 0101 and Design 1101.

#### 4.4 DOE IV Results

The following tables present the results from DOE IV. The simulations were performed with Ansoft Designer between 3 GHz and 11 GHz. Although each simulation consists of 300 frequency points, the following tables present the mean, minimum and maximum of the most important parameters. The statistical models were based on these responses and these results are explained later on. Finally, a comparison between designs establishes the effects that the variation in the level of each main factor has on the impedance bandwidth and the radiation characteristics of the antenna.

The purpose of this DOE is to find a solution to the problems in the radiation pattern of LPFSA with a scaling of 0.89 or less. Specifically, the proposed solution includes the etching of a phasing slot in the middle of each folded slot element to correct the phase of the Electric Field between the folded slot arms. The phasing slots insure that the magnetic currents in the folded slot arms are parallel.

**Table 4.14.** Mean and Minimum Values of the Reflection Coefficient of DOE IV.

<i>Experiment</i>	<i>Alternate Name</i>	<i>S11_mean(dB)</i>	<i>S11_min(dB)</i>	<i>S11_min(mag)</i>	<i>S11_mean(mag)</i>
1	0	-17.4565	-39.4023	0.0107	0.1633
A	1	-17.3339	-36.3666	0.0152	0.1627
B	10	-18.1580	-43.1023	0.0070	0.1524
Ba	11	-18.0565	-36.3890	0.0152	0.1523
C	100	-20.8443	-53.7577	0.0021	0.1232
Ca	101	-19.7277	-40.7999	0.0091	0.1273
Cb	110	-21.1532	-49.6952	0.0033	0.1171
Cba	111	-19.7087	-50.6519	0.0029	0.1280
D	1000	-17.3624	-40.0429	0.0100	0.1636
Da	1001	-17.3412	-32.4444	0.0239	0.1575
Db	1010	-16.8812	-44.3397	0.0061	0.1693
DbA	1011	-16.4743	-32.3089	0.0242	0.1686
Dc	1100	-10.9722	-21.6193	0.0830	0.2940
Dca	1101	-11.9389	-31.3920	0.0269	0.2696
Dcb	1110	-10.8921	-23.2511	0.0688	0.2971
dcba	1111	-11.9402	-29.1849	0.0347	0.2718

**Table 4.15.** Mean, Minimum and Maximum Values of VSWR and Input Resistance of DOE IV.

<i>Experiment</i>	<i>Alternate Name</i>	<i>VSWR(mean)</i>	<i>VSWR(min)</i>	<i>VSWR(max)</i>	<i>Rmean</i>	<i>Rmin</i>	<i>Rmax</i>
1	0	1.4480	1.0217	5.1508	52.2992	11.5274	131.1771
A	1	1.4500	1.0309	4.7848	56.7231	10.4913	183.9532
B	10	1.4099	1.0141	4.7135	53.0194	11.9674	142.6435
Ba	11	1.4175	1.0308	4.6339	58.5380	12.6782	174.4893
C	100	1.3177	1.0041	4.3276	55.1470	24.0644	194.9972
Ca	101	1.3253	1.0184	4.8617	57.8096	20.1153	96.0957
Cb	110	1.2964	1.0066	4.2269	55.2312	23.1279	159.7854
Cba	111	1.3215	1.0059	4.2702	59.0090	18.9608	96.6943
D	1000	1.4234	1.0201	2.9504	52.6477	18.8498	119.6390
Da	1001	1.4022	1.0489	3.0117	56.2922	19.6808	144.4902
Db	1010	1.4384	1.0122	2.6030	53.2758	19.2988	114.3475
DbA	1011	1.4330	1.0497	3.1895	57.4938	30.3547	146.4137
Dc	1100	1.8684	1.1810	3.5240	52.8262	23.8096	165.4430
Dca	1101	1.7720	1.0554	3.2491	55.2179	26.5256	151.7961
Dcb	1110	1.8825	1.1477	3.6419	53.1505	23.4455	160.0784
Dcba	1111	1.7840	1.0720	3.2985	56.2553	26.2109	149.9823

**Table 4.16.** Mean, Maximum and Minimum Values of the Gain of DOE IV.

<i>Experiment</i>	<i>Alternate Name</i>	<i>Gain_max(dB)</i>	<i>Gain_min(dB)</i>	<i>Gain_mean(Db)</i>
1	0	8.3373	1.8943	7.2540
A	1	8.0140	4.1749	7.3870
B	10	8.2526	3.0347	7.3380
Ba	11	8.0358	4.4854	7.4575
C	100	8.8745	2.9190	7.7337
Ca	101	8.4341	6.3067	7.8860
Cb	110	8.8407	2.9996	7.7704
Cba	111	8.5475	5.5272	7.9872
D	1000	8.2391	4.3542	7.4108
Da	1001	8.0686	4.7446	7.4374
Db	1010	8.2113	4.4843	7.4524
DbA	1011	8.0964	5.1076	7.4753
Dc	1100	8.7657	3.9012	7.9063
Dca	1101	8.6959	5.6527	7.9785
Dcb	1110	8.7447	4.8575	7.9515
Dcba	1111	8.7588	5.7403	8.0366

**Table 4.17.** Mean, Minimum and Maximum Values of VSWR and Input Resistance of DOE IV.

<i>Experiment</i>	<i>Alternate Name</i>	<i>Gain dB Std Deviation</i>	<i>Gain (dB) Variance</i>	<i>Input Resistance Variance</i>	<i>Input Resistance Std Deviation</i>
1	0	1.0696	1.1441	176.4677	13.28412
A	1	0.5344	0.2856	231.8504	15.22663
B	10	0.9455	0.8940	163.2265	12.77601
Ba	11	0.4934	0.2435	227.1347	15.07099
C	100	1.1389	1.2972	193.4178	13.90747
Ca	101	0.3786	0.1434	115.271	10.73643
Cb	110	1.0889	1.1857	135.1402	11.62498
Cba	111	0.5136	0.2638	112.3554	10.59978
D	1000	0.7958	0.6333	194.7917	13.95678
Da	1001	0.5003	0.2503	193.8007	13.92123
Db	1010	0.7261	0.5273	209.7045	14.48118
DbA	1011	0.4671	0.2182	221.0243	14.86689
Dc	1100	0.8175	0.6683	609.3653	24.68532
Dca	1101	0.4843	0.2345	546.6698	23.38097
Dcb	1110	0.7265	0.5278	632.7037	25.1536
Dcba	1111	0.4567	0.1113	574.6046	23.97091

#### 4.4.1 Model for the Minimum of the Gain

The following model tries to estimate the minimum of the gain. The model is important because it identifies the factors that cause the gain to drop dramatically. The minimum of the gain is a very important quantity even though only one point is analyzed for each experiment. The value allows us to establish which designs likely exhibit anomalies in the radiation will pattern even though the phasing slot is now being used to correct the problems in the radiation pattern. The Normal plot presented in Figure 4.4.1 establishes that the most influential factor in determining the minimum of the gain of the LPFSA with phasing slot is the length of the phasing slot. It also identifies that the impedance of the central line ( $Z$ ) is still an influential factor in the gain response. The widths of the slots play a minor role in the gain response along with the two way interaction between the width of the slots and the length of the phasing slot. The two way interaction of the impedance of the central line ( $Z$ ) and the length of the phasing slot

affects the response negatively because is located on the left side of the Normal plot. The objective here is to make the minimum value of the gain to be as big as possible. The model is presented in Equation 4.4.2.

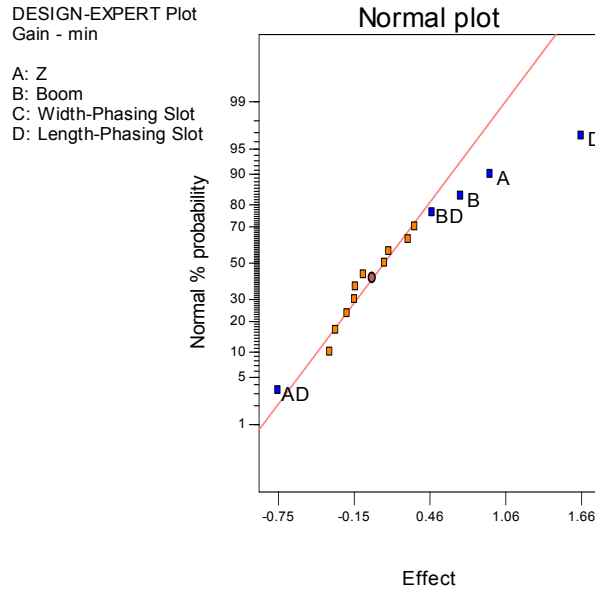


**Figure 4.4.1.** Graphical method for determining the parameters that affect the minimum of the gain using DOE IV data.

$$Gain (min) = 4.39 + 0.47A + 0.35B + 0.83D - 0.37AD + 0.24BD \quad (4.4.1)$$

To obtain the maximum value for the equation above is recommended to set the width of the slots and the length of the phasing slot to the high level and set the impedance of the central line (Z) to the low level. The model failed to point out the big influence that the impedance of the central line exerts on the response of the antenna. Interesting enough, if Z is set to the low level the term of the two way interaction between Z and the length of the phasing slot nearly cancels with the term related to the contribution of Z to the response.

The Normal plot of residuals (Figure A.12) follows a normal distribution. The residuals versus predicted values plot show random behavior in Figure A.12. This is what is expected of a good prediction model. The actual and predicted values are in very

good agreement. They are presented in Table A.12. These results are located in the appendix section.

#### 4.4.2 Model for the Minimum of the Reflection Coefficient

The following model estimates the minimum of the reflection coefficient. In this case, the minimum of the entire frequency range for each model is used to estimate the quantity. Even though one point is used for each experiment it is enough to determine the influential factors in the response. The Normal plot in Figure 4.4.2 shows that the most influential factors are the impedance of the central line and the two way interaction between the impedance of the central line and the width of the slots. Note that neither the width nor the length of the phasing slot affects the response negatively. The phasing slot helps the radiation characteristics of the antenna but does not affect the impedance response of the antenna. The equation describing the model is presented in Equation 4.4.3.

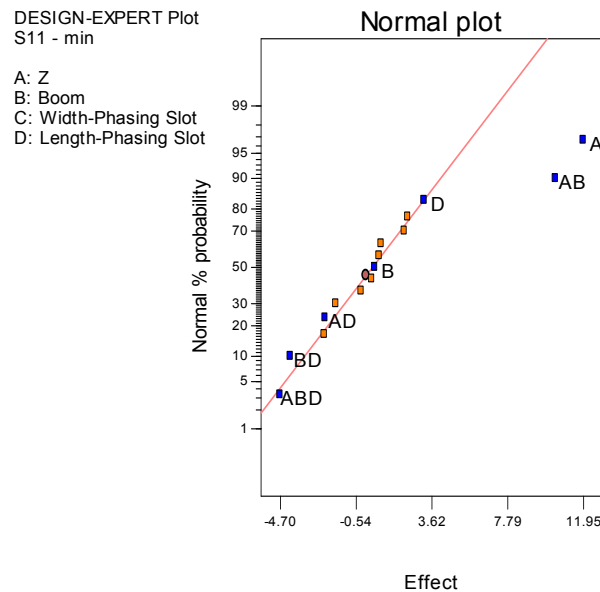


**Figure 4.4.2.** Graphical method for determining the parameters that affect the minimum of the reflection coefficient using DOE IV data.

$$S_{11} (\min) = -37.8 + 5.97A + 0.25B + 1.60D + 5.20AB - 1.11AD - 2.07BD - 2.35ABD \quad (4.4.2)$$

The objective with the model is to obtain the smallest value as possible. As mentioned before, the impedance of the central line ( $Z$ ) and the two way interaction between  $Z$  and the width of the slots affect the response negatively because it makes the value larger. The best settings to obtain the minimum value for the reflection coefficient is to set  $Z$  to low level and set the width of the slots to the high level. The width and length of the phasing slot is not important in the case under analysis but it is recommended to set the length of the phasing slot to the high level because it vastly improves the radiation pattern of the antenna.

Table A.13 shows the values predicted by the model as well as the actual values. There is very good agreement between the predicted and actual values. Figure A.13 shows that the residuals follow a normal distribution and also shows that the residuals present a random behavior. These are good signs that the model is accurate. These results are located in the appendix section.

#### **4.4.3 Model for the Maximum of the Input Resistance**

The next model estimates the maximum of the input resistance. It is important to maintain the maximum of the input impedance as small as possible. The smallest value possible for the maximum of the input resistance helps to maintain the  $V_{SWR} < 2$ . The Normal plot presented in Figure 4.4.3 shows that the impedance of the central line ( $Z$ ) affects the response negatively and the two way interaction between the length of the slots and the length of the phasing slot affects the response positively because it helps to reduce the maximum value. The two way interactions are very important for the model. The model is presented in Equation 4.4.4.

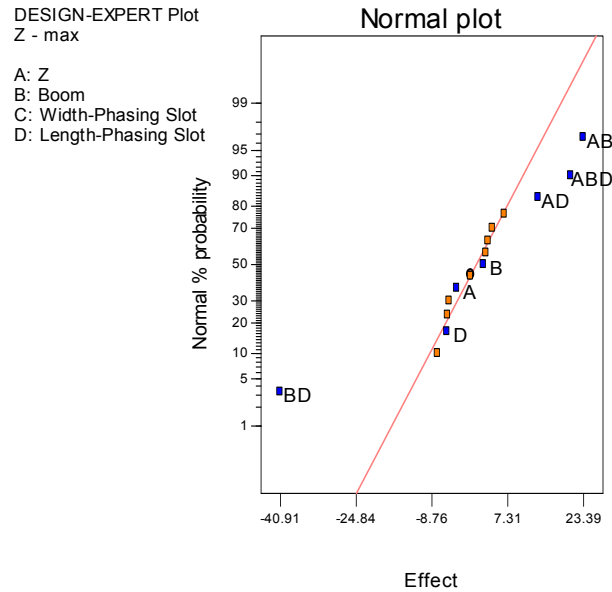


**Figure 4.4.3.** Graphical method for determining the parameters that affect the maximum of the input resistance using DOE IV data.

$$R (max) = 145.75 - 1.73A + 1.11B - 2.76D + 11.69AB + 6.91AD - 20.45BD + 10.37ABD \quad (4.4.3)$$

The minimum value for the equation above can be obtained by setting the impedance of the central line (factor A) to the low level and set the width of the slots (factor B) and the length of the phasing slot (factor D) to the high level. The biggest contribution comes from the two way interaction between the widths of the slots and the length of the phasing slot. Setting both factors to the high level will help to decrease the maximum value by 20. A reduction of 48 ohms in the maximum value of the input resistance is obtained by setting Z to the low level.

Figure A.14 strengthens the accuracy of the model because it shows the desirable characteristics of the residuals following a normal distribution and that the residuals present a random behavior. Table A.14 presents the predicted values using the model and the actual values. These results are located in the appendix section.

#### 4.4.4 Model for the Minimum of the Input Resistance

The remaining model estimates the minimum of the input resistance. The value should be as large as possible but less than 50 ohms to prevent a  $VSWR > 2$ . The Design Expert software recommended an inverse square transform to evaluate the model. After the transform was used, the Normal plot showed (Figure 4.4.4) that the influential factors in the response were the impedance of the central line ( $Z$ ) and the width of the slots and also the two way interaction between them. The proposed model is presented in Equation 4.4.5.

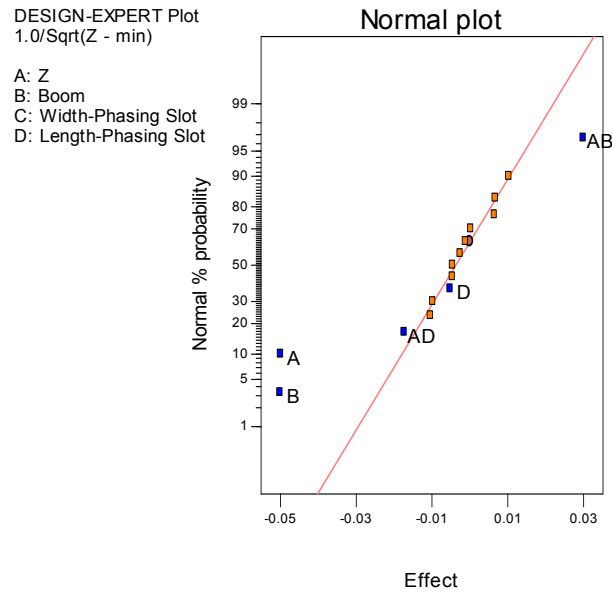


**Figure 4.4.4.** Graphical method for determining the parameters that affect the minimum of the input resistance using DOE IV data.

$$1.0/\text{sqrt}(R (\text{min})) = 0.23 - 0.02A - 0.02B - 0.004C - 0.00164D + 0.0015AB - 0.0075AD + 0.0058BC \quad (4.4.4)$$

To increase the minimum value of the input resistance, the impedance of the central line ( $Z$ ) must be set to low level because it has been proved that for the configuration higher values of  $Z$  the frequency response worsens. The remaining factors,

the width of the slots and the length of the phasing slot must be set to high level because they help to increase the minimum value of the input resistance. According to the model, the width of the phasing slot has a small negative effect in the response. Therefore, the width of the phasing slot must be set to the lower level.

Table A.15 shows the values predicted by the model as well as the actual values. There is very good agreement between the predicted and actual values. Figure A.15 shows that the residuals follow a normal distribution and also shows that the residuals present a random behavior. These are good signs that the model is accurate. These results are located in the appendix section.

#### **4.4.5 Effects in the Antenna Parameters**

The DOE consisted of 16 runs. One way to evaluate the effects that each level has on the frequency response of the designs is to compare the frequency response of two designs at a time. This helps us to confirm the findings from the different statistical models based on one response for each design. In this case, the frequency response consists of 300 frequency points equally spaced between 3 and 11 GHz.

##### **4.4.5.1 Effects of the Width of the Phasing Slot in the Return Loss Response and Radiation Pattern**

The width of the phasing slots was varied between  $.17S$  and  $.33S$  for DOE IV. The objective was to analyze the impact of the width of the phasing slots in the impedance bandwidth and the radiation characteristics of the antenna. The return loss response between designs 0001 (a) and 0011 (ba) is presented in Figure 4.4.5. The difference in the return loss response between the two designs is minimal. All the designs exhibited the same behavior: the width of the phasing slot makes no difference in the return loss of the antenna. The radiation characteristics remained also unchanged when the width of the phasing slot was varied between two values. The gain in the direction of maximum radiation of some designs is presented in Figure 4.4.6 and 4.4.7.

Note that the gain remains stable when designs 0001 (a) and 0011 (ba) are compared against each other. Likewise, big drops in gain are still observed when designs 0010 (b) and 0011 (ba) are compared against each other. The drops in gain are present because the length of the phasing slot is not sufficient to correct the problem in the radiation pattern. Therefore, the variation in the width of the phasing slot did not change the radiation characteristics of the antenna.

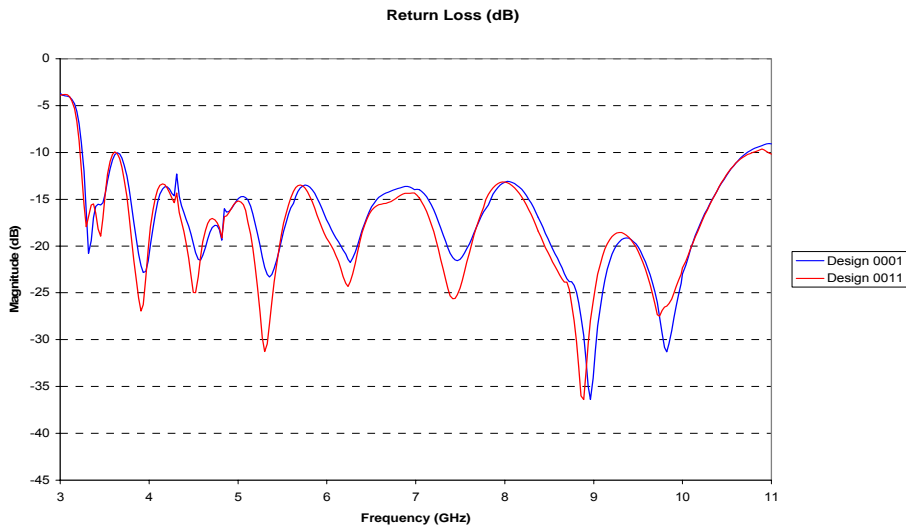


**Figure 4.4.5.** Return Loss Response for DOE IV Design 0001 and Design 0011.

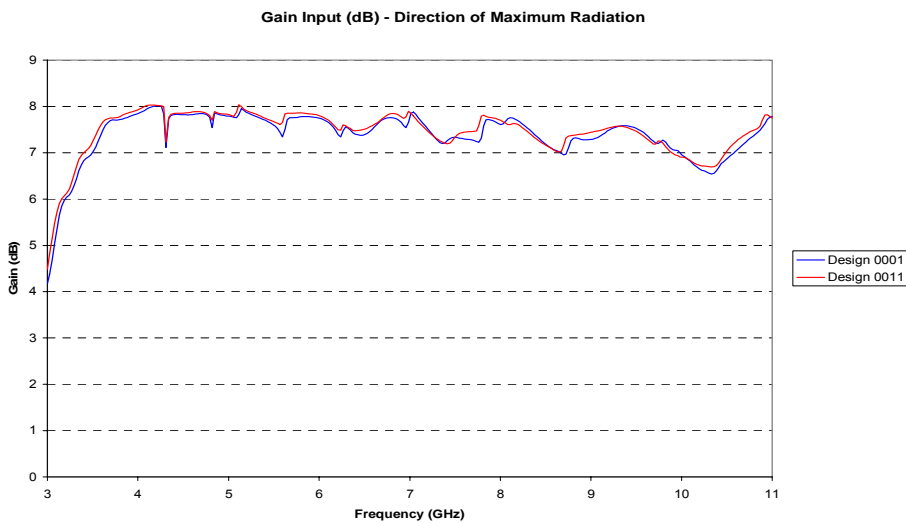


**Figure 4.4.6.** Gain in the Direction of Maximum Radiation for DOE IV Design 0001 and Design 0011.

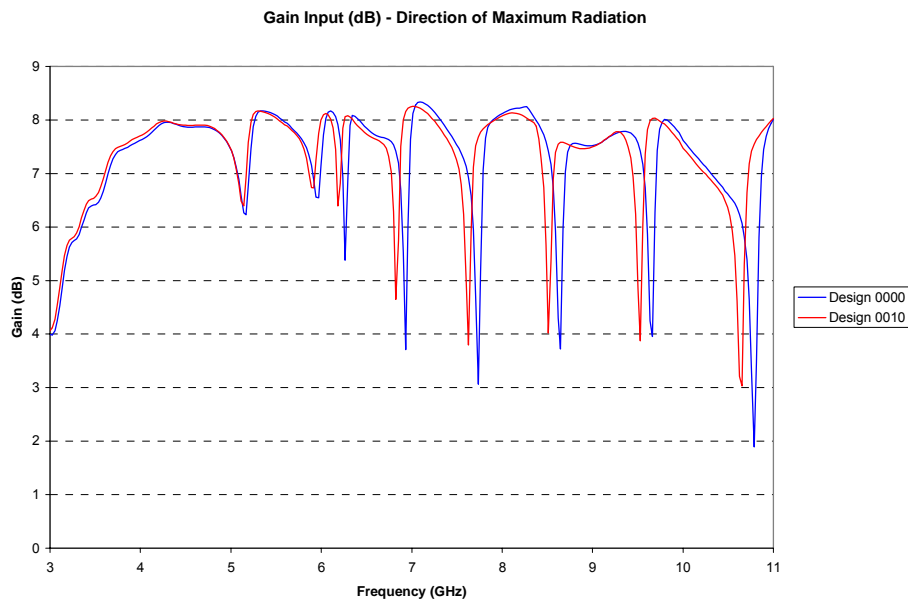


**Figure 4.4.7.** Gain in the Direction of Maximum Radiation for DOE IV Design 0000 and Design 0010.

#### 4.4.5.2 Effects of the Length of the Phasing Slot in the Return Loss Response and Radiation Pattern

The length of the phasing slots in the log periodic folded slot antenna configuration was varied between  $0.75\alpha$  and  $1.15\alpha$ . The length of a folded slot element in the LPFSA is  $2\alpha$ . A phasing slot was added to correct the problems with the radiation pattern of the baseline configuration. The return loss response between designs 0010 (b) and 0011 (ba) is presented in Figure 4.4.8. The plot shows that the return loss is not affected negatively if the length of the phasing slot is varied between  $0.75\alpha$  and  $1.15\alpha$ . The same behavior was observed for all the designs. On the other hand, the radiation characteristics are vastly improved when the length of the phasing slots is increased to  $1.15\alpha$ .

A comparison between the gain of designs 0010 (b) and 0011 (ba) at the direction of maximum radiation is presented in Figure 4.4.9. The huge drops in gain that are related to the instability of the radiation pattern disappear. Now, the drops in gain are

less than 1 dB for the entire frequency range. This behavior can be explained from the fact that now the phasing slot insure that the magnetic currents in the folded slot arms are parallel. The phase of the electric field on both folded slots arms along with the  $180^\circ$  phase difference between successive elements provided by the Coplanar Waveguide Feedline now insure a stable radiation pattern.



**Figure 4.4.8.** Return Loss Response for DOE IV Design 0010 and Design 0011.

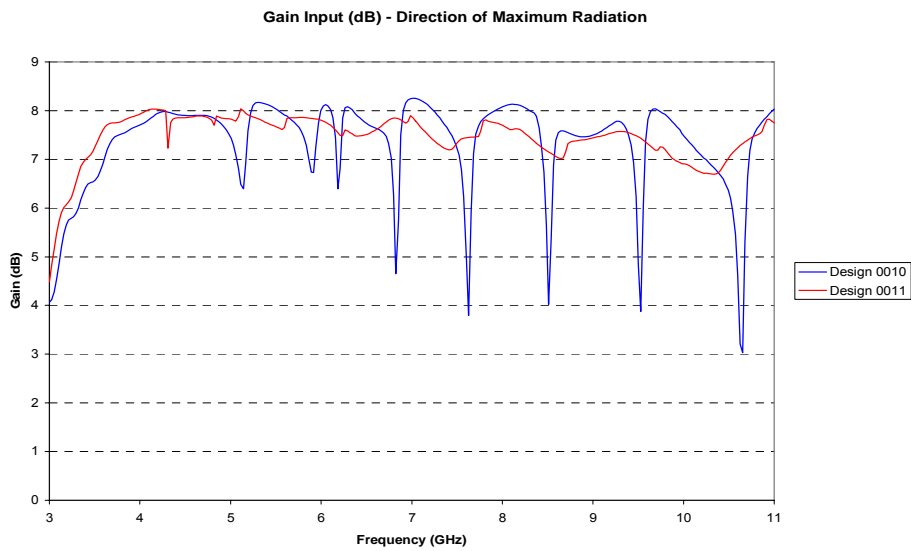


**Figure 4.4.9.** Gain in the Direction of Maximum Radiation for DOE IV Design 0010 and Design 0011.

### 4.4.5.3 Effects of the Boom Length in the Return Loss Response and Radiation Pattern

The boom length has been identified as one of the factors that affect the frequency response of log periodic folded slot antennas the most. The effect of increasing the boom length is evaluated now that phasing slots have been added to the configuration to improve the radiation characteristics of the antenna. In Figures 4.4.10 and 4.4.11, the return loss responses of designs 1011 (dba) and 1111 (dcba) and also designs 0001 (a) and 0101 (ca) are presented. The return loss of design 1111 (dcba) is near the -10 dB line (VSWR < 2) for the most part of the frequency band.

On the other hand, the return loss response of design 1011 (dba) is near -15 dB line for the most part of the frequency band. Since smaller values in the return loss response means less reflections design 1011 (dba) (the design with the boom length set to the lower level) is the winner in this case. In this particular case, the VSWR and the reflections increase. But, the reflections are in the same level when designs 0001 (a) and 0101 (ca) are compared. Then, the VSWR of the antenna won't increase by simply increasing the boom length. However, the VSWR and the reflections increase considerably when the boom length and the impedance of the central line are set to the high level at the same time as is the case of Figure 4.4.12.

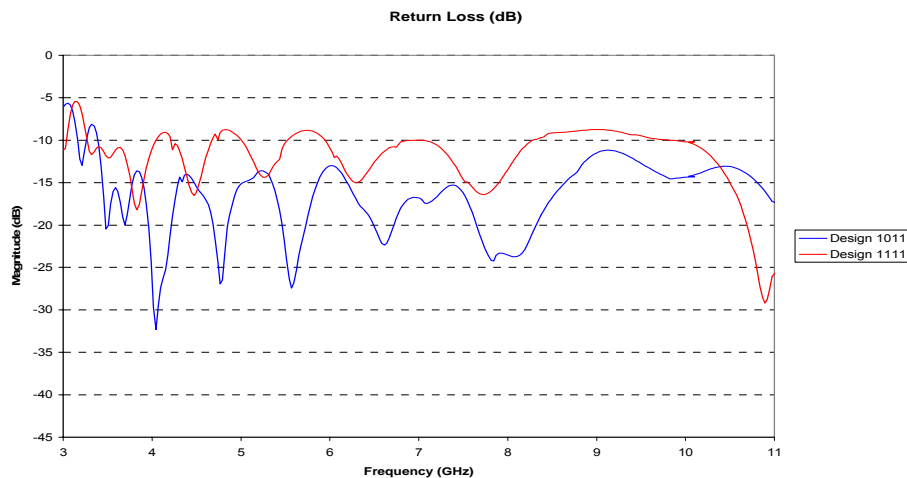
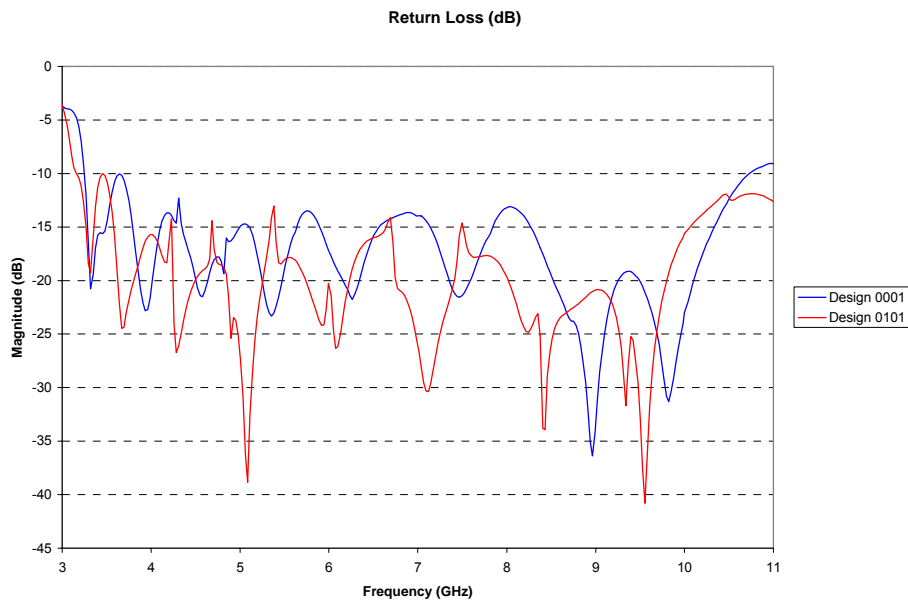
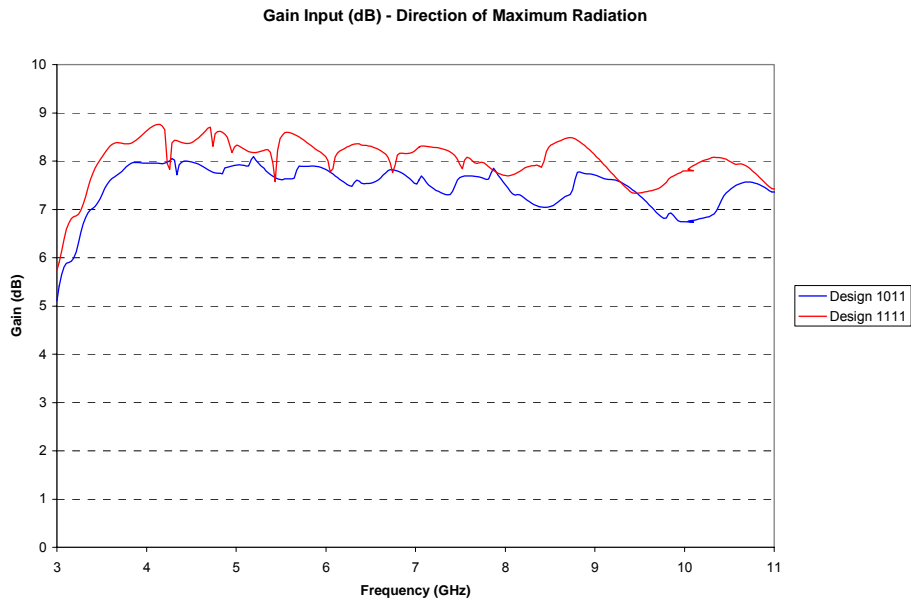


Figure 4.4.10. Return Loss Response for DOE IV Design 1011 and Design 1111.



**Figure 4.4.11.** Return Loss Response for DOE IV Design 0001 and Design 0101.

Although the return loss response is not affected if the impedance of the central line is kept at the low level, the radiation characteristics are affected when the boom length is set to the high level. The radiation characteristics deteriorate and drops in gain are observed again even though the phasing slot of optimal length is one feature of the design. The comparison of the gain between designs 1011 (dba) and 1111 (dcba) and also between designs 0011 (ba) and 0111 (cba) indicates that the designs with a stable radiation pattern are designs 1011 (dba) and 0011 (ba). Those designs have the boom length set to the low level. The same behavior was observed on the other designs: the boom length must be kept at the low level to obtain a stable radiation pattern.



**Figure 4.4.12.** Gain in the Direction of Maximum Radiation for DOE IV Design 1011 and Design 1111.

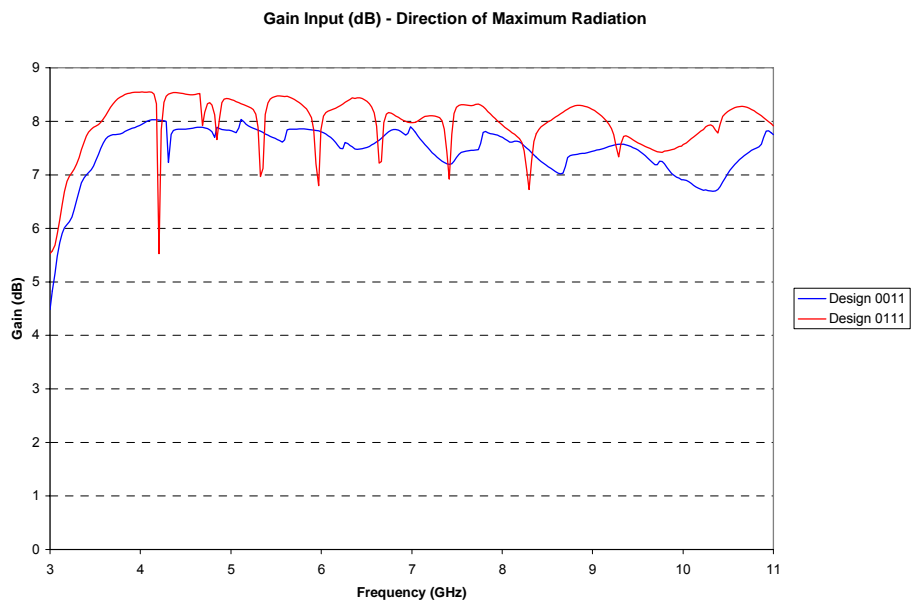


**Figure 4.4.13.** Gain in the Direction of Maximum Radiation for DOE IV Design 0011 and Design 0111.

Below, two views from the radiation pattern at one frequency confirms the stability of the radiation pattern while using the phasing slot. The 3-D view shows no

sidelobes or backlobes on the radiation pattern while the 2-D view of the pattern at  $f=5.67$  GHz establishes that the front to back ratio is over 30 dB.

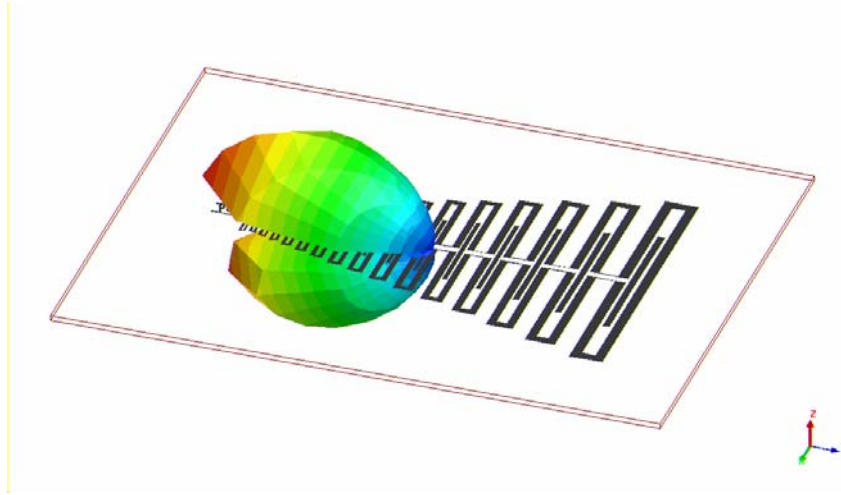


**Figure 4.4.14.** 3-D View of Radiation Pattern for DOE IV Design 0011 ( $f = 5.67$  GHz).

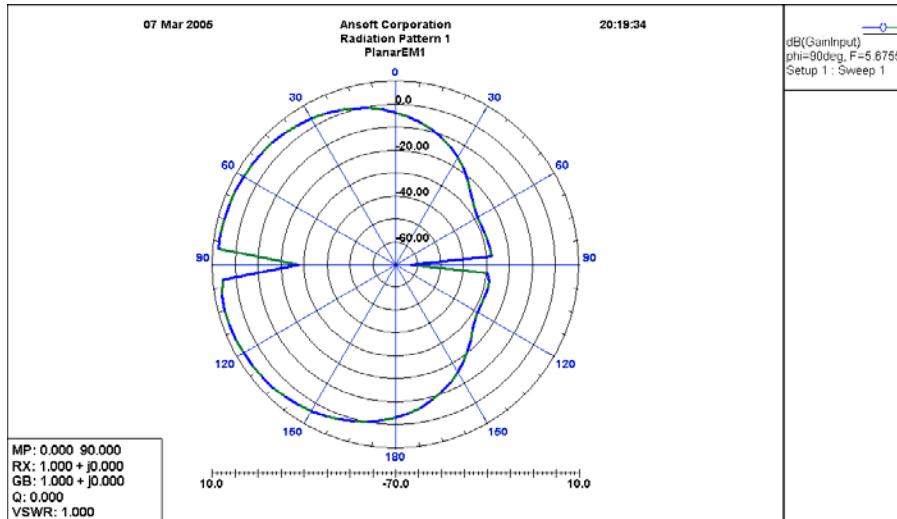


**Figure 4.4.15.** Radiation Pattern ( $\phi=90^\circ$ ) for DOE IV Design 0011 ( $f = 5.67$  GHz)

#### 4.4.5.4 Effects of the Impedance of the Central Line in the Return Loss Response and Radiation Pattern

All the statistical models agree on the fact that the most important factor in the design of log periodic folded slot antennas is the impedance of the central line ( $Z$ ). The effect that could be experienced when the value of  $Z$  is varied between two levels will be studied in this section. The return loss response of design 1111 (dcba) is above the  $VSWR > 2$  in some parts of the frequency band as observed in Figure 4.4.16. On the other hand, the  $VSWR < 2$  for design 0111 (cba). The difference is that the impedance of the central line for design 1111 (dcba) is 85 ohms while for design 0111 (cba) is 65 ohms. From DOE I, it was concluded that the response of design 1111 (dcba) would look worse if the impedance of the central line is increased above 85 ohms. In Figure 4.4.17, both designs exhibit a  $VSWR < 2$  for the band of operation. The difference here is that the boom length is set to the low level and that helps the antenna to maintain a  $VSWR < 2$ . Nonetheless, the impedance of the central is an important factor in the factor and must be kept near 65 ohms. The radiation characteristics of the antenna are not affected when the impedance of the line is increased to 85 ohms. This can be observed in Figures 4.4.18 and 4.4.19. But this is the case because  $Z$  is varied between 65 and 85 ohms. If the range of variation of  $Z$  is expanded between 74 and 150 like in DOE I, the radiation characteristics will be affected as explained in a previous section.

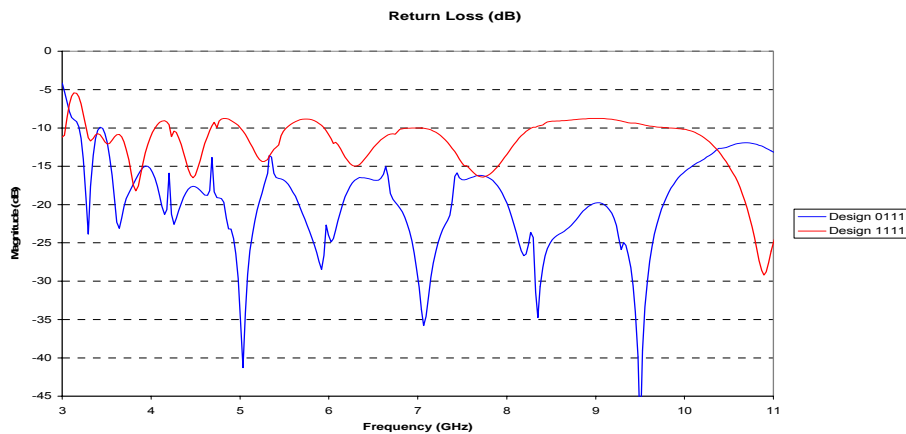


**Figure 4.4.16.** Return Loss Response for DOE IV Design 0111 and Design 1111.

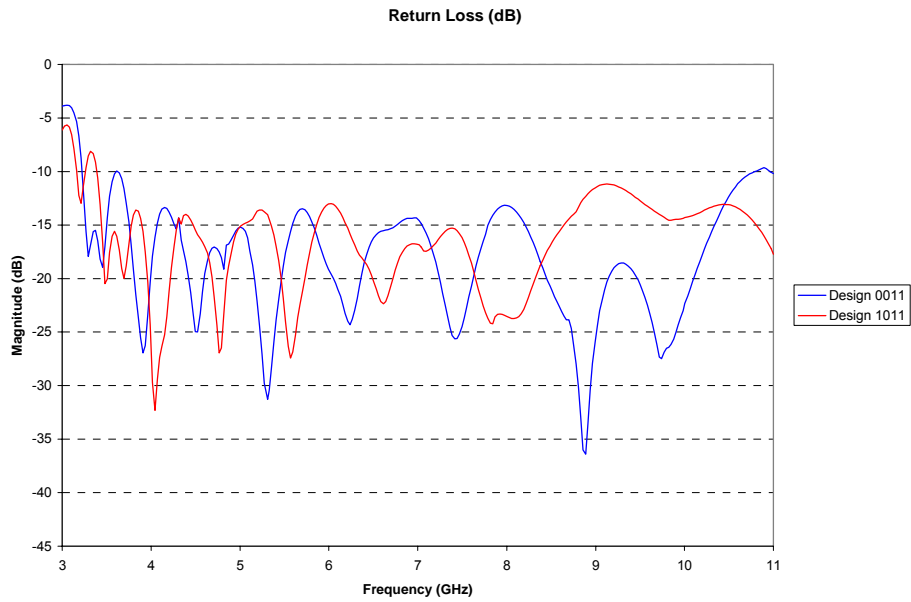


**Figure 4.4.17.** Return Loss Response for DOE IV Design 0011 and Design 1011.

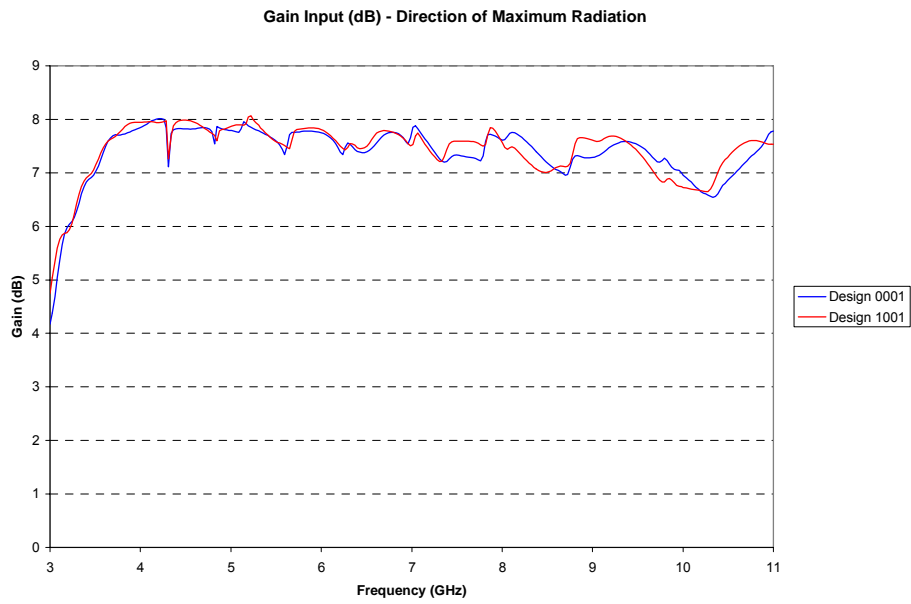


**Figure 4.4.18.** Gain in the Direction of Maximum Radiation for DOE IV Design 0001 and Design 1001.

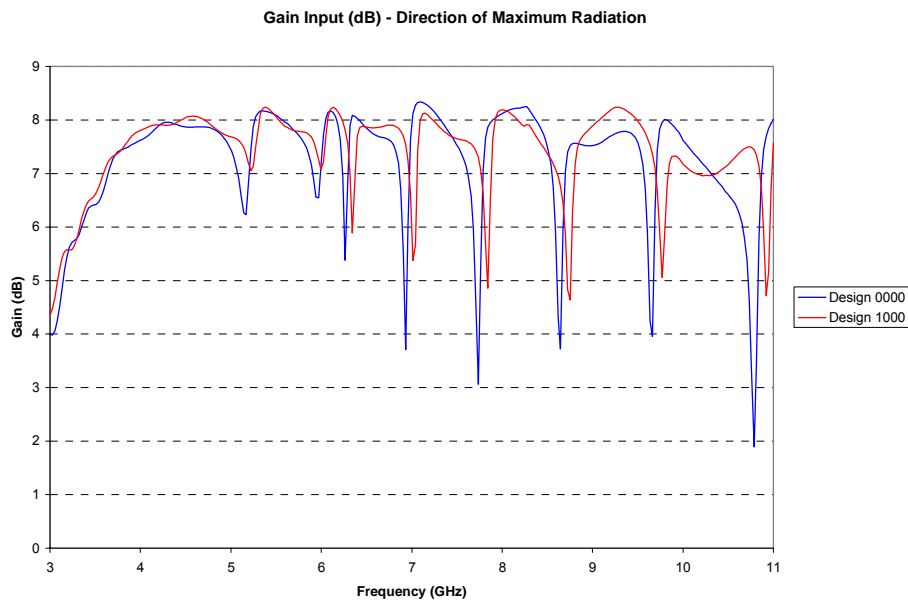


**Figure 4.4.19.** Gain in the Direction of Maximum Radiation for DOE IV Design 0000 and Design 1000.

## 4.5 Time Domain Analysis

In this section, the time domain response to a Gaussian monopulse of the different log periodic folded slot antenna configurations studied in this work will be analyzed. The results are obtained by using the time domain analysis procedure outlined in Chapter 3.

In this case, the time domain analysis was performed on design 00000 from DOE2 with 16 folded slot elements. It is important to point out that the transfer function and the received waveform are calculated at a single point ( $\theta=85^\circ$ ,  $\phi=90^\circ$ ). This is the angle of maximum radiation. The first plot shows the shape of the transmitted pulse in the time domain. A .2 ns Gaussian monopulse is transmitted and then received by another log periodic folded slot antenna.

The transfer function is then calculated with the data from Ansoft Designer. The magnitude and the phase of the transfer function are shown in Figure 4.5.1. Note that the magnitude of the transfer function is almost flat. On the other hand, the phase of the

transfer function changes by 360 degrees very often. This implies that the group delay is not constant. Then, the clean pulse transmission is thwarted by the phase changes by 360 degrees very often. For clean pulse transmission, the phase of the transfer function must be linear and the changes in the phase by 360 degrees must be minimal.

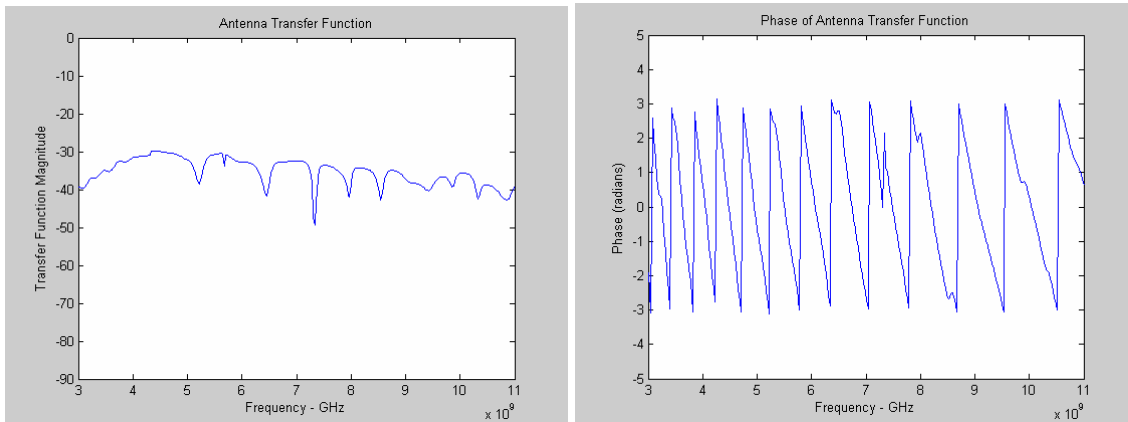


**Figure 4.5.1.** Magnitude and Phase of the Transfer Function from design 00000 from DOE II.

The frequency content of the received and transmitted pulse is presented in Figure 4.5.2. Note that the frequency content of the received pulse does not resemble the transmitted pulse. Instead, the frequency content of the received pulse is distorted completely and cannot be recognized as a Gaussian monopulse.

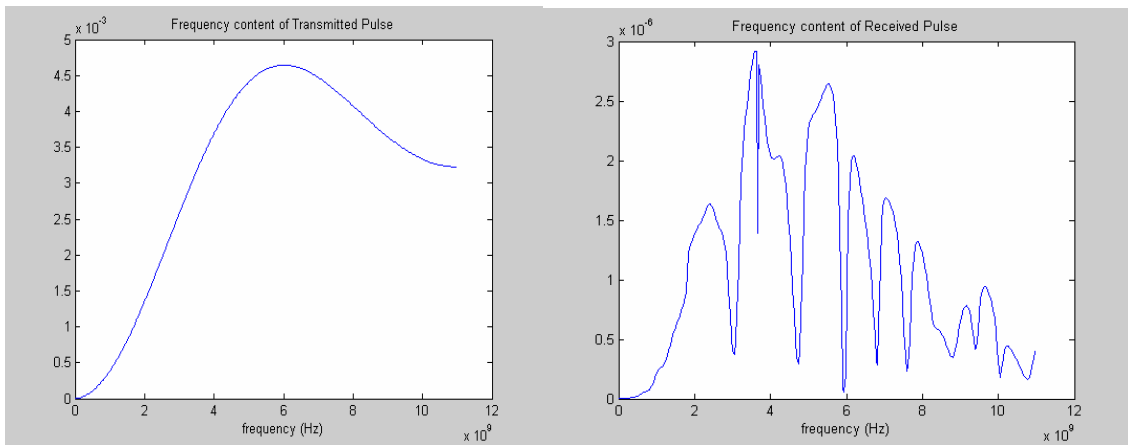


**Figure 4.5.2.** Frequency Content of Transmitted and Received Pulse from design 00000 from DOE II.

When the received waveform is transformed back to the time domain it seems that noise was received by the log periodic antenna. Actually, it is a Gaussian monopulse with components of different frequencies arriving at different times. The end result is that the pulse transmission is elongated in time which prevents the successful transmission and detection of subsequent pulses. This behavior is observed in Figure 4.5.3 where the transmitted and received pulse is presented.

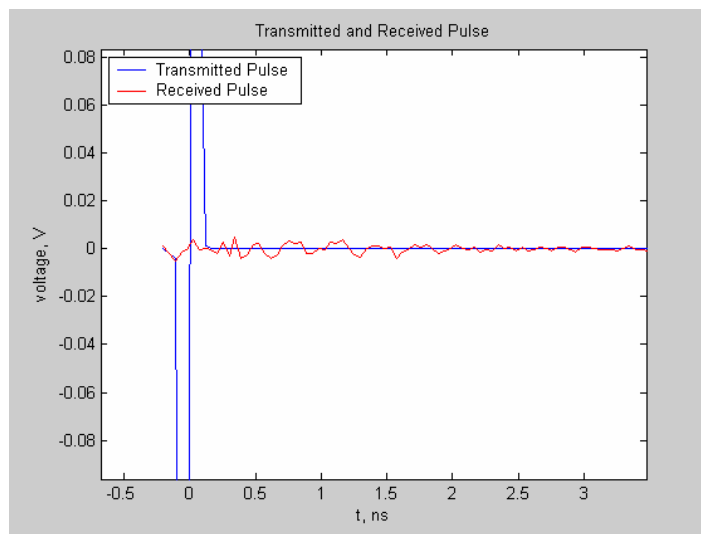


**Figure 4.5.3.** Transmitted and Received Pulse using design 00000 from DOE 2.

The same procedure is repeated for design 00010 (b) from DOE2 with 33 folded slot elements. The magnitude and phase of the transfer function is shown in Figure 4.5.4. More elements in the antenna contribute to more phase changes by 360 degrees. The reason for this is simple, everytime the frequency changes from  $f$  to  $\tau f$ , the phase of the Electric Field changes by 360 degrees. Then, when more elements are added the phase of the transfer function changes by 360 degrees more often which in turn distorts the received pulse even more.

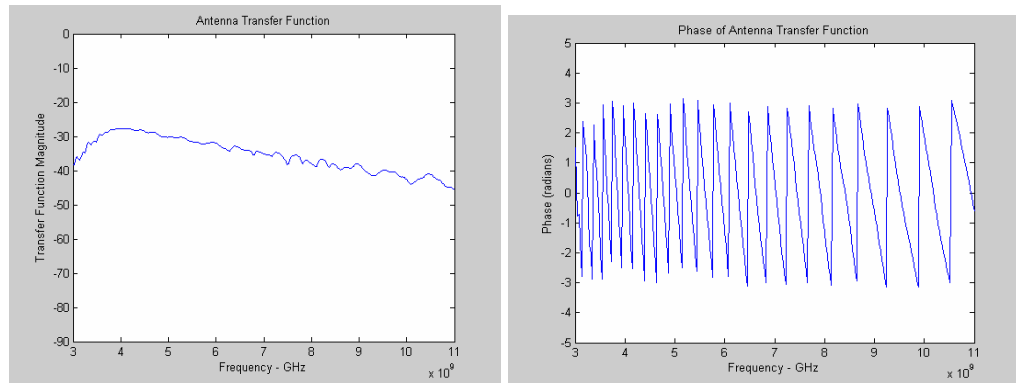


**Figure 4.5.4.** Phase and Magnitude of the Transfer Function from design 00010 from DOE II.

The frequency content and the time domain response of the pulse are shown in Figure 4.5.5. Now, the received pulse and its frequency content looks more distorted than the received pulse from design 00000 which confirms the fact that when more elements are added the received pulse is distorted even more.

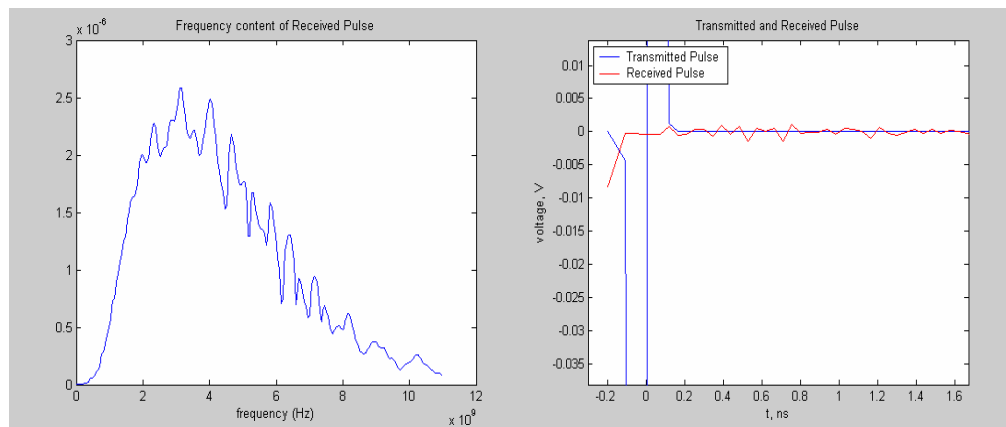


**Figure 4.5.5.** Frequency content of the Received Pulse and Transmitted and Received pulse using design 00010 from DOE II.

The time domain analysis procedure is now applied to design 0010 (b) from DOE III with 12 folded elements. This design stabilizes the radiation pattern of the LPFSA by making the side slots of each element wider.

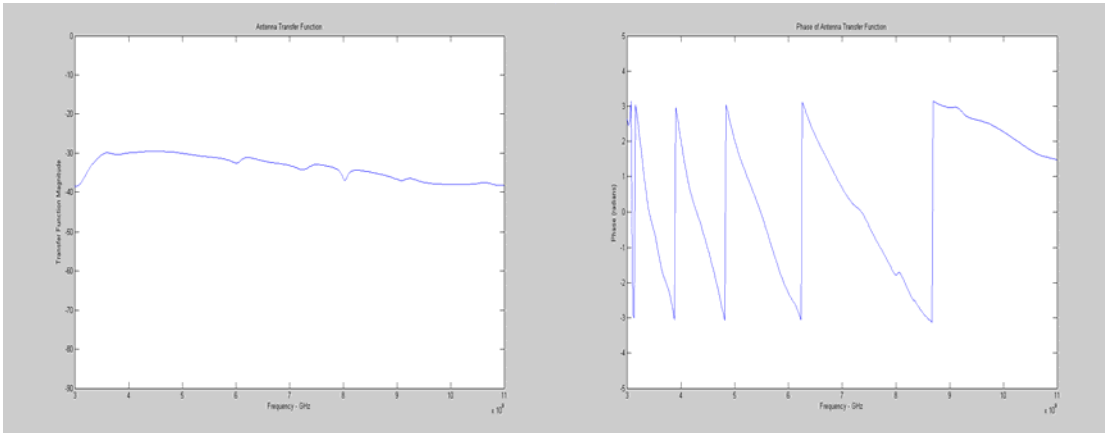


**Figure 4.5.6.** Phase and Magnitude of the Transfer Function from design 00010 from DOE III.

It is very important to point out that the phase of the transfer function changes by 360 degrees just five times. Since the antenna has 12 folded slot elements operating between 3 and 12 GHz more changes in the phase of the transfer function should be observed since the phase changes are proportional to the number of elements in the antenna. This behavior is observed in Figure 4.5.1 where 13 phase changes by 360 degrees are observed in the transfer function. The only reason why 13 phase changes are observed instead of 16 (the number of elements in the antenna) is because there are elements in the antenna that resonate above 11 GHz and those phase changes are not observed here. The important aspect to consider is that antennas designed for UWB applications such as those presented in [18] present changes in the phase of the Electric field by 360 degrees just two times in the entire frequency band. The key in reducing pulse distortion is to make the magnitude of the transfer function flat and its phase linear. Therefore, the log periodic antenna that presents fewer changes in the phase of the transfer function would be more suitable for pulse transmission. Although the antenna with 12 folded slot elements (design 0010 from DOE III) cannot transmit a clean short pulse as presented in Figure 4.5.7 it would be more suitable for such uses than previous designs.

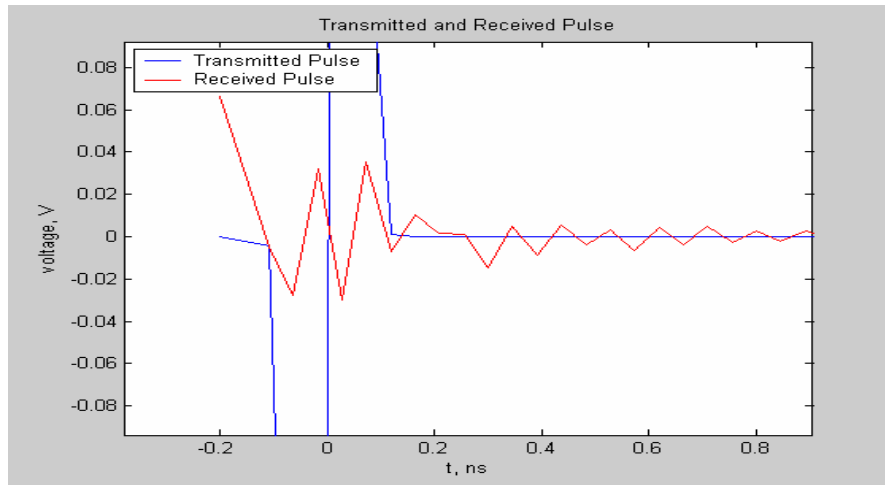


**Figure 4.5.7.** Transmitted and Received Pulse using design 0010 from DOE III.

## 4.6 Modulated Impedance Feeder

This section deals with the idea of scaling the dimensions of the central line by the scaling factor. The idea is to see what benefits can be obtained from the idea. Does the radiation pattern become stable? What effect does the modulated impedance feeder has on the impedance bandwidth of the antenna? These questions will be answered in this section.

The modulated impedance feeder configuration is presented in Figure 4.6.1. It is similar to the baseline configuration (Figure 3.1.1). The only difference between this configuration and the baseline configuration is that the impedance of the central line is constant and the dimensions do not change. On the other hand, the dimensions of the central line for the modulated impedance feeder are modified by the scaling factor. This in turn implies that the impedance will also vary along the line but the variation is not dictated by the scaling factor.

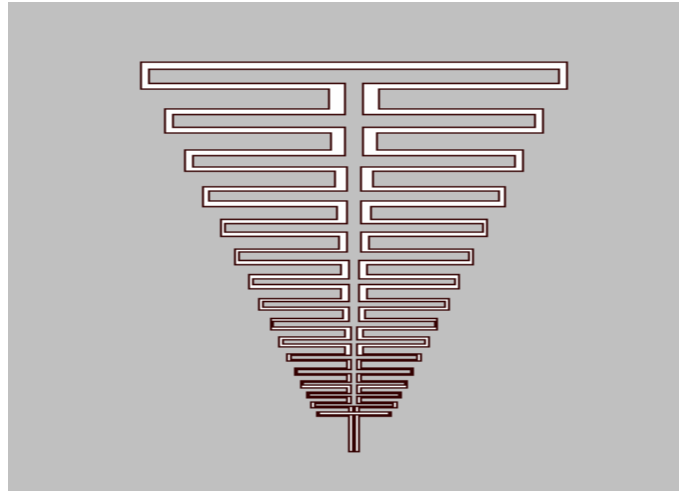


**Figure 4.6.1.** Modulated Impedance Feeder Configuration.

First, the effect on the radiation pattern is analyzed. Since the dimensions of the central line are being varied using the scaling factor, the line connected to the largest element will have the largest impedance while the line connected to the smaller element will have the smallest impedance. First, the intention was to vary the impedance values of the central line with the scaling factor. But this idea yielded unrealistic dimensions when the impedance values were scaled. Then, it was decided to vary the physical dimensions of the central line. The change in impedance values using this method is around 20 ohms from the largest to the smallest element. Figure 4.6.2 shows the gain of the different designs. Unfortunately, it is evident from the graph that the modulated impedance feeder does nothing to improve the radiation pattern of a log periodic folded slot antenna with 17 elements. The antenna with the largest value for impedance ( $Z$  between 140 and 115 ohms) shows a peak of 13 dB for the gain at maximum radiation. It is important to point out that the radiation pattern is not improved, it does not look drastically different. Even more, when the same antenna was simulated using a constant 150 ohm line the gain dropped to negative values. That behavior is not observed here.

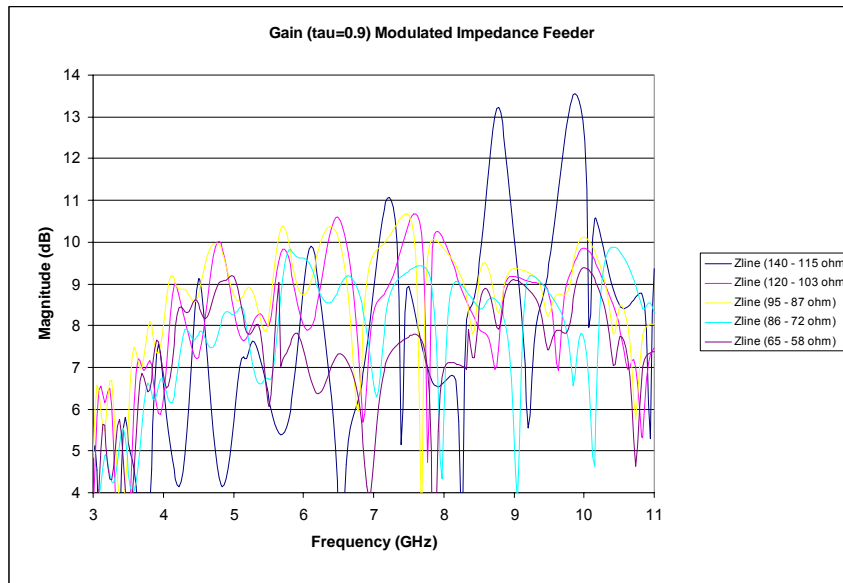


**Figure 4.6.2.** Gain in the direction of maximum radiation for designs using the modulated impedance feeder.

Then, the effects on the impedance bandwidth of the antenna were investigated. By looking at the VSWR, Input Impedance and Return Loss plots it was concluded that the modulated impedance feeder has very negative effects on the impedance bandwidth of the antenna when  $Z$  starts at a big value. In Figure 4.6.3 it can be observed that the bandwidth of the antenna is negligible (VSWR  $< 2$ ) when  $Z$  varies between 120 and 104 ohms. The addition of a phasing slot using the same line improves the return loss response but the bandwidth continues to be negligible. However, when the values for  $Z$  are reduced and  $Z$  varies between 86 and 72 ohms the return loss response looks much better and the bandwidth of the antenna starts from 5 to 11 GHz. Certainly, the bandwidth is reduced.

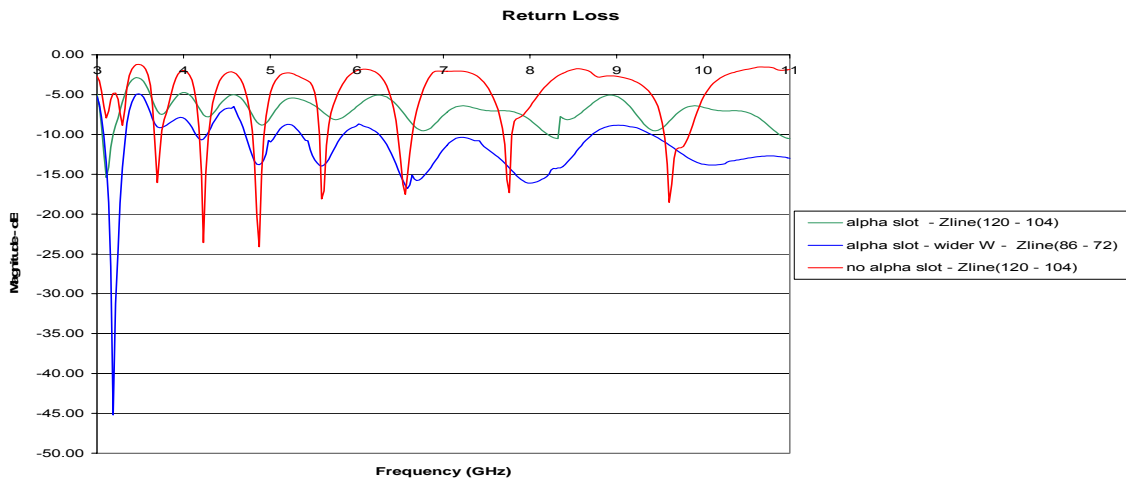


**Figure 4.6.3.** Return Loss Response for designs using the modulated impedance feeder.

The bandwidth reduction problem is also experienced when other values for  $Z$  are used (see Figure 4.6.4). As expected, the bandwidth of the antenna is negligible when the values for  $Z$  vary between 140 and 116 ohms. When the values are reduced the return loss response gets better using phasing slots but the bandwidth is reduced when the designs with the modulated impedance feeder are compared to similar designs without using the modulated impedance feeder.

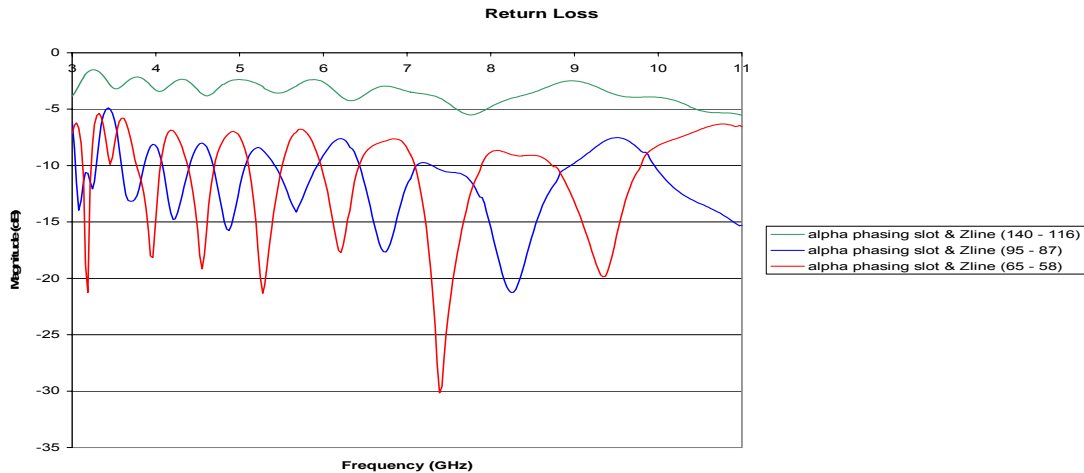


**Figure 4.6.4.** Return Loss Response for designs using the modulated impedance feeder.

Then, neither the impedance bandwidth nor the radiation pattern is improved while using a modulated impedance feeder. The impedance bandwidth is reduced and the radiation pattern still looks bad when the phasing slot is not used.

## **4.7 Measured Results**

In order to validate the simulated results, some prototypes were fabricated using the milling machine and also using etching. The milling machine can make slots as small as 0.15 mm but some designs especially those with a phasing slot had slots smaller than 0.15 mm. Therefore, those antennas were built using etching. In the next few paragraphs, a comparison between the simulated and measured results will be presented.

DOE II Design 00000 antenna was built using both the milling machine and the etching technique. The results for the return loss response are presented in Figure 4.7.1. The reason why the results do not look extremely similar to each other is due to the fact that the 3.5 mm SMA connector changes the input impedance response of the antenna because there is no ground below the antenna and the connector must be soldered in a special way to prevent a short circuit at the connector. The VSWR response is shown in Figure 4.7.2 and the important result here is that the design shows  $VSWR < 2$  for the majority of the frequency band just like Ansoft Designer predicted. However, the VSWR increases and it's nearly 5 at the end of the frequency band, something Designer did not show during the simulation.

Measurements of the field pattern were taken using the Near Field anechoic chamber facility at UPRM Radiation Laboratory. Then, the near field measurements were converted to the Far field using NSI control program. The far field data shows that the radiation pattern is stable until 8 GHz for both cases of DOE II Design 00000, one built using the milling machine and the other using etching. The measurements were

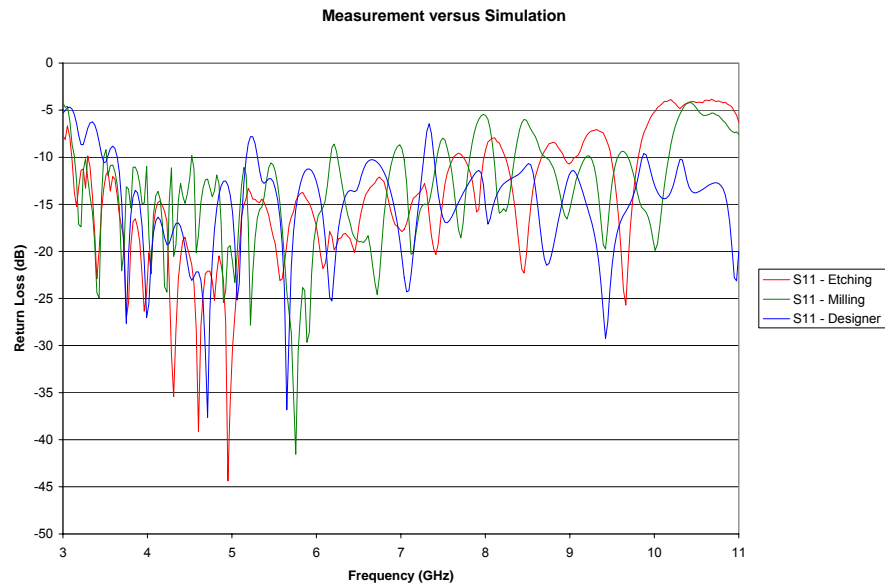


**Figure 4.7.1.** Simulated versus Measured Results of Return Loss Response of DOE II Design 00000.

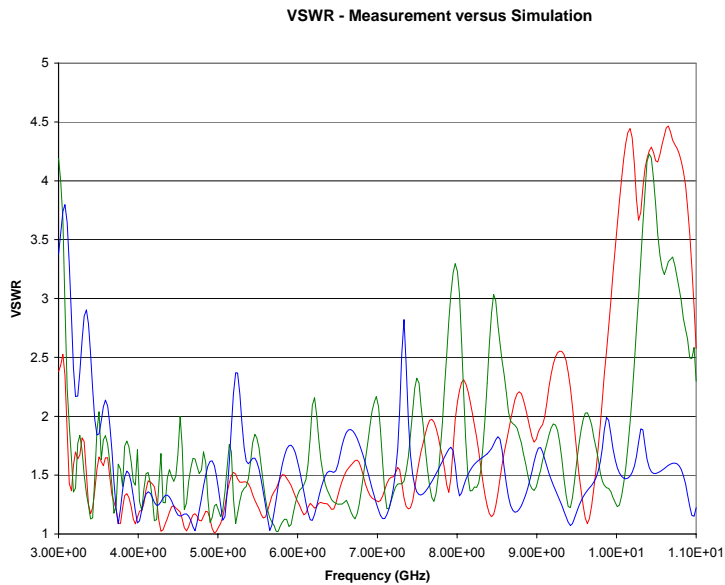


**Figure 4.7.2.** Simulated versus Measured Results of VSWR Response of DOE II Design 00000.

taken 250 MHz apart between each frequency point and it took an average of 32 minutes to complete the measurement at each frequency point. The effect of instability in the radiation pattern was not observed at low frequencies but at 5.25 GHz a drop of 2 dB in

the directivity was observed. It is important to point out that Designer did not predict instability in the radiation pattern. Figure 4.7.3 shows the measured radiation pattern of DOE II Design 00000 built using etching at 6 GHz on the H plane. The directivity at this point in frequency is around 8.26 dB. The front to back ratio is about 20 dB and the null is about -15 dB, this null should be deeper but all the measurements taken exhibited a similar behavior. The directivity is stable until reaching 8 GHz when it increases to 10 dB to then drop to 8 dB and then again increase to 10 dB. The measured radiation pattern at 8.4 GHz is observed in Figure 4.7.4. The control program reported a directivity of 10.43 dB at this point in frequency. Note that the front to back ratio is around 10 dB and that there are lots of ripples while the radiation pattern shown in Figure 4.7.3 is smooth. This behavior is observed throughout the rest of the band.

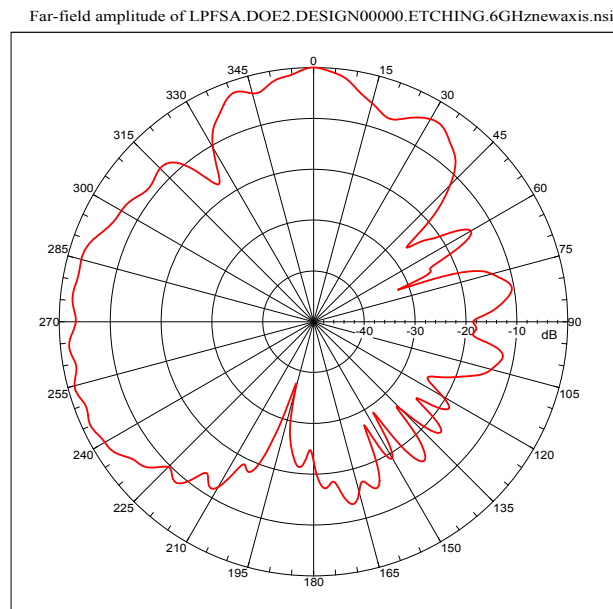


**Figure 4.7.3.** Far Field Pattern (H-plane) of DOE II Design 00000 (etching),  $f=6$  GHz. Feed pointing to  $325^\circ$ , ground plane is normal to the page.

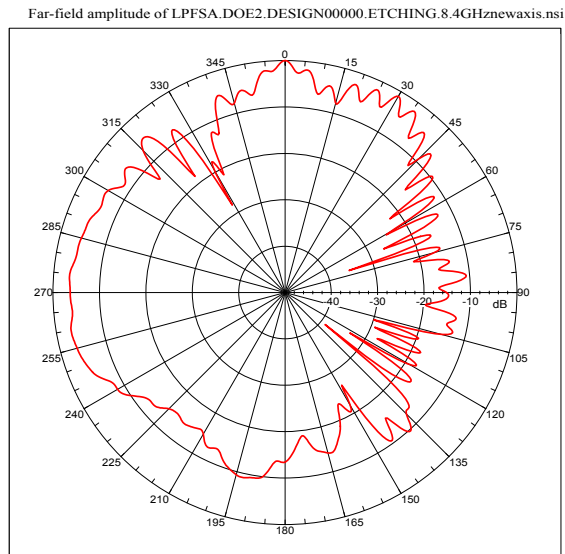


**Figure 4.7.4.** Far Field Pattern (H-plane) of DOE II Design 00000 (etching),  $f=8.4$  GHz. Feed pointing to  $330^\circ$ , ground plane is normal to the page.

The next design was built using only the etching technique. DOE II Design 00101 (ca) was chosen because the design has the boom length and the impedance of the central line ( $Z$ ) set to the high level. According to all the statistical models, this combination produces a VSWR  $>2$  which is not desired. Figure 4.7.5 shows the return loss response and it shows that the return loss response is above  $-10$  dB which means that the VSWR  $> 2$ .

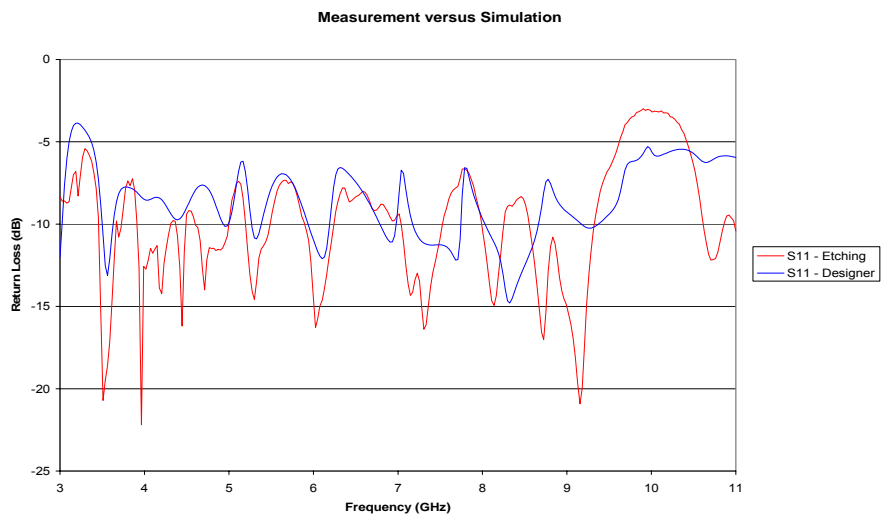


**Figure 4.7.5.** Simulated versus Measured Results of Return Loss Response of DOE II Design 00101.

DOE III Design 0010 (b) proved to be one of the best designs of all the experiments performed. This design provided a stable radiation pattern along with a good impedance bandwidth with a VSWR < 2.5. This design also is very compact and the time domain response although is not perfect it certainly distorts the transmitted pulse less than other designs. The return loss response and the VSWR between the simulated and measured results on a prototype built using the milling machine are shown in Figure 4.7.6 and Figure 4.7.7 respectively.

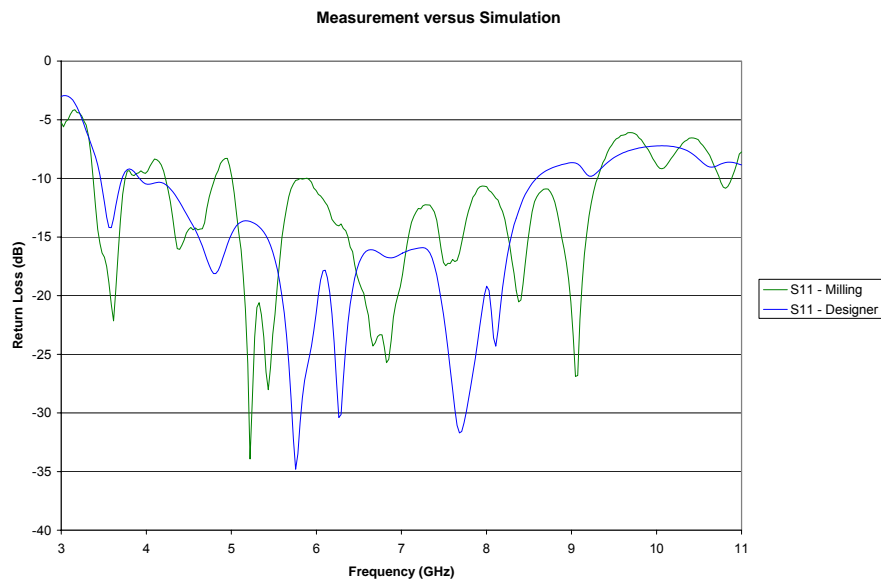


**Figure 4.7.6.** Simulated versus Measured Results of Return Loss Response of DOE III Design 0010.

The near field pattern of DOE III Design 0010 (b) was also measured at the UPRM Radiation Laboratory facility. The directivity observed throughout the frequency band was around 8 dB. The pattern looks unstable after 8.6 GHz where a directivity of 9.5 dB was reported. This is not surprising because the bandwidth of the antenna is reduced when the side slots are made wider than the top and bottom slots. It is important to point out that the measured patterns look better than those from DOE II Design 00000 at all frequencies. Measurements taken on another design with wider side slots also agree with the fact that the pattern is improved.

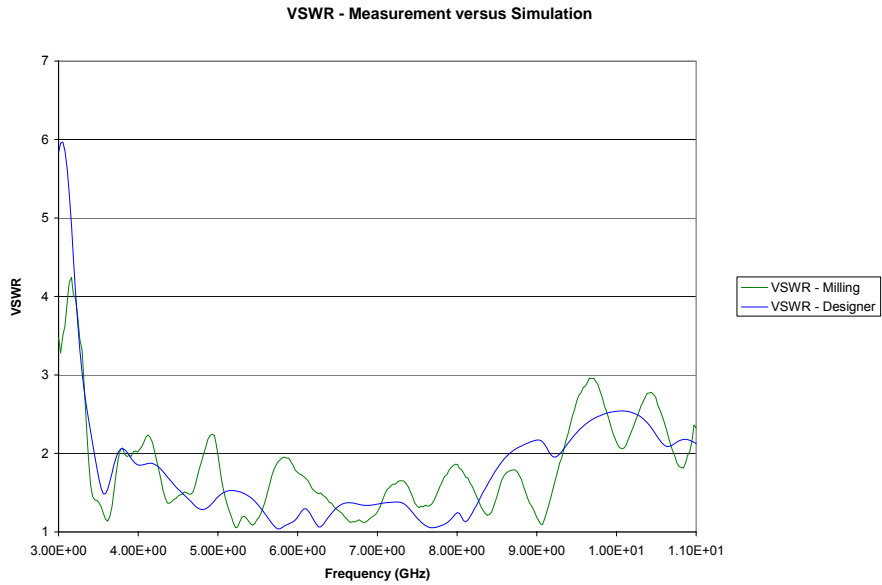


**Figure 4.7.7.** Simulated versus Measured Results of VSWR Response of DOE III Design 0010.

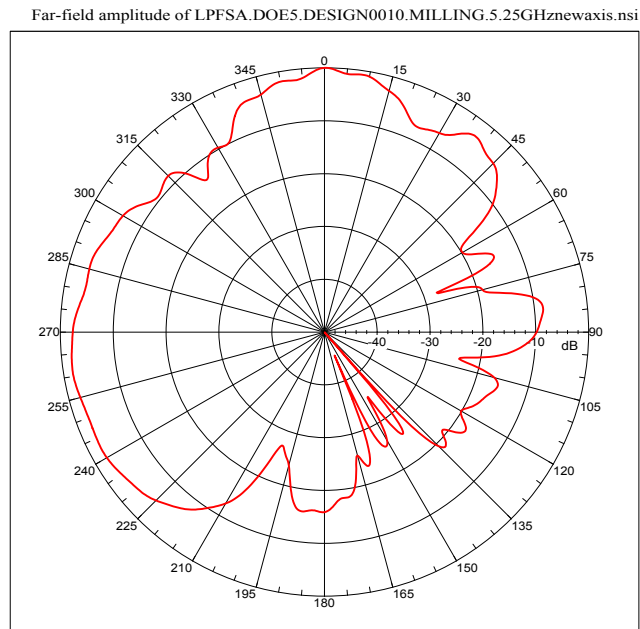


**Figure 4.7.8.** Far Field Pattern (H-plane) of DOE III Design 0010 (b) (milling),  $f=5.25$  GHz. Feed pointing to  $325^\circ$ , ground plane is normal to the page.

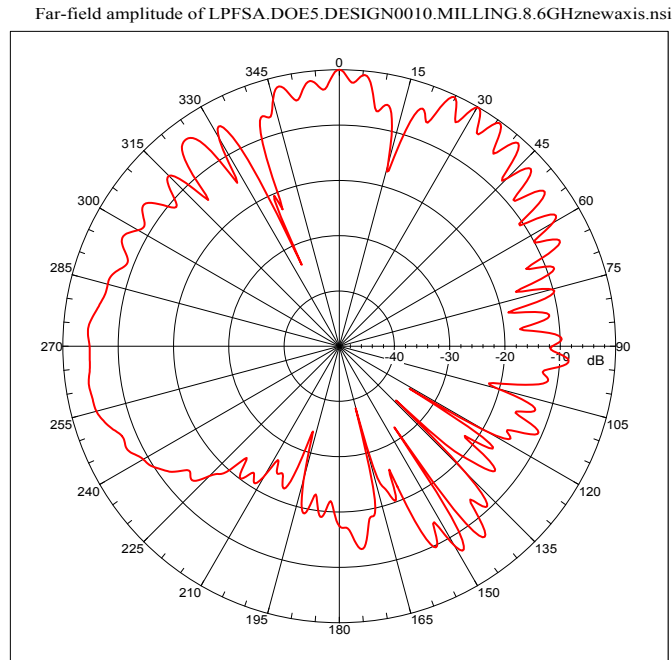


**Figure 4.7.9.** Far Field Pattern (H-plane) of DOE III Design 0010 (b) (milling),  $f=8.6$  GHz. Feed pointing to  $335^\circ$ , ground plane is normal to the page.

One of the most important designs is DOE IV Design 0011 (ba) because it provides a decent impedance bandwidth and a stable radiation pattern. Figure 4.7.10 shows the return loss response and it shows that the results agree up until 9 GHz when the VSWR  $> 3$ .

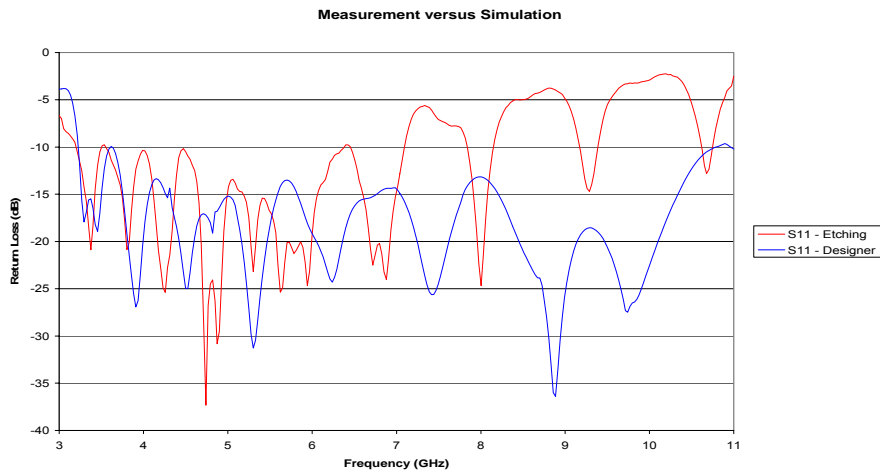


**Figure 4.7.10.** Simulated versus Measured Results of Return Loss Response of DOE IV Design 0011.

## 5 Conclusions and Recommendations

### 5.1 Conclusions

Three configurations of the log periodic folded slot antenna were analyzed on this work. The antennas built on top of a substrate with  $\epsilon_r=3.48$  with  $h=0.762$  mm were studied using Design of Experiments techniques. The three configurations studied shown in Figure 3.1.1 are based on the log periodic folded slot antenna and two modifications to the design to improve the radiation characteristics.

According to the experiments conducted on the baseline configuration, the most influential factors in the frequency response of the antenna are the impedance of the central line that connects all the folded slot elements in the antenna and also the boom length of the antenna. The experiments showed that if the impedance of the central line is increased beyond 85 ohms, the impedance bandwidth and the radiation characteristics deteriorate and a VSWR more than three and big dropouts in gain at high frequencies are experienced. These results come from DOE I where the impedance of the central line had a value of 150 ohms at the high level and none of the 16 designs that used the 150 ohm line worked. The designs that worked using the baseline configuration exhibited an unstable radiation pattern when the scaling factor was set to .89. The designs with a scaling factor of .95 exhibited a stable radiation pattern as long as the impedance of the central line was kept below 85 ohms. All sorts of problems in the radiation pattern were experienced because the electric field between the top and bottom slots of each folded slot element was not in phase.

Attempts to match the antenna to 50 ohms by changing the folded slot dimensions and keeping the 150 ohm line were made and eventually were successful. This was achieved by making the side slots of each folded slot element five times wider than before while keeping the rest of the dimensions constant. However, the range of values used for the impedance of the central line moved from 65 to 85 ohms to between 115 to 150 ohms. The main purpose of making the side slots wider was to try to correct the

problem of the unstable radiation pattern for small scaling factor values. The results showed that the radiation pattern became stable and dropouts in gain in the direction of maximum radiation and sidelobes and big backlobes were no longer experienced even for a scaling factor of 0.85 and just 12 folded slot elements. Unfortunately, the bandwidth of the antenna is reduced by 27% when compared to other designs especially at high frequencies. A  $VSWR > 3$  is experienced for frequencies above 8.6 GHz. Attempts to correct this problem by adding more folded slots elements have been unsuccessful.

The other configuration studied included the addition of a phasing slot to stabilize the radiation pattern of the LPFSA for small values of the scaling factor. In this case, the radiation pattern became stable when the length of the phasing slot was around  $1.15\alpha$ . Experiments with a shorter phasing slot did not solve the problem of instability in the radiation pattern. It is important to point that the impedance bandwidth of the antenna was not deteriorated and designs with a stable radiation pattern with the desired impedance bandwidth between 3 and 11 GHz were achieved. One drop back of the configuration is that the width phasing slot elements become very small at high frequencies which make prototype construction with a milling machine very difficult.

In terms of time domain analysis, all the antennas configurations examined showed poor performance for short pulse transmission. This is due to the fact that the frequency components of the signal are transmitted at different times due to the way the antenna is fed. However, the transmitted pulse is less distorted while using the configuration with wider side slots mainly because the phase of the electric field does not change by 360 degrees when the frequency is increased from  $f$  to  $f/\tau$ , a characteristic feature of log periodic antennas.

The DOE techniques used for the analysis of the log periodic folded slot antennas proved to be useful because it allowed us to identify the influential factors using just one point to describe the behavior of 300 frequency points for each experiment. Also, side by side comparisons between results of experiments for the entire frequency band where

when just one factor was varied was the most useful analysis tool because it helped to confirm the results from the statistical models and helped to interpret the models better.

## **5.2 Recommendations**

It is important to investigate on how to improve the impedance bandwidth of the wider side slots configuration. This configuration provides a stable radiation pattern, is smaller and does not distort transmitted pulses as much as other configurations. One way to achieve this is to use a DOE with multiple levels on a single factor. The width of the side slots, the boom length and the scaling factor need to be studied using more levels instead of two. Specifically, it is very important to study more profoundly the effect of that the width of the side slots has on the impedance bandwidth of the antenna using multiple levels.

## 6 Bibliography

- [1] D.E. Isbell, “Log-Periodic Dipole Arrays” *Antennas and Propagation, IEEE Transactions on*, Volume: 8 Issue: 3, May 1960. Page(s): 260 – 267.
- [2] R. L. Carrel, “Analysis and Design of the Log-Periodic Dipole Antenna,” Ph.D. Dissertation, Electrical Engineering Department, University of Illinois, 1961.
- [3] R.H. DuHamel, and M.E. Armstrong, “Log-Periodic Transmission Line Circuits-Part I: One Port Circuits” *Microwave Theory and Techniques, IEEE Transactions on*, Volume: 14 Issue: 6, Jun. 1966. Page(s): 264 – 274.
- [4] K.G. Balmain, C. Bantin, C. Oakes, and L. David, “Optimization of Log-Periodic Dipole Antennas” *Antennas and Propagation, IEEE Transactions on*, Volume: 19 Issue: 2, Mar. 1971. Page(s): 286 – 288.
- [5] P.G. Ingeron, P. Mayes, and C. McBride, “Frequency Independent Excitation of Higher Mode Elements on Log-Periodic Antennas” *Antennas and Propagation, Society International Symposium*, Volume: 6, Sep. 1968. Page(s): 247 – 248.
- [6] G. De Vito, and G. Stracca, “Comments on the Design of Log-Periodic Dipole Antennas” *Antennas and Propagation, IEEE Transactions on*, Volume: 21 Issue: 3, May 1973. Page(s): 303 – 308.
- [7] P.G. Ingeron, and P. Mayes, “Log Periodic Antennas with Modulated Impedance Feeders” *Antennas and Propagation, IEEE Transactions on*, Volume: 16 Issue: 6, Nov 1968. Page(s): 633 – 642.
- [8] W. Sorgel, C. Waldschmidt, and W. Wiesbeck, “Transient Responses of a Vivaldi Antenna and a Logarithmic Periodic Dipole Array” *Antennas and Propagation, Society International Symposium*, Volume: 3, June 2003. Page(s): 592 – 595.
- [9] D.M. Pozar, “Waveform Optimizations for Ultrawideband Radio Systems” *Antennas and Propagation, IEEE Transactions on*, Volume: 51 Issue: 9, Sep 2003. Page(s): 2335 – 2345.
- [10] J. McLean, And R. Sutton, “A Log-Periodic Dipole Antenna Employing a Forward-firing Feed Mechanism for Pulse Radiation” *Antennas and Propagation, Society International Symposium*, Volume: 3, June 2003. Page(s): 571 – 574.
- [11] P.S. Excell, and A.D. Tinniswood, and R.W. Clarke, “An Independently Fed Log-Periodic Antenna For Directed Pulsed Radiation” *Electromagnetic Compatibility, IEEE Transactions on*, Volume: 41 Issue: 4, Nov 1999. Page(s): 344 – 349.

- [12] H.S. Tsai, and R.A. York, “Applications of planar multiple-slot antennas for impedance control, and analysis using FDTD with Berenger’s PML method” Antennas and Propagation Society International Symposium, 1995. AP-S. Digest, Volume: 1, 1995. Page(s): 370 -373.
- [13] M H.S. Tsai, and R.A. York, “FDTD analysis of CPW-fed folded-slot and multiple slot antennas on thin substrates” Antennas and Propagation, IEEE Transactions on , Volume: 44 Issue: 2, Feb. 1996. Page(s): 217 -226.
- [14] R.A. Rodríguez Solís, “Analysis and Design of a Microwave Three-Dimensional Frequency-Independent Phased Array Antenna Using Folded Slots” PhD Dissertation, Department of Electrical Engineering, The Pennsylvania State University, 1997.
- [15] Chung You Chung, and R. Haupt, “Log-period dipole array optimization” Aerospace Conference Proceedings, 2000. Volume: 4 , March 2000. Page(s):449 – 455.
- [16] A.U. Bhode, C.L. Holloway, M. Picket-May, and R. Hall, “Wide-band slot antennas with CPW feed lines: hybrid and log periodic designs” Antennas and Propagation, IEEE Transactions on, Volume: 52 Issue: 10, Oct. 2004. Page(s): 2545 -2554.
- [17] W.E. McKinzie III, J.J. Moncada, and T.L. Anderson, “A microstrip-fed log-periodic slot array” Antennas and Propagation Society International Symposium, 1994. AP-S. Digest , Volume: 2 , 1994. Page(s):1278 – 1281.
- [18] M. Tzyh-Ghuang, and J. Shyh-Kang, “A compact tapered-slot-feed annular slot antenna for ultra-wideband application” Antennas and Propagation Society International Symposium, 2004. AP-S. Digest, Volume: 3, 2004. Page(s): 2943 - 2946.
- [19] Y. Pinhasi, A. Yahalom, O. Harpaz, and G. Vilner, “Study of ultrawide-band transmission in the extremely high frequency (EHF) band” Antennas and Propagation, IEEE Transactions on, Volume: 52 Issue: 11, Nov. 2004. Page(s): 2833 -2842.
- [20] T.M. Weller, L.P.B Katehi, and G.M. Rebeiz, “Single and double folded-slot antennas on semi-infinite substrates” Antennas and Propagation, IEEE Transactions on, Volume: 43 Issue: 12, Dec. 1995. Page(s): 1423 -1428.
- [21] C.A. Balanis, *Antenna Theory: Analysis and Design*, Second Edition. New York: John Wiley and Sons, 1996.

- [22] N.D. López Rivera, "Characterization and Modeling of Folded Slot Antenas" MS Dissertation, Department of Electrical Engineering, University of Puerto Rico, 2003.
- [23] O.E. Allen, D.A. Hill, and A.R. Ondrejka, "Time-domain antenna characterizations" *Electromagnetic Compability*, IEEE Transactions on, Volume: 35 Issue: 3, Aug. 1993. Page(s): 339 -346.
- [24] A. Shlivinski, E. Heyman, and R. Kastner, "Antenna characterization in the time domain" *Antennas and Propagation*, IEEE Transactions on, Volume: 45 Issue: 8, Jul. 1997. Page(s): 1140 -1149.
- [25] R.C. Johnson, *Antenna Engineering Handbook*, Third Edition. Columbus, OH. McGraw-Hill, 2001
- [26] K. Beilenhoff, and W. Heinrich, "Parasitic parallel-plate line mode coupling at coplanar discontinuities" *Institut fur Hochfrequenztechnik. TUD.* Page(s): 44 -47.
- [27] D.C. Montgomery, *Design and Analysis of Experiments*, Fifth Edition. New York: John Wiley and Sons, 2001.
- [28] <http://www.isixsigma.com>.
- [29] J.D. Kraus and R.J. Marhefka, *Antennas*, Third Edition. Columbus, OH: McGraw-Hill, 2001.

## 7 Appendix

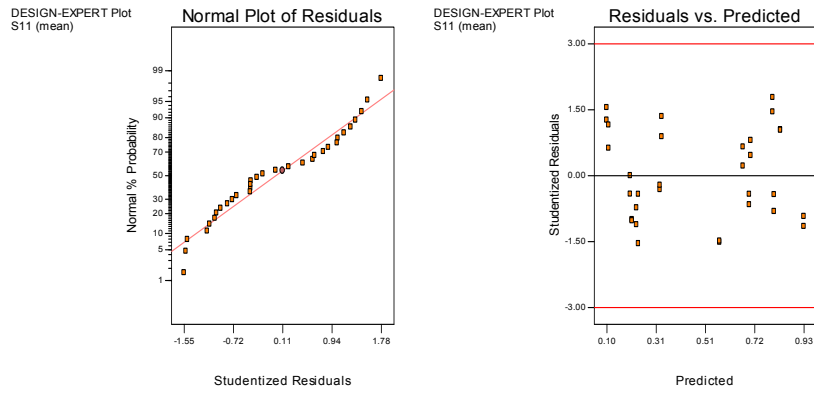


Figure A.1. Normal Plot of Residuals and Residuals versus Predicted Values Plot for S11 (mean) model for DOE I.

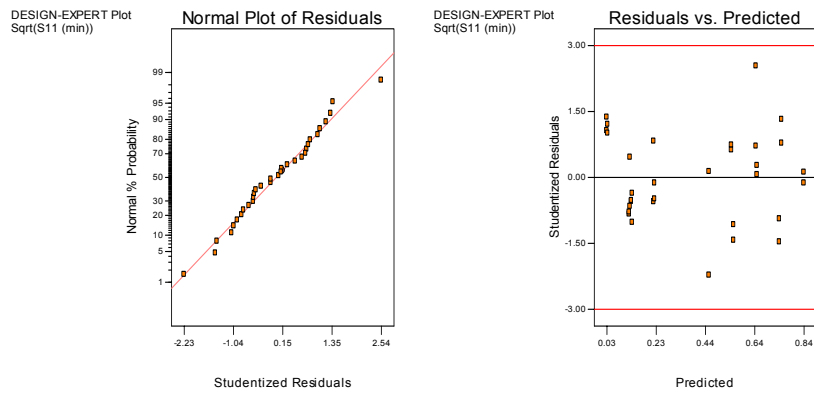


Figure A.2. Normal Plot of Residuals and Residuals versus Predicted Values Plot for S11 (min) model for DOE I.

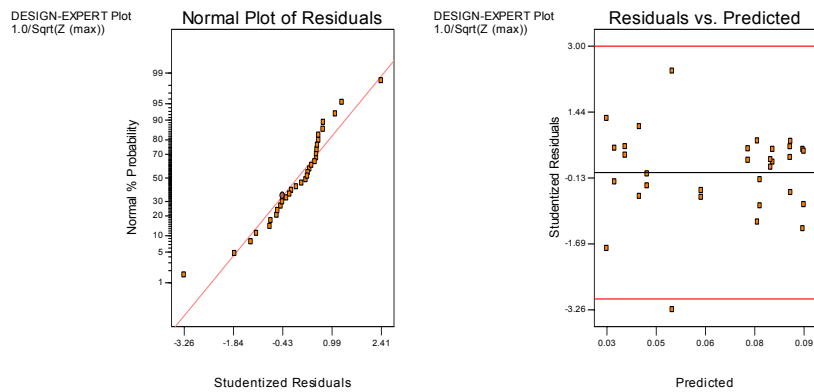


Figure A.3. Normal Plot of Residuals and Residuals versus Predicted Values Plot for the maximum value of the input resistance model for DOE I.

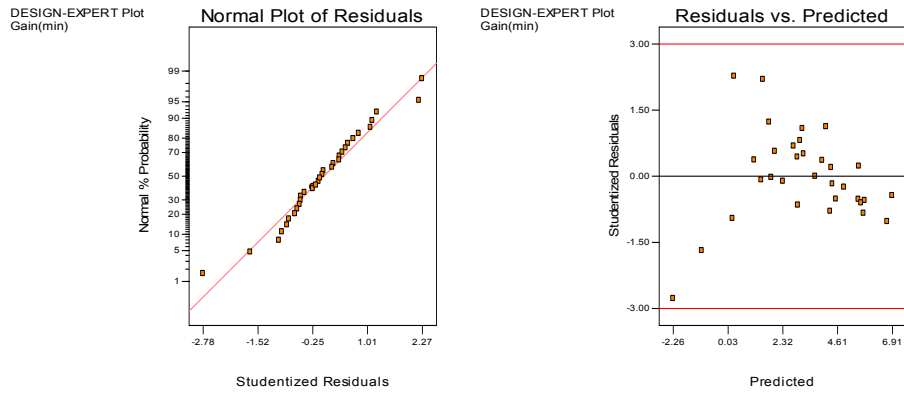


Figure A.4. Normal Plot of Residuals and Residuals versus Predicted Values Plot for Gain (min) model for DOE II.

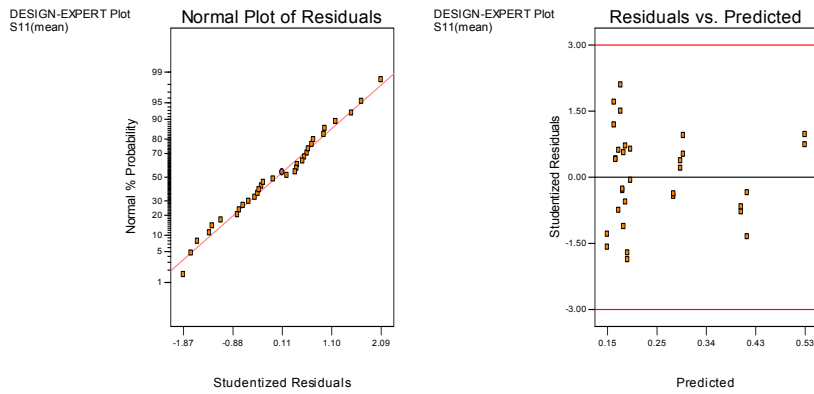


Figure A.5. Normal Plot of Residuals and Residuals versus Predicted Values Plot for S11 (mean) model for DOE II.

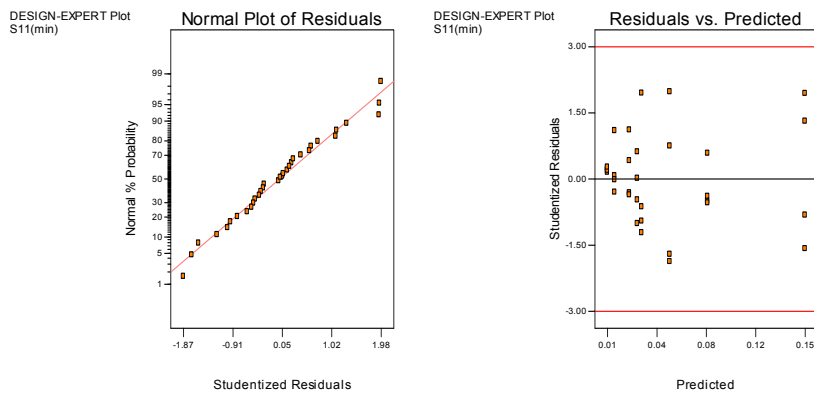


Figure A.6. Normal Plot of Residuals and Residuals versus Predicted Values Plot for S11 (min) model for DOE II.

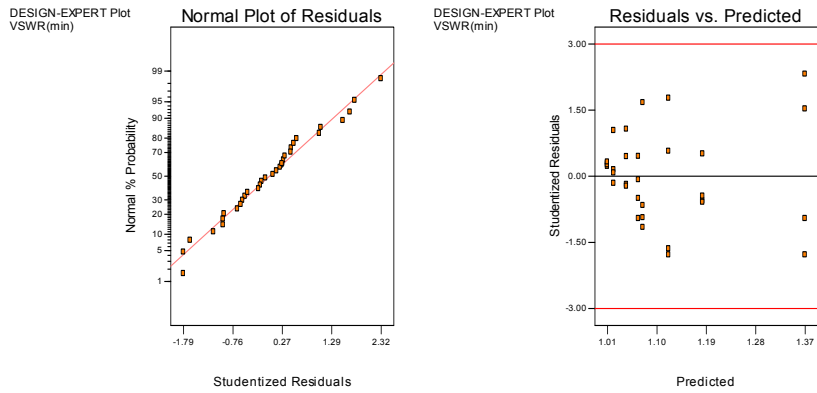


Figure A.7. Normal Plot of Residuals and Residuals versus Predicted Values Plot for VSWR (min) model for DOE II.

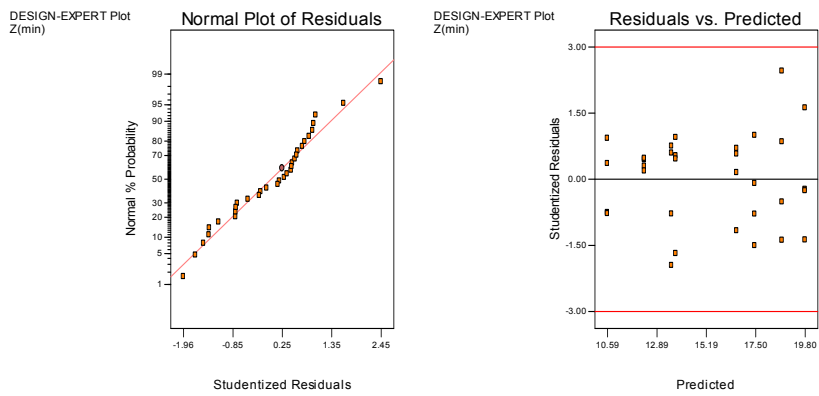


Figure A.8. Normal Plot of Residuals and Residuals versus Predicted Values Plot for the minimum of the input resistance model for DOE II.

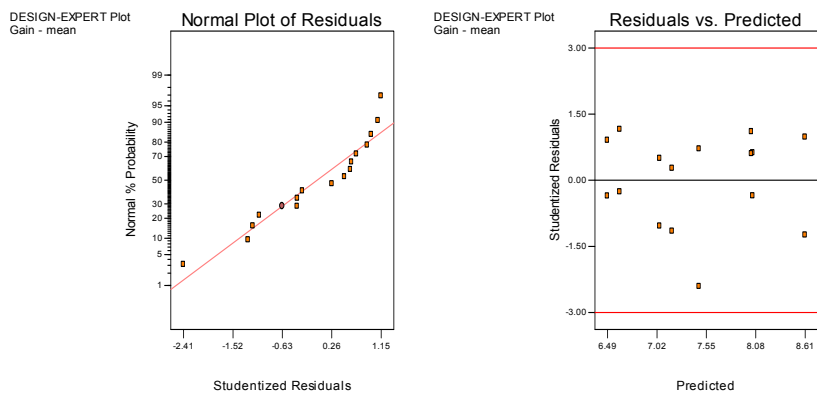


Figure A.9. Normal Plot of Residuals and Residuals versus Predicted Values Plot for Gain (mean) model for DOE III.

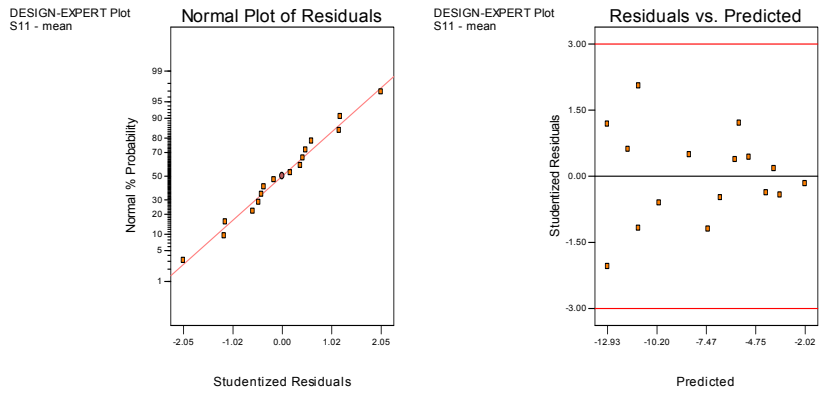


Figure A.10. Normal Plot of Residuals and Residuals versus Predicted Values Plot for S11 (mean) model for DOE III.

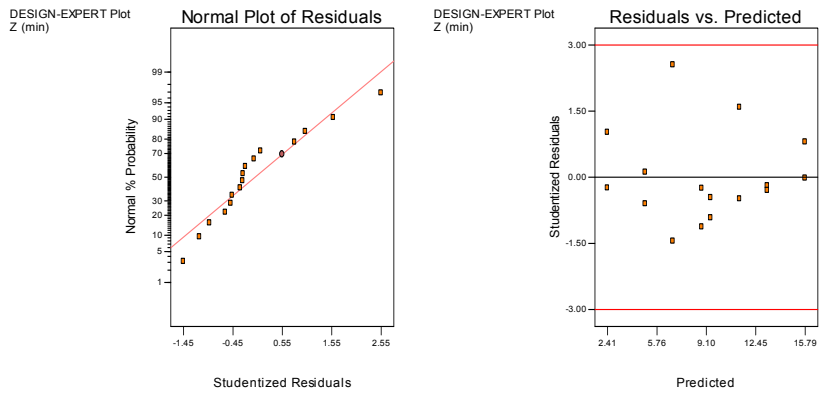


Figure A.11. Normal Plot of Residuals and Residuals versus Predicted Values Plot for minimum of the input resistance model for DOE III.

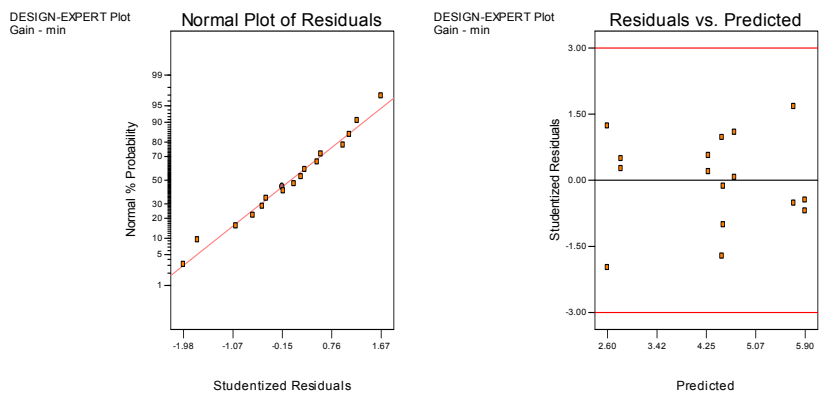


Figure A.12. Normal Plot of Residuals and Residuals versus Predicted Values Plot for Gain (min) model for DOE IV.

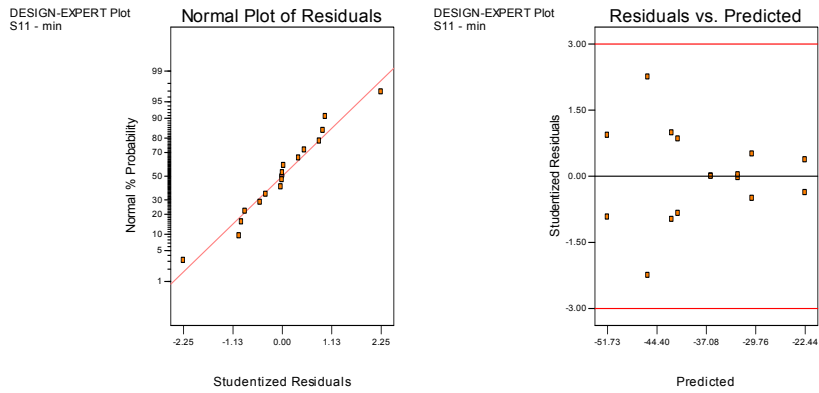


Figure A.13. Normal Plot of Residuals and Residuals versus Predicted Values Plot for S11 (min) model for DOE IV.

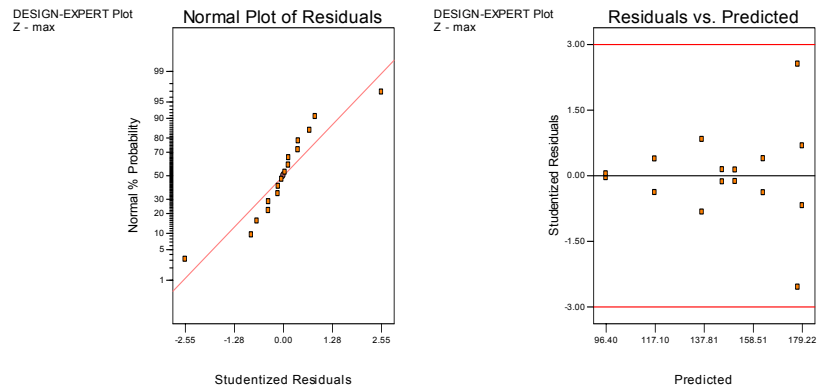


Figure A.14. Normal Plot of Residuals and Residuals versus Predicted Values Plot for the maximum of the input resistance model for DOE IV.

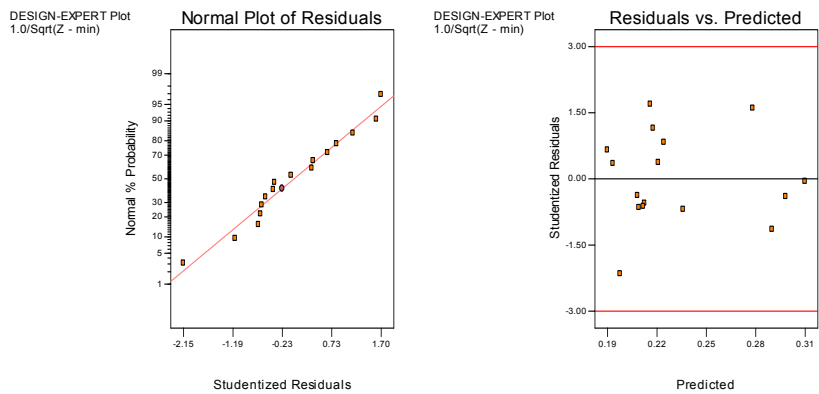


Figure A.15. Normal Plot of Residuals and Residuals versus Predicted Values Plot for the minimum of the input resistance model for DOE IV.

**Table A.1.** Actual and Predicted Values of the Model

Diagnostics Case Statistics					
Experiment	Actual	Predicted			
Number	Value	Value			
00000	0.20	0.20	00001	0.70	0.67
01000	0.18	0.20	01001	0.68	0.67
10000	0.15	0.10	10001	0.52	0.57
11000	0.14	0.10	11001	0.52	0.57
00100	0.31	0.32	00101	0.85	0.80
01100	0.32	0.32	01101	0.86	0.80
10100	0.19	0.23	10101	0.68	0.70
11100	0.20	0.23	11101	0.68	0.70
00010	0.17	0.21	00011	0.79	0.80
01010	0.17	0.21	01011	0.78	0.80
10010	0.15	0.11	10011	0.73	0.70
11010	0.13	0.11	11011	0.72	0.70
00110	0.36	0.33	00111	0.89	0.93
01110	0.38	0.33	01111	0.90	0.93
10110	0.18	0.23	10111	0.87	0.83
11110	0.22	0.23	11111	0.87	0.83

**Table A.2.** Actual and Predicted Values of the Model

Diagnostics Case Statistics					
Experiment	Actual	Predicted			
Number	Value	Value			
00000	0.01	0.05	00001	0.33	0.26
01000	0.01	0.05	01001	0.34	0.26
10000	0.01	0.03	10001	0.11	0.18
11000	0.01	0.03	11001	0.21	0.18
00100	0.07	0.07	00101	0.46	0.45
01100	0.04	0.07	01101	0.60	0.45
10100	0.01	0.01	10101	0.24	0.37
11100	0.01	0.01	11101	0.23	0.37
00010	0.02	0.05	00011	0.47	0.51
01010	0.01	0.05	01011	0.44	0.51
10010	0.01	0.03	10011	0.42	0.43
11010	0.01	0.03	11011	0.44	0.43
00110	0.05	0.07	00111	0.69	0.69
01110	0.04	0.07	01111	0.71	0.69
10110	0.01	0.01	10111	0.67	0.61
11110	0.01	0.01	11111	0.62	0.61

**Table A.3.** Actual and Predicted Values of the Model

Diagnostics Case Statistics					
Experiment	Actual	Predicted			
Number	Value	Value			
00000	0.0918	0.0894	00001	0.0584	0.0608
01000	0.0908	0.0894	01001	0.0591	0.0608
10000	0.0957	0.0935	10001	0.0781	0.0759
11000	0.0882	0.0935	11001	0.0770	0.0759
00100	0.0790	0.0797	00101	0.0387	0.0363
01100	0.0766	0.0797	01101	0.0379	0.0363
10100	0.0848	0.0838	10101	0.0609	0.0514
11100	0.0860	0.0838	11101	0.0386	0.0514
00010	0.0742	0.0789	00011	0.0432	0.0434
01010	0.0818	0.0789	01011	0.0421	0.0434
10010	0.0877	0.0896	10011	0.0386	0.0408
11010	0.0925	0.0896	11011	0.0451	0.0408
00110	0.0836	0.0831	00111	0.0352	0.0329
01110	0.0844	0.0831	01111	0.0320	0.0329
10110	0.0908	0.0938	10111	0.0233	0.0304
11110	0.0958	0.0938	11111	0.0355	0.0304

**Table A.4.** Actual and Predicted Values of the Model

Diagnostics Case Statistics					
Experiment	Actual	Predicted			
Number	Value	Value			
00000	-4.73	-2.26	00001	-0.63	0.23
01000	2.31	0.30	01001	3.39	2.78
10000	1.46	1.13	10001	1.82	1.85
11000	3.68	3.69	11001	4.25	4.40
00100	-2.56	-1.06	00101	1.35	1.43
01100	3.45	1.50	01101	4.30	3.98
10100	2.23	2.34	10101	3.77	3.05
11100	4.67	4.89	11101	5.07	5.61
00010	2.50	2.00	00011	2.85	1.76
01010	4.09	4.55	01011	3.60	4.31
10010	3.33	2.94	10011	4.11	3.15
11010	5.02	5.49	11011	4.96	5.70
00110	3.65	3.20	00111	2.38	2.96
01110	5.26	5.76	01111	5.72	5.51
10110	5.14	4.14	10111	4.53	4.35
11110	5.78	6.70	11111	6.52	6.91

**Table A.5.** Actual and Predicted Values of the Model

Diagnostics Case Statistics					
Experiment	Actual	Predicted			
Number	Value	Value			
00000	0.2076	0.2383	00001	0.1089	0.1535
01000	0.2666	0.2383	01001	0.2666	0.2788
10000	0.1539	0.1773	10001	0.2682	0.2788
11000	0.1920	0.1773	11001	0.1812	0.1696
00100	0.2150	0.2186	00101	0.1808	0.1696
01100	0.1952	0.2186	01101	0.3839	0.4061
10100	0.1530	0.1575	10101	0.3871	0.4061
11100	0.2000	0.1575	11101	0.3114	0.2968
00010	0.1391	0.2130	00011	0.3233	0.2968
01010	0.1435	0.2130	01011	0.3021	0.2916
10010	0.2208	0.1519	10011	0.2973	0.2916
11010	0.2375	0.1519	11011	0.1738	0.1824
00110	0.2140	0.1932	00111	0.1748	0.1824
01110	0.1995	0.1932	01111	0.5474	0.5267
10110	0.1172	0.1322	10111	0.5538	0.5267
11110	0.1089	0.1322	11111	0.3796	0.4174

**Table A.6.** Actual and Predicted Values of the Model

Diagnostics Case Statistics					
Experiment	Actual	Predicted			
Number	Value	Value			
00000	0.0132	0.0116	00001	0.0130	0.0529
01000	0.0350	0.0116	01001	0.0165	0.0529
10000	0.0071	0.0286	10001	0.0159	0.0226
11000	0.0185	0.0286	11001	0.0463	0.0226
00100	0.0185	0.0319	00101	0.1821	0.1542
01100	0.0115	0.0319	01101	0.1206	0.1542
10100	0.0094	0.0062	10101	0.0937	0.0812
11100	0.0112	0.0062	11101	0.0705	0.0812
00010	0.0113	0.0116	00011	0.0951	0.0529
01010	0.0053	0.0116	01011	0.0689	0.0529
10010	0.0417	0.0286	10011	0.0315	0.0226
11010	0.0290	0.0286	11011	0.0150	0.0226
00110	0.0734	0.0319	00111	0.1367	0.1542
01110	0.0060	0.0319	01111	0.1955	0.1542
10110	0.0104	0.0062	10111	0.0697	0.0812
11110	0.0119	0.0062	11111	0.0729	0.0812

**Table A.7.** Actual and Predicted Values of the Model

Diagnostics Case Statistics					
Experiment	Actual	Predicted			
Number	Value	Value			
00000	1.0267	1.0190	00001	1.0264	1.1187
01000	1.0725	1.0190	01001	1.0336	1.1187
10000	1.0142	1.0638	10001	1.0323	1.0421
11000	1.0377	1.0638	11001	1.0972	1.0421
00100	1.0376	1.0720	00101	1.4453	1.3664
01100	1.0233	1.0720	01101	1.2742	1.3664
10100	1.0190	1.0075	10101	1.2067	1.1805
11100	1.0226	1.0075	11101	1.1516	1.1805
00010	1.0228	1.0190	00011	1.2102	1.1187
01010	1.0107	1.0190	01011	1.1479	1.1187
10010	1.0871	1.0638	10011	1.0650	1.0421
11010	1.0596	1.0638	11011	1.0304	1.0421
00110	1.1583	1.0720	00111	1.3167	1.3664
01110	1.0120	1.0720	01111	1.4861	1.3664
10110	1.0209	1.0075	10111	1.1499	1.1805
11110	1.0242	1.0075	11111	1.1572	1.1805

**Table A.8.** Actual and Predicted Values of the Model

Diagnostics Case Statistics					
Standard	Actual	Predicted			
Order	Value	Value			
Experiment	13	12	00001	15	14
Number	13	12	01001	16	14
00000	15	14	10001	19	20
01000	9	14	11001	23	20
10000	14	17	00101	11	11
11000	16	17	01101	13	11
00100	24	19	10101	18	17
01100	21	19	11101	18	17
10100	13	12	00011	10	14
11100	13	12	01011	15	14
00010	15	14	10011	17	20
01010	12	14	11011	19	20
10010	17	17	00111	9	11
11010	20	17	01111	9	11
00110	18	19	10111	17	17
01110	16	19	11111	14	17

**Table A.9.** Actual and Predicted Values of the Model

Diagnostics Case Statistics		
Experiment	Actual	Predicted
Number	Value	Value
0000	6.55	6.62
1000	6.40	6.49
0100	6.91	6.62
1100	6.71	6.49
0010	6.89	7.18
1010	6.79	7.05
0110	7.25	7.18
1110	7.17	7.05
0001	7.96	8.05
1001	7.65	7.47
0101	8.20	8.05
1101	6.86	7.47
0011	8.29	8.61
1011	8.18	8.03
0111	8.85	8.61
1111	8.31	8.03

**Table A.10.** Actual and Predicted Values of the Model

Diagnostics Case Statistics		
Experiment	Actual	Predicted
Number	Value	Value
0000	-8.1505	-8.4112
1000	-5.6794	-5.8816
0100	-4.8869	-5.1164
1100	-3.6459	-3.7366
0010	-14.0151	-12.9177
1010	-12.2960	-12.9286
0110	-11.4655	-11.7910
1110	-8.0119	-7.3680
0001	-6.9558	-6.6952
1001	-4.3677	-4.1655
0101	-3.6298	-3.4003
1101	-2.1113	-2.0205
0011	-10.1042	-11.2016
1011	-11.8451	-11.2125
0111	-10.4005	-10.0749
1111	-5.0081	-5.6520

**Table A.11.** Actual and Predicted Values of the Model

Diagnostics Case Statistics		
Experiment	Actual	Predicted
Number	Value	Value
0000	15.50	11.36
1000	8.15	8.80
0100	10.07	11.36
1100	5.86	8.80
0010	15.74	15.79
1010	12.73	13.24
0110	17.88	15.79
1110	12.45	13.24
0001	5.27	4.97
1001	5.07	2.41
0101	3.39	4.97
1101	1.78	2.41
0011	7.00	9.40
1011	13.51	6.85
0111	8.19	9.40
1111	3.06	6.85

**Table A.12.** Actual and Predicted Values of the Model

Diagnostics Case Statistics		
Experiment	Actual	Predicted
Number	Value	Value
0000	1.89	2.60
1000	4.35	4.29
0100	2.92	2.83
1100	3.90	4.51
0010	3.03	2.60
1010	4.48	4.29
0110	3.00	2.83
1110	4.86	4.51
0001	4.17	4.53
1001	4.74	4.72
0101	6.31	5.71
1101	5.65	5.90
0011	4.49	4.53
1011	5.11	4.72
0111	5.53	5.71
1111	5.74	5.90

**Table A.13.** Actual and Predicted Values of the Model

Diagnostics Case Statistics		
Experiment	Actual	Predicted
Number	Value	Value
0000	-39.40	-41.25
1000	-40.04	-42.19
0100	-53.76	-51.73
1100	-21.62	-22.44
0010	-43.10	-41.25
1010	-44.34	-42.19
0110	-49.70	-51.73
1110	-23.25	-22.44
0001	-36.37	-36.38
1001	-32.44	-32.38
0101	-40.80	-45.73
1101	-31.39	-30.29
0011	-36.39	-36.38
1011	-32.31	-32.38
0111	-50.65	-45.73
1111	-29.18	-30.29

**Table A.14.** Actual and Predicted Values of the Model

Diagnostics Case Statistics		
Experiment	Actual	Predicted
Number	Value	Value
0000	131.18	136.91
1000	119.64	116.99
0100	195.00	177.39
1100	165.44	162.76
0010	142.64	136.91
1010	114.35	116.99
0110	159.79	177.39
1110	160.08	162.76
0001	183.95	179.22
1001	144.49	145.45
0101	96.10	96.40
1101	151.80	150.89
0011	174.49	179.22
1011	146.41	145.45
0111	96.69	96.40
1111	149.98	150.89

**Table A.15.** Actual and Predicted Values of the Model

Diagnostics Case Statistics		
Experiment	Actual	Predicted
Number	Value	Value
0000	0.2945	0.2974
1000	0.2303	0.2353
0100	0.2039	0.2086
1100	0.2049	0.2077
0010	0.2891	0.2775
1010	0.2276	0.2154
0110	0.2079	0.2119
1110	0.2065	0.2111
0001	0.3087	0.3091
1001	0.2254	0.2171
0101	0.2230	0.2203
1101	0.1942	0.1894
0011	0.2808	0.2892
1011	0.1815	0.1971
0111	0.2297	0.2236
1111	0.1953	0.1928